FINAL REPORT

Mechanochemical Nitration of Organic Compounds

SERDP Project WP19-1383

JULY 2021

Edward L. Dreizin
New Jersey Institute of Technology

Leah Wingard
Army Research Laboratory

SERDP
DOD ▪ EPA ▪ DOE

REPORT DOCUMENTATION PAGE

Form Approved
OMB No. 0704-0188

1. REPORT DATE *(DD-MM-YYYY)*	**2. REPORT TYPE**	**3. DATES COVERED** *(From - To)*
27/07/2021	SERDP Final Report	2/1/2019 - 7/28/2022

4. TITLE AND SUBTITLE

Mechanochemical Nitration of Organic Compounds

5a. CONTRACT NUMBER
19-P-0007

5b. GRANT NUMBER

5c. PROGRAM ELEMENT NUMBER

6. AUTHOR(S)
Edward L. Dreizin
New Jersey Institute of Technology

Leah Wingard
Army Research Laboratory

5d. PROJECT NUMBER
WP19-1383

5e. TASK NUMBER

5f. WORK UNIT NUMBER

7. PERFORMING ORGANIZATION NAME(S) AND ADDRESS(ES)
New Jersey Institute of Technology
University Heights
Newark, NJ 07102

8. PERFORMING ORGANIZATION REPORT NUMBER
WP19-1383

9. SPONSORING/MONITORING AGENCY NAME(S) AND ADDRESS(ES)
Strategic Environmental Research and Development Program (SERDP)
4800 Mark Center Drive, Suite 16F16
Alexandria, VA 22350-3605

10. SPONSOR/MONITOR'S ACRONYM(S)
SERDP

11. SPONSOR/MONITOR'S REPORT NUMBER(S)
WP19-1383

12. DISTRIBUTION/AVAILABILITY STATEMENT

DISTRIBUTION STATEMENT A. Approved for public release: distribution unlimited.

13. SUPPLEMENTARY NOTES

14. ABSTRACT

Nitro-products of organic compounds are useful in many applications; they are widely employed as precursors or components of energetic materials. Industrial nitration generates substantial waste and uses aggressive chemicals, making the process unsafe and environmentally objectionable. This work advances the solvent-free process of mechanochemical nitration of aromatic compounds. Feasibility of such nitration with high yield and rate was shown. Nitration is achieved during mechanical milling of the organic precursor, solid powder catalyst, and nitrate, serving as a source of nitronium. However, it remained unclear how important are the choices of the catalyst, organic compound to be nitrated, and nitronium source. Quantifying and understanding such effects will advance the proposed mechanochemical nitration technique and build the foundation for the follow-up work identifying the reaction mechanisms and scaling the process up to pilot-plant level.

15. SUBJECT TERMS

Mechanochemical Nitration, Organic Compounds

16. SECURITY CLASSIFICATION OF:			**17. LIMITATION OF ABSTRACT**	**18. NUMBER OF PAGES**	**19a. NAME OF RESPONSIBLE PERSON**
a. REPORT	**b. ABSTRACT**	**c. THIS PAGE**			Edward L. Dreizin
UNCLASS	UNCLASS	UNCLASS	UNCLASS	91	**19b. TELEPHONE NUMBER** *(Include area code)* 973-596-5751

Contents

LIST OF FIGURES

LIST OF TABLES

LIST OF ABBREVIATIONS

Abbreviation	Meaning
PM	Planetary mill
GC-MS	Gas chromatography-Mass spectrometery
XRD	X-ray Diffraction
BET	Brunauer-Emmett-Teller theory
NT	Nitrotoluene
MNT	Mononitrotoluene
DNT	Dinitrotoluene
p/o	Para:ortho isomer ratio
P	Product
NP	Nitroproduct
AIC	Akaike Information criterion

Abstract

Introduction and Objectives: Nitro-products of organic compounds are useful in many applications; they are widely employed as precursors or components of energetic materials. Industrial nitration generates substantial waste and uses aggressive chemicals, making the process unsafe and environmentally objectionable. This work advances the solvent-free process of mechanochemical nitration of aromatic compounds. Feasibility of such nitration with high yield and rate was shown. Nitration is achieved during mechanical milling of the organic precursor, solid powder catalyst, and nitrate, serving as a source of nitronium. However, it remained unclear how important are the choices of the catalyst, organic compound to be nitrated, and nitronium source. Quantifying and understanding such effects will advance the proposed mechanochemical nitration technique and build the foundation for the follow-up work identifying the reaction mechanisms and scaling the process up to pilot-plant level.

Technical Approach: A laboratory planetary mill is used for experiments. The type of catalyst, the organic compounds to be nitrated, and the nitrates, serving to provide nitronium were varied systematically. The products were analyzed using gas chromatography–mass spectrometry. Aside from milling parameters, the amounts of liquid organic precursor and nitrate were varied. The results were analyzed correlating properties of catalysts, precursors, and nitronium sources with the rate of reaction, yield of nitro-products, selectivity, and production of byproducts.

Results: Mechanochemical nitration was successful for multiple useful aromatic compounds. The reaction rate and yield are increased when solid catalysts have high acidity and contain both, Bronsted and Lewis sites. Among the tested materials, MoO_3 was the preferred catalyst. Homogenizing the catalyst with nitrate by a preliminary milling step accelerates ensuing mechanochemical nitration significantly. The selectivity was enhanced and the yield of the nitroproduct was increased when the volume of the aromatic precursor was reduced while the mass of metal oxide catalyst was fixed. The formation of nitroproducts depends on the aromatic activation by the functional group, gas basicity and enthalpy of vaporization of the aromatic precursor. Reaction enthalpies and kinematic viscosity were found to be important as well. Different nitration rates were observed for different nitrates used as nitronium sources with the highest nitration rate observed for $Cu(NO_3)_2$. The reaction rate correlated with the enthalpy of the global nitration reaction for which the decomposition of the nitrate was assumed to form the corresponding metal hydroxide. More exothermic global reactions led to higher reaction yields and rates. A second nitration of the aromatic ring was observed for all the precursors tested. Nearly complete mechanochemical nitration could be achieved in many experiments. In this work, achieving the complete nitration was not targeted; instead, conditions, materials, and process parameters affecting the reaction were established.

Benefits: A path is established to further scale-up and optimize solvent-free mechanochemical nitration of organic compounds. Catalysts are benign, reusable or recyclable. Reaction rate is controllable and yield is high. Found relationships between the process parameters, materials, and yield and reaction rate for the nitro-products will guide future mechanistic and scale-up efforts. Design of pilot-plant production of single-nitrated products can be a logical next step.

Objective

Specific objectives of this proposed effort are to extend the previous effort to systematically include mechanochemical nitration of differently activated aromatics, and other classes of organic compounds, and to quantify the respective reaction mechanism.

In the previous SEED program, it has been established that mechanochemical nitration of organic compounds, such as toluene is feasible. It was further shown that varying milling process parameters, it is possible to reach high, practically significant yields (ca. 90%) of synthesizing mono-nitrotoluene (MNT) using toluene as a precursor and using sodium nitrate as a source of nitronium ions. The amounts of MNT isomers formed indicated a surface reaction with para/ortho ratios in the relatively narrow range of 1.1 – 1.4. The main undesirable byproducts were benzaldehyde and toluene dimers, 2- and 4-methylphenyl-phenylmethanone. The yield and selectivity of production of MNT were found to be sensitive to the type of milling media (size and material of balls), ball to powder mass ratio, and milling temperature. It was further found that combining the catalyst, MoO_3, with a high-surface area support material, such as SiO_2, led to increase in the yield of mechanochemically produced MNT. Thus, mechanochemical synthesis of nitrated organic compounds could be readily controlled; it could certainly be further optimized. However, the mechanism of mechanochemical nitration using a solid catalyst and a solid nitrate source has been unclear. Previous research suggests that heteropoly acids are excellent nitration catalysts due to the effectively high surface area, exposing active centers to the reactants [1-4]. However, catalysts with these cage structures decay over time, and need to be regenerated before they can be reused. Mechanical milling provides an alternative to this approach via continuous generation of fresh surface, thereby exposing catalytically active centers volumetrically. On the other hand, mechanical milling stresses the organic substrate by localized (mm scale), and short-term (μs scale) temperature fluctuations. Quantifying details of this process balance, and illuminating other aspects of the mechanochemical nitration process will be important goals of the proposed research. *Specific experimental objective of this effort was to systematically quantify the effects of properties and type of organic substrate, solid catalyst, nitronium source, and process parameters on nitration of different organic compounds.* This work is expected to lead to further studies aimed to:

- Formulating a quantitative mechanism of interaction between starting components and catalysts leading to mechanochemical nitration reactions.
- Identify pathways for scaling-up the mechanochemical synthesis of organic nitrated compounds while reusing or recycling spent milling media and catalysts.

The long-term focus of the research is to develop an environmentally friendly technology for manufacturing nitrated organic compounds with minimized energy consumption, complete conversion of starting materials, and enabling reuse and recycling of spent catalysts and milling media. The successful demonstration of the feasibility of the mechanochemical synthesis approach in the previous SEED program paved the way for this study focused strategically on the reaction mechanisms, synthesis optimization, and scale-up.

Process safety is an important consideration while developing the proposed technology. The present approach enables one to set up the mechanochemical synthesis so that the mass and, more importantly, heat capacity of milling media is substantially greater than that of the precursors and formed products. Thus, in case of an accidental mechanical initiation of a produced energetic material, the reaction will be effectively suppressed by heat removal into high heat capacity milling media. Additional safeguards will also be considered.

Background

Mechanochemical processing was recently developed into a versatile and economically viable materials synthesis method suitable for preparation of an essentially unlimited range of both inorganic and organic compounds [5]. This method uses no solvents; it is readily scalable and relatively inexpensive. Generated wastes include used milling media and catalysts. All are solids, which are typically environmentally benign and easy to recycle or reuse. In this effort, mechanochemistry has been adapted to nitrate organic compounds to serve as energetic materials or their precursors or components.

Some of the most common and important organic reactions involve nitration of various organic compounds [6], which find wide use in many applications. Majority of energetic materials are organic compounds, which derive their energy from the nitro group [7]. Nitrated aromatics are of particular interest as they are used as solvents, dyes [8], explosives [9], pharmaceuticals [10], and perfumes [11]. In addition, they serve as intermediates in preparation of other compounds, particularly amines [12]. Nitrotoluene (NT), for example, is the first precursor in the synthesis of trinitrotoluene or TNT – a common explosive [13]. In addition, NT is used in synthesis of toluidine, nitrobenzaldehyde, and chloronitrotoluenes, which are the intermediates for the production of dyes, resin modifiers, optical brighteners and suntan lotions [14]. Other nitrated compounds, such as nitrocellulose and nitroglycerine also have a number of applications in energetic formulations (propellants, explosives, pyrotechnics) [15] and in pharmaceuticals [14]. The nitrating agent for these reactions has traditionally been fuming nitric acid combined with another strong acid, e.g., sulfuric acid, perchloric acid, selenic acid, hydrofluoric acid, boron triflouride, or an ion-exchange resin containing sulfonic acid groups. These strong acids are catalysts that result in formation of nitronium ion, NO_2^+. Sulfuric acid is almost always used industrially since it is both effective and relatively inexpensive [16-18].

The common nitration methods involving strong acids have a number of disadvantages; perhaps the most significant being the production of large quantities of spent acids, which must be regenerated because their neutralization and disposal on a large scale are environmentally and economically unsound [19]. Another issue is generation of considerable amounts of environmentally harmful waste during the purification of the products [18]. Additional disadvantages include the hazards associated with handling the nitrating agents, as well as over nitration [20]. The reactions are not selective, and usually yield a mixture of isomers some of which are less desirable than others. For example, toluene nitration using this method produces a mixture of 55-60% of ortho- or o-NT, 35-40% of para- or p-NT, and 3-4% of meta-, or m-NT [21]. This leads to large quantities of unwanted product because the demand for p-NT is greater

than for the other isomers [18, 22]. The conventional techniques used to increase the ratio of p- to o- isomers, such as nitration in the presence of phosphoric acid or in the presence of aromatic sulfonic acids increase the p/o ratio from 0.6 to 1.1-1.5 [23], require additional use of environmentally harmful reactants. Another challenge associated with this reaction is the formation of oxidative byproducts. The addition of the nitro group to the aromatic ring of toluene strongly activates its methyl group making it susceptible to oxidation. Therefore, industrial nitration of toluene must be carried out at low temperatures to minimize formation of the undesired oxidation products [18]. In a batch process, for example, the acids are added at 25°C and the reaction is carried out at 35 – 40°C [18]. The total NT yield in this reaction is 96% for a batch process, but most patents for continuous processes report yields of up to 50% [18].

The disadvantages of the conventional nitration methods motivated research aimed at finding cleaner, safer, and more efficient techniques. In one approach, liquid sulfuric acid is replaced with solid catalysts, which tend to be safer, environmentally friendlier, and easier to separate from the reaction solution than sulfuric acid. In addition, in the case of toluene nitration, surface reaction tends to favor formation of the desirable p-isomer [18]. In Ref. [18], toluene was nitrated in the vapor phase using fuming nitric acid over solid acid catalysts. Several catalysts were tested, including zeolites and non-zeolitic materials. The reactions were carried out in a fixed bed reactor at atmospheric pressure with temperatures ranging from 130 to 160 °C. NT yield fluctuated around 20% for the reaction carried out without solid acid catalyst and around 40% for Deloxan catalyzed reaction. Para/ortho ratio was approximately 0.7 for the uncatalyzed reaction and 0.8 for the reaction catalyzed with Deloxan®. NT yields for the zeolite-catalyzed reaction stayed close to 20%, but the p/o ratio varied from about 0.7 to about 1.1. Only some zeolites (namely H-beta) actually catalyzed the reaction, causing it to take place on the surface and thus resulting in a higher p/o ratio. Preshaped silica pellets impregnated with H_2SO_4 were found to be the only catalyst among those considered that produced NT yields of up to 60%, and even that only when the samples with high content of sulfuric acid were used. Unfortunately, this approach still uses fuming nitric acid as well as significant quantities of concentrated sulfuric acid. The latter, despite being attached to silica, gets used up and cannot be regenerated. Therefore the environmental and safety concerns associated with the traditional nitration methods remain.

More recently Gong et al. [24] carried out liquid phase nitration of toluene using dilute nitric acid (50%) over silica supported Cs salt of phosphomolybdic acid ($Cs_{2.5}H_{0.5}PMoO_{40}$) and achieved remarkably high yields of up to 99.6% NT. The reaction was carried out in a stirred batch reactor with the highest product yields achieved at the reaction times of over 4 hrs. It was also found that the catalyst could be easily regenerated and reused. This method eliminated the need for sulfuric acid, while still using diluted nitric acid. Unfortunately, the p/o isomer ratio did not exceed 0.66, thus the problem of unwanted product accumulation was not resolved. Somewhat similarly, Adamiak et al. [20] achieved high yields of mono- and di- nitrotoluenes by nitrating toluene with fuming nitric acid over MoO_3/SiO_2 catalyst modified with H_3PO_4. The characterization of catalyst showed that phosphoric acid reacted with molybdenum oxide forming phosphomolybdic acid, which is a heteropoly acid with a cage-like structure, and

catalyzes the nitration reaction by effectively exposing the catalytically active [MoO_6] centers to the reactants. Good para- selectivity was observed for this process with p/o ratios greater than 1 and reaching 2.09 in one case. Unfortunately, these approaches still use nitric acid as the nitrating agent, which is difficult to handle and hard to dispose of. Thus, other sources of nitronium ion were considered. Peng et al. [25] carried out nitration of toluene using liquid NO_2 and molecular oxygen over zeolite catalysts and achieved p/o ratio as high as 14 using HZSM-5. Perves et al., [26] used nitronium tetraflouroborate as a source of nitronium ion. These methods, while achieving promising results, rely on impractical, exotic and expensive reactants and/or catalysts.

A new and potentially promising approach to this problem is to carry out the nitration in solid phase using nitrate salts as sources of nitronium ion, driving the reaction mechanochemically. Eliminating solvents and acids offers substantial reduction of the environmental impact of nitration; using inexpensive and readily available nitrogen sources and catalysts offers potential cost benefits as well. Although the concept of carrying out reactions in solid phase by mechanical agitation, known as mechanochemistry, existed for centuries, its application has traditionally been limited to insoluble materials [27]. Last several decades have witnessed a steadily and rapidly increasing interest to mechanochemical synthesis, and the manifestation of the versatility and the potential of this approach [5, 28-39]. There are two reasons behind the tremendous interest in mechanochemical research. First, it is becoming increasingly clear that this approach can be effective and advantageous for a wide range of materials. Second, there is an increasing awareness that our current dependence on solvents is both wasteful of fossil derived materials and harmful to the environment; thus it is unsustainable [40].

Despite significant progress, our current understanding of the mechanisms of mechanochemical reactions remains deficient. It is generally understood that the reactions occur at points of contact between solid surfaces, and there are various theories explaining such reactions. One possibility is that mechanical impact causes dramatic increase in lattice stress. This stress then relaxes, either physically, by emission of heat, or chemically, by ejection of atoms or electrons, formation of excited states on the surface, bond breakage, and other chemical transformations [41]. This can cause chemical reactions to occur in the field of mechanical stress or even after the stress is removed, by the action of reactive species such as free radicals formed under the action of mechanical stress, that can now cause the reaction to propagate further [42]. Other models discussed in the literature include the “hot-spot” theory and the “magma-plasma model” [43]. In both cases, impacts are predicted to cause a localized temperature increase up to ca. 10^4 K. Such high temperatures stimulate reactions; however, it is unlikely for such heating to occur for organic reactions, which would decompose most of the involved species [43]. Instead, covalent bond forming organic reactions have been suggested to occur through the formation of intermediate liquid eutectic phases [44]. There has been little done to customize these mechanisms for specific reactions, despite the fact that parameters affecting reactions depend significantly on such mechanisms. Lowering temperature, for example, usually improves the effectiveness of milling processes, and can improve the rate of reactions caused by formation of

surface defects. If, however, the reaction proceeds through the formation of a localized liquid phase and/or is thermally activated, its rate is likely to drop when the temperature is lowered.

Despite a wide variety of reactions that have been carried out mechanochemically to date, nitration of aromatics has been largely overlooked. An exception is the work of Albadi et al. [42] who nitrated a number of aromatic compounds in a mortar using sodium nitrate in the presence of melamine trisulfonic acid as a source of nitronium ion. All the compounds nitrated were activated by strongly electron donating substituents such as –OH, -OMe, or $–N(CH_3)_2$ groups. Nitration of toluene, whose methyl group is less activating in an electrophilic substitution reaction than the above listed groups, was not reported.

In the previous SEED program, the approach of mechanochemical nitration using nitrates was adopted to nitrate toluene and modified further by using environmentally benign catalysts, such as MoO_3 or combinations of MoO_3 and SiO_2. The catalytic activity of MoO_3, particularly in hydrocarbon oxidation reactions has long been known, and many studies have been performed examining its use in partial oxidation of methanol [13, 42] and other compounds [45]. Although the mechanism of these reactions is subject to much debate in the literature [46], there is evidence, based on atomic force microscopy studies [45], that the uncoordinated Mo^{6+} cations on step edges and defects are the active sites for oxidation of alcohols. These Lewis acid sites are effective to form the nitronium ion from the nitrate. Thus, the ball milling process, which continuously generates fresh surfaces and new defects may greatly enhance the Lewis acid properties of MoO_3 making it an effective catalyst in mechanochemical aromatic nitration.

It has been established that high, practically significant yields of MNT, are attainable by mechanochemical reaction of toluene and sodium nitrate with molybdenum oxide as a catalyst, and without any added solvents. The reaction occurs with a high MNT yield when the ratio of reactant to catalyst is low, so that toluene is effectively spread as a monolayer on the surface of the catalyst. The rate of the mechanochemical nitration increases with the number of collisions; the reaction efficiency is also strongly affected by the energy dissipated in the collisions. Adding silica to the catalyst MoO_3 increases efficiency of the mechanochemical nitration of toluene as long as a sufficient amount of the catalyst remains available. The results suggested that introducing one global reaction may be inadequate for modeling mechanochemical nitration of toluene. Yields, which were optimized at a specific milling time and with specific silica content, will need to be described using additional reactions. Additional reactions are also necessary to describe the observed formation of byproducts observed in the experiments, which were also affected by the milling temperature. At low concentrations of catalyst, direct oxidation of toluene by sodium nitrate can generate benzaldehyde, one of the main byproducts. No evidence is found of formation of dimers, 2-methylphenyl-phenylmethanone and 4-methylphenyl-phenylmethanone, other significant byproducts, by reactions directly involving toluene. Further work is needed to understand the reason for reduced yield and recovery at longer milling times; use of other solvents or other extraction techniques is necessary

Although not discussed above, nitration of naphthalene and anisole was also observed. Thus, nitration of aromatic compounds is feasible using mechanochemical reaction without involving

any solvents and/or strong acids. Product yield and selectivity depend on milling conditions, particularly milling dose. A weak Lewis acid, MoO_3 is found to be an attractive candidate for mechanochemical nitration. It is hypothesized here that the mechanochemical approach can further be developed to produce a broad range of organic nitro compounds with high purity and on a practically attractive scale, without strong acids and solvents employed in the present technologies.

Technical approach

This program was aimed to explore further mechanochemical nitration of organic compounds, starting with toluene, as an important organic liquid precursor for many energetic materials. This effort was a collaboration between Prof. Dreizin's research group at NJIT and scientists at the Army Research Laboratory (ARL) led by Dr. L. Wingard. ARL guided NJIT researchers in selecting compounds to be nitrated of particular interest to DOD. Jointly, NJIT and ARL researchers assessed the products generated and study the reaction mechanisms based on diverse analytical techniques and methods. ARL played the key role in efforts aimed at extending this technology to specific materials of interest to DOD.

In this, limited scope study, the focus has been to understand and quantitatively describe the mechanism of mechanochemical nitration. Achieving this understanding relied on a detailed experimental study aimed to identify the *key process parameters and characteristics of precursor materials and catalysts* used in reaction, which affect the yield and selectivity of nitration.

Both *reaction mechanisms and scale up methods* will be addressed in the follow-up research. Establishing the effect of *catalyst, precursor, and nitronium source* on the nitration of organic compounds is considered the key for the success of the follow-up research.

General experimental approach followed that developed in the previous SEED effort. Specifically, different pairs of precursors, e.g., toluene and sodium nitrate, were blended with a catalyst, e.g., MoO_3, and milled to achieve nitration. The starting milling conditions were selected based on the previous work, in which high yields of MNT were achieved. These conditions suggested a relatively high solids loading with a small amount of organic compound, which likely forms a thin, discontinuous coating on the catalyst particles. Following the milling runs, the products were extracted and analyzed using gas chromatography combined with mass spectroscopy (GCMS). Additional measurements and analyses are described specifically for different chapters listed below.

Results and Discussion

Chapter 1: Mechanochemical nitration of toluene with metal oxide catalysts

1.1. Abstract

Results of an experimental study of the mechanochemical nitration of toluene are presented. The focus is on the effect of acidity of metal oxide catalysts on the yield of mononitrotoluene. No solvents were used during the reaction. Sodium nitrate served as a source of nitronium. Gas chromatography-mass spectrometry of the products showed that the nitration rate scaled with the

catalyst's acidity and specific surface area. Homogenizing $NaNO_3$ with the catalyst by additional milling prior to reaction with toluene led to a rapid, nearly complete nitration. Distribution of nitrate over the surface of catalyst is likely rate limiting when toluene is mechanochemically nitrated without the preliminary milling step. The observed for varied reactant ratios trends in yield and isomer ratios suggest that nitronium participates in the nitration while localized on the active sites of the catalyst. Excess of toluene blocks acid sites, inhibiting the formation of nitronium and impeding the nitration.

1.2. Introduction

There has been a significant rise in the use of green synthesis methods in the chemical industry with focus on using renewable raw materials, eliminating waste, and reducing use of hazardous reagents and solvents in the production of chemicals [1, 2]. Nitration methods used in the industry commonly rely on mixed acids with an excess of nitric acid [3]. These methods have a number of drawbacks, such as low selectivity of desirable isomers, generation of waste acid and evolution of NO_x fumes among other safety concerns [4]. Disposal of the produced waste acids is costly [4, 5]. Heterogeneous catalysis of nitration of a variety of aromatics used gas-solid and liquid-solid systems. The solid catalysts used, which include metal oxides and zeolites, were found to be effective because of their acidity. The acid sites on the surface of a solid catalyst were required for generation of NO_2^+ (nitronium ion) from NO_3^+ (nitrate ion) [6, 7]. Effectively, solid acids can play the role of sulfuric acid by assisting in the formation of the nitronium ion while providing easy separation of product and reduced quantities of hazardous waste [8]. Commonly used solid catalysts include Lewis acids, such as molybdenum and tungsten oxides on supports, such as silica and titanium oxide [8-13], or zeolites, such as HZSM-5, H-Y, H-beta, and H-mordenite [5, 14-17]. Although the use of sulfuric acid can thus be avoided, the nitration still often requires nitric acid and associated wastes. Water generated through usage of nitric acid necessitated the use of acetic anhydride [12]. Liquid nitric acid is the most common source of the nitro group [5, 9, 18-22], although gaseous sources [13, 23-29] and inorganic nitrates [23, 230-33] were also explored.

Recently, mechanochemical nitration of aromatics was reported using a solid catalyst and an inorganic nitrate as the source for nitronium [34, 35]. Reaction (1) was carried out in a high-energy ball mill producing MNT.

$$C_7H_8 + NaNO_3 \xrightarrow[MoO_3]{} C_7H_7NO_2 + NaOH \qquad (1)$$

The mechanochemical process continuously generates fresh catalytic surface, and brings it in contact with the aromatic and the nitrate. It eliminates the need for liquid reagents other than the aromatic precursor. The solid catalyst and nitrates are environmentally benign. However, the mechanism of nitration in this process is not yet well understood. Previous work [35, 36] explored the reaction of toluene and sodium nitrate, as shown in reaction (1), using molybdenum oxide as a catalyst. The effects of milling parameters, including the milling ball diameter, temperature, and milling time were initially characterized. The present experiments are focused on the catalyst acidity, surface area available, and distribution of the nitrate over the catalyst surface.

1.3. Experimental

Reactants and catalysts

Starting chemical reactants were toluene (Startex, solvent grade) and sodium nitrate (Alfa Aesar, 99%). Experiments were performed with a range of catalysts, which included metal oxides and zeolites listed in Table 1.1. The catalysts were chosen based on the nature of acid sites (considering categories described in the literature [37]) and overall acidity as reported in Refs. [37, 38]. The commercial availability of materials was also a factor when selecting catalysts in each category. Catalysts with minimal Bronsted acid sites (TiO_2 and Fe_2O_3) were considered to elucidate the effect of Lewis vs. Bronsted acid sites. Some active catalysts, such as CrO_3, were not included because of their toxicity and poor compatibility with the solvents. Because the minimum acid strength required to catalyze the reaction was not known a priori, tests were performed with materials with a broad range of acidities.

Table 1.1. Materials tested as catalysts for mechanochemical nitration of toluene

Material	Supplier and nominal purity	Relative Acidity, [38]	Type of acidity [37]
Molybdenum oxide, MoO_3	Alfa Aesar, 99.95 %	5.35	Medium Bronsted + Strong Lewis sites
Tungsten oxide, WO_3	Alfa Aesar, 99.95 %	5.05	
Vanadium oxide, V_2O_5	Acros organics, 99.6 %	4.54	
Manganese oxide, MnO_2	Alfa Aesar, 99.9 %	3.65	Not specified
γ- alumina, Al_2O_3	Alfa Aesar, 99.9 %	2.28	Strong Lewis sites*
Titanium oxide, TiO_2	Alfa Aesar, 99.9 %	3.05	Medium Lewis sites
Iron oxide, Fe_2O_3	Alfa Aesar, 99.5 %	2.5	
Bismuth oxide, Bi_2O_3	Alfa Aesar, 99 %		Medium Lewis + Basic sites**
Zeolite HZSM-5, Si/Al 38	ACS chemicals		Bronsted + Lewis sites**
Zeolite HZSM-5, Si/Al 360			

* Alumina phase was not specified in ref. [38]
** Acidity values not stated in literature

In preliminary experiments in which the products were extracted and analyzed as described below, only the three catalysts with the highest relative acidity, MoO_3, WO_3, and V_2O_5, were identified as generating detectable amounts of MNT. Further experiments focused on these three materials.

Surface area of the catalyst powders was measured by nitrogen adsorption using the Brunauer-Emmett-Teller (BET) method on a Quantochrome Instruments Autosorb IQ ASIQM000000-6. Surface area measurements were carried out also for the solid fraction extracted after milling. The powder was dried and degassed at 350 °C for 8 h to remove residual organics. Catalysts were also examined using x-ray diffraction (XRD). A Panalytical Empyrean x-ray diffractometer operated at 45 kV and 40 mA using unfiltered Cu K_α radiation (λ= 1.5438 Å) was used.

The effect of the catalyst surface area at the beginning of the reaction was tested by pre-milling the catalyst for a fixed time before adding the reactants toluene and sodium nitrate. The catalysts were pre-milled for 15, 30 and 120 minutes. In some experiments, as discussed further, the catalyst was pre-milled with sodium nitrate.

Following pre-milling, the reactants toluene and sodium nitrate (unless the nitrate was introduced during pre-milling) were added and milled further. The milling time with toluene following pre-milling is referred to as reaction time. In one series of experiments, catalysts powders were pre-milled for 15, 30, and, in some cases, 120 minutes; the toluene was then added and the reaction time was fixed at 30 minutes. In separate experiments, the reaction times varied between 15 and 45 minutes for both pre-milled and as-received catalyst powders. In yet another set of experiments using MoO_3 as a catalyst, the $NaNO_3$/toluene ratio was changed while fixing the amount of either

toluene or sodium nitrate and varying the amount of the other reactant; the reaction time was again fixed at 30 min. The same series of experiments was performed for sodium nitrate pre-milled with MoO_3 for up to 120 min.

Reaction Milling

Milling was carried out in a Retsch PM 400MA planetary mill. An air conditioner set at 15.5 ^{o}C was installed to cool the compartment containing the milling vials. The rotation direction was changed every 15 minutes and regular, 500-cm^3 hardened steel milling vials were used. For reactions using pre-milled catalysts, the vials were allowed to cool for 10 minutes before adding reactant(s). Milling parameters pre-set for the initial set of experiments are shown in Table 1.2 following Ref. [35]. The milling media, the mass of catalyst, ball to powder mass ratio, and milling speed shown in Table 1.2 were used throughout this study. The reaction time, mass of sodium nitrate and volume of toluene shown in Table 1.2 were used in most experiments; however, these parameters were varied in selected experiments.

Table 1.2. Milling parameters pre-set for initial experiments comparing different catalysts.

Used in all experiments				Varied in selected experiments, see text		
Milling Media (steel balls) diameter, mm	Ball to powder ratio	Milling speed (rpm)	Mass of catalyst (g)	Mass of sodium nitrate (g)	Volume of toluene (ml)	Reaction time (minutes)
12.7	3	350	41.63	1.67	0.5	30

Product extraction

The products were extracted using ethyl acetate (ACS, 99.8%), which dissolves MNT readily. Milling vials were opened in an argon-filled glovebox, 150 ml of ethyl acetate were added, and vials were closed and transferred back to the ball mill. The vials with added solvent were milled for one additional minute. Milling balls were separated from the resulting suspension using a No. 8 sieve (2.34 mm diameter openings). The suspension was allowed to settle for a day and centrifuged for 5 minutes in a LW Scientific Ultra 8F-centrifuge to remove all solids before its composition was analyzed using gas chromatography–mass spectrometry (GC-MS).

GC-MS analysis

The yield of MNT and formed by-products were quantified using an HP 6890 gas chromatograph. The injection port was held at 200 °C, and the column was heated to 250 °C at 5 °C /min. An HP G2350A mass spectrometer was used to identify the species evolved using the in-built NIST 08 Mass spectral library. In all experiments, xylene (solvent grade, by Sunnyside) was added to the solution as internal standard with a concentration of 4.06 mmol/L. A commercially available MNT, 4-nitrotoluene (Sigma Aldrich, 99%) served as an external standard to calibrate the GC-MS. A calibration curve was obtained comparing peak areas for MNT and xylene using a set of solutions with commercial MNT/xylene ratio varied from 0.2 to 2.2. The percentage of MNT present in a sample was calculated using the calibration curve.

The detection limit for the GC-MS system used is specified as 1 pg/µl for octafluoronaphthalene for the signal to noise ratio of 60. Assuming this detection limit to remain approximately similar for different compounds, for a 1-ml sample, 1 ng of the product of interest could be detected. The catalysts without recognizable peaks for MNT were thus assumed to generate less than 1 ng of MNT or have less than 0.000027 % yield.

Sources of errors and uncertainties

The inconsistencies in the reported results could be caused both by lack of reproducibility in the milling experiments and by measurement techniques used to characterize the nitration products. The reproducibility of the milling experiments could be affected by catalyst caked in selected runs, presence of iron impurities from the milling media, and slight differences between individual milling vials. These issues can be addressed by repeating multiple experiments. Indeed, some of our tests were repeated; in such cases, error bars showing standard deviations of results are shown. Generally, such error bars are smaller than the meaningful changes in the measured quantities reported and discussed here. Further reduction of the error bars could be achieved by additional experiments, which were outside the scope of this effort.

The errors in the concentration measurements are first associated with the efficiency of extraction of the reaction products. This efficiency is hard to access; however, the procedure used here was refined to achieve reproducible results in multiple repeated experiments performed in this and previous similar studies [35, 36]. The errors in GS-MS analysis can be assessed based on the relative standard deviation for selected repeated experiments as not exceeding 5% of the measured value for the signal to noise ratio of 60.

1.4. Results

In initial experiments, all catalysts listed in Table 1.1 were tested. DetecTable 1.yields of MNT were obtained only for MoO_3, WO_3, and V_2O_5. Accordingly, these catalysts were used for further experiments. The complete summary of results for all performed experiments is given in the supplement, Tables S1 – S3. Most important results are discussed here with more details provided.

Surface area and structure of catalysts

The specific surface area of the different catalysts as a function of pre-milling time is shown in Fig. 1.1. Longer pre-milling results in a greater surface area for all three oxides. The greatest increase in surface area was observed for pre-milled V_2O_5. The change in the surface area caused by milling correlates with mechanical properties of oxides. For example, bulk modulus values calculated using density functional theory (BLYP method) for WO_3, MoO_3 [39], and V_2O_5 [40] were 257, 195.7, and 87 GPa, respectively. Greater bulk moduli thus correlate with the slower surface area increase during milling. Note that the observed surface increase for MoO_3 is less significant if the reactant $NaNO_3$ is added (in the amount shown in Table 1.2) before pre-milling. Surface areas for the recovered solids were also measured after the mechanochemical nitration of

toluene. The results for all surface area measurements, before and after the reaction, are summarized in Table 1.3. For pre-milled oxides, a relatively minor change in the specific surface area after nitration runs is observed. In most cases, the surface area is somewhat decreased. Conversely, samples with pre-milled MoO_3 and $NaNO_3$ show a noticeable increase in the solids' surface area after the reaction.

Initial experiments were carried out to test the effect of pre-milling sodium nitrate with all three oxides, MoO_3, WO_3 and V_2O_5 on the nitration rate. Results of these experiments shown in the supplement, Table 1.S1 suggest that the MNT yield was higher for MoO_3 than for the other two oxides. Respectively, further experiments involving pre-milled sodium nitrate and catalyst focused on using MoO_3.

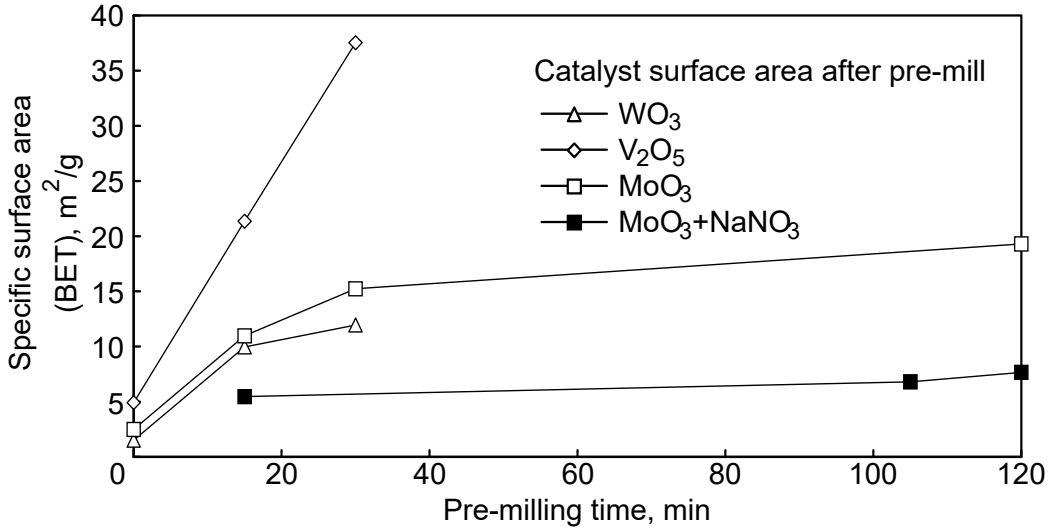

Figure 1.1. Specific surface area of different powders as a function of the pre-milling time

XRD patterns for several MoO_3- based powders used as catalysts are shown in Fig 2. The bottom pattern represents as-received MoO_3. The second and third patterns from the bottom show powders pre-milled for 15 and 30 min. Finally, the top three patterns show MoO_3 and $NaNO_3$ powders pre-milled for different times. With the increase in milling time, the MoO_3 peaks broaden suggesting a reduction in the crystallite sizes. No other changes in the XRD are noted, suggesting that any reaction occurring during pre-milling is negligible.

Table 1.3. Specific surface areas measured for different catalysts prior to mechanochemical nitration and for respective solids recovered after the reaction.

Catalyst	**Surface area, m^2/g**									
	Prior to reaction, pre-milling time, min					Reaction time: 30 min, pre-milling time, min				
	0	15	30	105	120	0	15	30	105	120
MoO_3	2.5	10.97	15.24		19.3	8.6	9.02	9.57		14.70
WO_3	1.5	9.96	11.96			5.7	7.14	9.20		
V_2O_5	4.91	21.35	37.54			37.54	26.65	34.12		
MoO_3 + $NaNO_3$		5.46		6.8	7.66		9.74		12.26	14.85

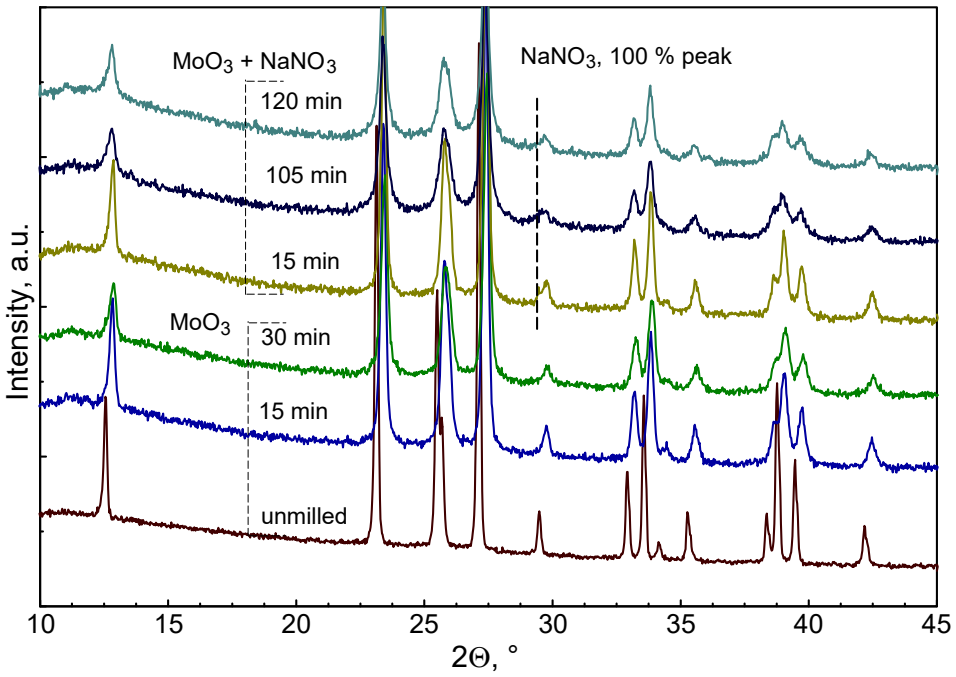

Figure 1.2. X-ray diffraction patterns for the catalyst powders based on MoO_3. The times shown are for pre-milling with or without added $NaNO_3$

Using Williamson-Hall method, crystallite sizes for some of the powders were evaluated as shown in Fig. 1.3. The reduction in the crystallite size is noted for MoO_3 milled with and without $NaNO_3$. Extended milling times, in excess of ca. 100 min do not lead to further reduction in the crystallite sizes.

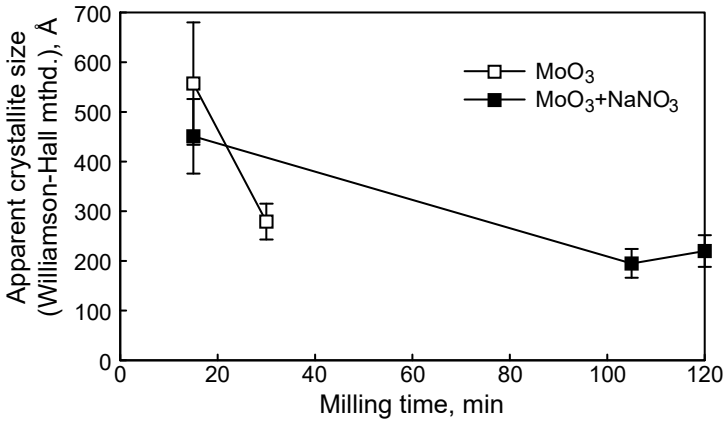

Figure 1.3. Apparent crystallite sizes for different catalyst powders as a function of the pre-milling time.

MNT production

Results for a set of nitration experiments with 30-min reaction time employing the as-received and pre-milled catalysts V_2O_5, WO_3, and MoO_3 are shown in Fig. 1.4. Yields are shown in Fig. 1.4a in terms of conversion of the initially used toluene. The yield is higher for MoO_3 while the yields for V_2O_5 and WO_3 are comparable to each other. For both, MoO_3 and V_2O_5, pre-milling results in increased yield. However, this trend is not as clearly observed for WO_3. The effect of acidity (quantified using the relative scale from Ref. [38], see Table 1.1) is not clearly observed either, at least comparing WO_3 and V_2O_5.

The same results are shown in Fig. 1.4b in terms of the absolute amount of MNT produced per unit of surface area of the catalyst. For this presentation, the surface areas were measured for solids recovered after the nitration runs (Table 1.3). Fig. 1.4b shows a clear correlation of amount of MNT produced and the catalyst's relative acidity.

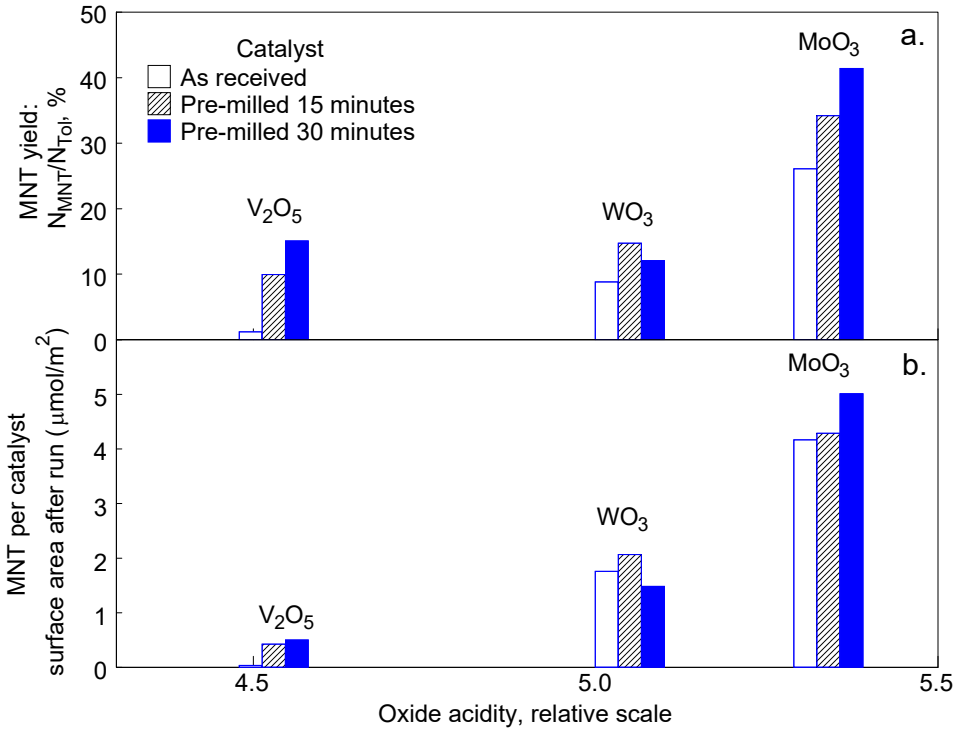

Figure 1.4. MNT yield for different catalysts plotted as a function of relative acidity scale: a. Yield of MNT; b. MNT normalized per catalyst surface area measured after run.

For MoO_3, showing the highest yield of MNT, the effect of pre-milling times longer than 30 min was further investigated. In addition, results compared yields of MNT for MoO_3 pre-milled with $NaNO_3$ for different times. These comparisons are shown in Fig. 1.5; as before, the reaction time was fixed at 30 min. Longer pre-milling does not result in significant increase in the surface area of MoO_3 (cf. Table 1.3). The MNT yield is lower at 120 min pre-milling despite nearly the same surface areas observed for the solids after reaction for pre-milling times of 30 and 120 min. Conversely, for MoO_3 pre-milled with $NaNO_3$, the yield increases with an increase in the pre-milling time (as does the surface area, cf. Table 1.2). The amount of MNT produced per unit of the surface area also increases, nearly linearly.

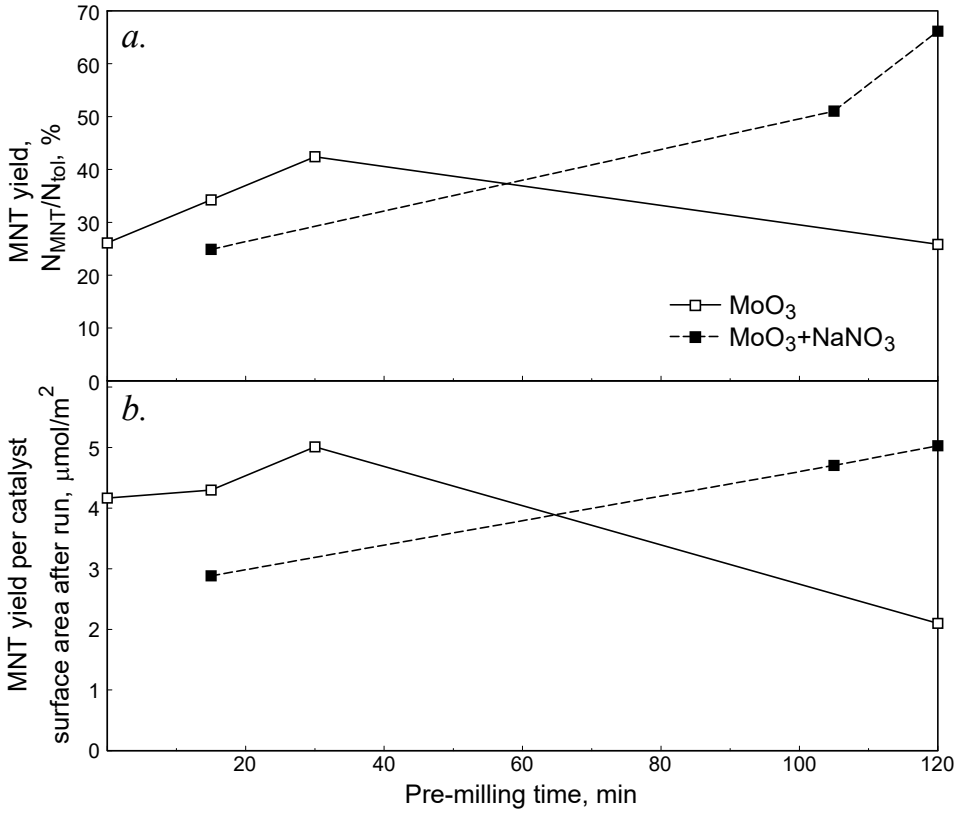

Figure 1.5. Effect of pre-milling time on MNT production: a. Yield; b. MNT normalized per catalyst surface area measured after run.

Effect of the reaction time on MNT yield

The effect of reaction time on MNT yield is shown in Fig. 1.6; the complete set of results is given in the supplement, Table 1.S2. The error bars representing the relative standard deviations are shown for selected repeated measurements. For other measurements, as mentioned above, the error is expected to be within 5 %. Both as-received and pre-milled catalyst powders were used. It is observed that for MoO_3 and WO_3, the effect of pre-milling the catalyst is negligible. For these catalysts, there is a general, rather weak trend of yield increasing with the reaction time. For MoO_3 pre-milled with $NaNO_3$, the results look qualitatively different. First, there is a significant yield observed even without milling, when the composite MoO_3/$NaNO_3$ catalyst is brought in contact with toluene. In this case, the product was agitated for one minute when it was being extracted with ethyl acetate. The yield increases with the reaction time very rapidly reaching a relatively stable plateau after 15 min. The absolute yield observed in these experiments exceeds significantly that observed when the catalyst was not pre-milled with $NaNO_3$. These results suggest that the distribution of the solid reactant $NaNO_3$ over the catalyst during milling limits the MNT formation rate in the present experiments, in which MoO_3 and $NaNO_3$ are not pre-milled together.

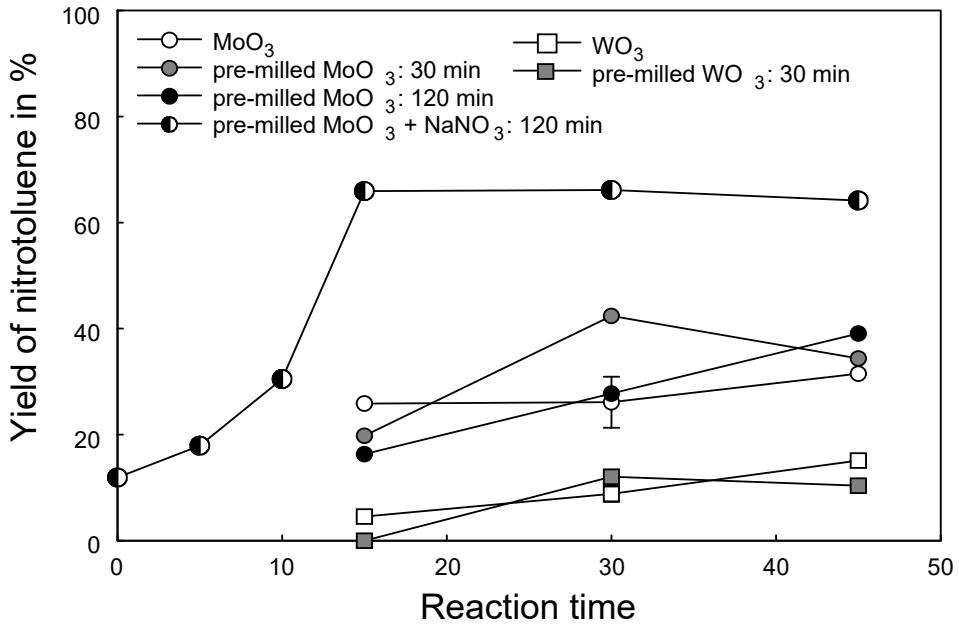

Figure 1.6. Effect of reaction time (milling pre-milled catalyst with toluene and $NaNO_3$) on yield of MNT.

Effect of reactant ratio on MNT yield and reaction selectivity

The effect of $NaNO_3$/toluene ratio on yield of MNT and on the reaction selectivity was investigated in three sets of experiments. First, the amount of toluene was kept constant at 1.5 ml and the amount of sodium nitrate varied from 0.305 to 4 g. Then, the amount of sodium nitrate was fixed at 1.67 g and the toluene amount varied from 0.1 to 8 ml. In both cases, pre-milled MoO_3 served as catalyst in the amount shown in Table 1.2. Figure 1.7 illustrates these experimental series. Finally, the third set of experiments used pre-milled $NaNO_3$ and MoO_3 (in the amounts shown in Table 1.2), and the amount of toluene varied from 0.305 to 4 g, just like in the first set. The complete set of results is shown in the supplement, Table 1.S3.

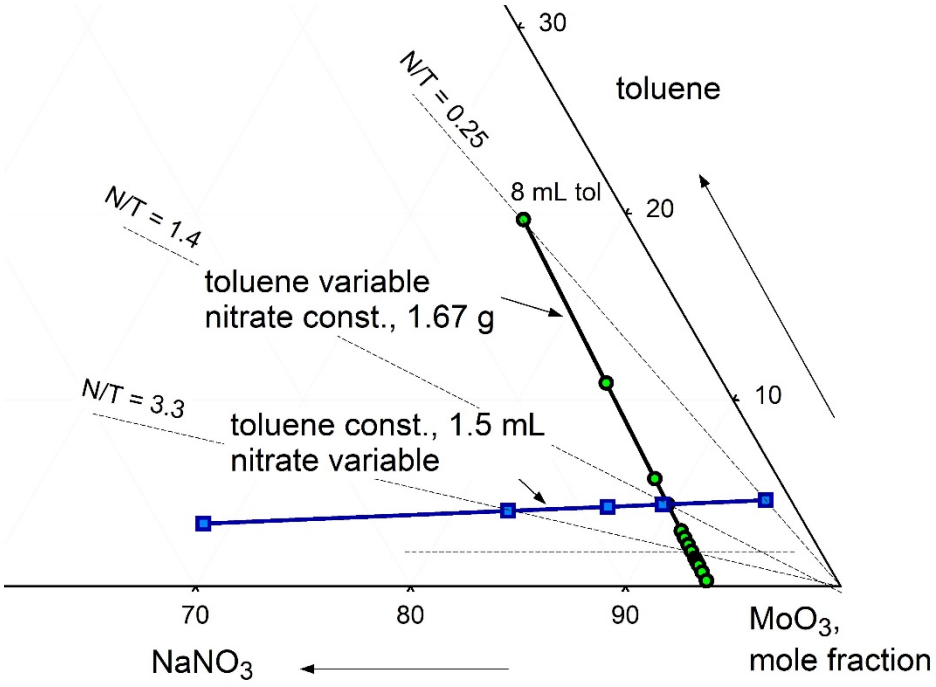

Figure 1.7. Ternary plot with the molar fractions of catalyst, nitrate and toluene

The results are shown in Fig. 1.8 in terms of MNT produced per surface area of the catalyst (measured after the run), para/ortho ratio for the produced MNT, and amount of benzaldehyde, a main byproduct of MNT oxidation observed in each run. In agreement with data shown in Fig. 1.6, the yield for the runs using $NaNO_3$ pre-milled with MoO_3 is much higher than for other conditions. In both cases where $NaNO_3$ was held constant and the amount of toluene varied, the maximum yield is observed for the nitrate to toluene mole ratio in the range of 2 – 5. At higher ratios, the amount of MNT produced gradually decreases. No similar effect could be clearly detected when the amount of toluene remained constant, while the same range of the nitrate to toluene ratios was covered. It is interesting that using $NaNO_3$ pre-milled with MoO_3 leads not only to a greater yield but also to a minimized amount of benzaldehyde, an undesirable byproduct. In other words, the production of benzaldehyde does not directly correlate with production of MNT. Finally, the p/o ratio clearly increases when toluene was the limiting reactant, i.e., for nitrate to toluene ratios of 1 or more. It is also greater for the runs with higher yield per surface area of the catalyst.

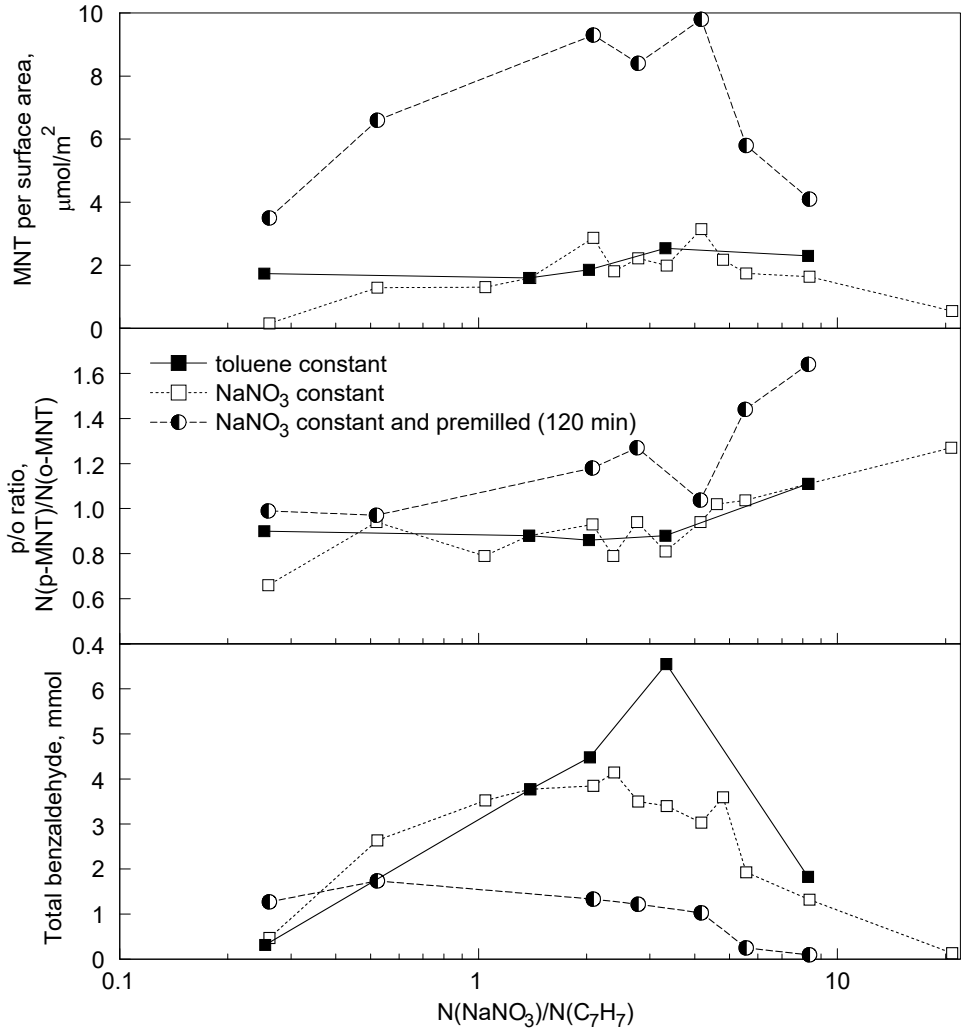

Figure 1.8. Effect of nitrate to toluene mole ratio on yield of MNT, benzaldehyde, and p/o ratio.

1.5. Discussion

Under the conditions tested here, toluene nitration occurred only for relative catalyst acidities of 4.5 and higher. Less acidic catalysts, including zeolites, showed no detectable nitration. The situation for zeolites may be confounded by the porosity restricting the bulk of the surface area [14]. For the three catalysts where nitration was observed (Fig. 1.4), the MNT yield scales with acidity and surface area of the catalyst.

The catalyst and the nitrate reactant are solids, and for toluene nitration to occur, all reactants and the catalyst must be brought in contact with each other. During milling, the reaction mixture homogenizes, the reactants are brought in contact with the catalyst, and the reaction (1) occurs. Under conditions where all reactants are introduced in the mill simultaneously, the amount of MNT produced increases with reaction milling time (Fig. 1.6). If, however, the nitrate and the catalyst are milled prior to reaction with toluene, the yield becomes remarkably high after a much shorter milling time compared to previous work [35]. After that short milling time, the

duration of reaction milling has virtually no effect on the amount of MNT observed after reaction.

The above observations strongly suggest that among all the conceivable processes occurring during milling, the distribution of the nitrate over the catalyst surface has been rate limiting for mechanochemical nitration in this, as well as in earlier work [35, 36].

Our results have several further implications. The near constant ~70 % yield of MNT observed after reaction with pre-milled $NaNO_3$ on the MoO_3 catalyst, even at short reaction times (Fig. 1.6), likely represents the maximum observable amount under the current milling and extraction conditions, and therefore full conversion of the toluene. Indeed, at the temperature of ca. 50 °C in the milling vial, the toluene vapor pressure is close to 0.13 bar. For the toluene load of 0.5 ml (Table 1.2), and vial volume of 500 cm^3, this would cause about 50 % of the loaded toluene to be in the gas phase, reacting less effectively. Estimating that approximately 10 % of toluene could have formed products other than MNT, e.g. benzaldehyde, or MNT that was not recovered, the full conversion of toluene is supported.

Further, the MNT formation over the pre-milled $NaNO_3$-MoO_3 catalyst is not instantaneous, suggesting that the distribution of toluene over the available catalysts surface occurs at a finite rate. This rate is likely affected by the milling intensity.

Additionally, the general notion that milling continuously generates fresh surface and therefore new catalytically active surface sites is challenged by the high yield observed when nitrate and catalyst are homogenized prior to reaction. Generation of additional catalytic surface sites appears to be secondary if the bulk of the nitrate is already in contact with the catalyst, and the gradual increase in MNT produced if all reactants are introduced at the same time is unlikely due to the generation of fresh catalyst surface.

It is finally of interest to understand the mechanism of nitration in this system, and initial guidance is given by results shown in Fig. 1.8. The results can be considered in the context of previous reports, essentially identifying two distinct reaction pathways for catalytic nitration of toluene [7, 41]. Toluene can be nitrated reacting with nitronium complexes attached to acid sites [7]. This preferentially produces the para isomer p-MNT. Conversely, toluene can be attached to a Lewis acid site prior to reaction [41, 42] forming para and ortho isomers in equal proportions. In the present experiments, the p/o ratio is generally high (Fig. 1.8), particularly for conditions when toluene amounts were reduced while pre-milled $NaNO_3$ and MoO_3 were used. This observation points out to a preferential reaction pathway of toluene reacting with nitronium complexes attached to the acid sites. It is interesting that both yield of MNT and p-MNT selectivity are reduced simultaneously when the amounts of toluene are increased. The trend is qualitatively similar, although it is less well resolved for the experiments using MoO_3 and $NaNO_3$ without pre-milling. An explanation can be that excess of toluene may be blocking acid sites preventing attachment or formation of nitronium. Furthermore, formation of nitronium also involves interaction of dissolved $NaNO_3$ with Bronsted acid sites similar to nitric acid [11, 32]; thus, blocked acid sites may lead to a less effective production of nitronium slowing down nitration occurring by both catalytic pathways.

The results shown in Fig. 1.8 for the formation of benzaldehyde suggest that it forms directly from toluene rather than from oxidized MNT. Indeed, such benzaldehyde formation accounting for toluene adsorbed to Lewis sites was described in Ref. [41]. This side reaction involving toluene adsorption onto the Lewis sites appears to be less favored with the pre-milled MoO_3 and $NaNO_3$ samples when amounts of the produced benzaldehyde are reduced. That is likely because $NaNO_3$ is well distributed for the samples containing pre-milled MoO_3 and $NaNO_3$ making fewer Lewis sites available to adsorb toluene. The effect is stronger for smaller amounts of toluene used, clearly because fewer toluene molecules remain available to be adsorbed and oxidized.

1.6. Conclusions

Effective mechanochemical nitration of toluene requires solid catalysts with high acidity and both, Bronsted and Lewis sites. Among several tested materials, molybdenum oxide was the preferred catalyst. High catalyst surface area available for mechanochemical nitration accelerates the reaction. When the catalyst and sodium nitrate are homogenized by a preliminary milling step, the reaction rate of the nitrate with toluene increases significantly. Nearly complete conversion of toluene to mononitrotoluene was readily achieved after the solid powders were homogenized. Effect of nitrate to toluene mole ratio and of the total amount of toluene used in the experiments on the yield, p/o ratio, and formation of byproducts suggests that the reaction primarily involves nitronium ions attached to acid sites of the catalyst. The amount of toluene in the reactor should be limited to avoid blocking catalyst's acid sites required to generate nitronium and later retain it at the catalyst surface prior to the nitration reaction.

1.7. SUPPLEMENTARY INFORMATION

The complete set of experimental results is reported in Tables 1.S1 – 1.S3.

Table 1.S1 . Nitration of 0.5 ml of toluene with 1.67 g of $NaNO_3$, 41.63 g catalyst, 30 min reaction time. Variables include the pre-milling time and the materials being pre-milled.

Pre-milled catalyst (and nitrate)	Pre-milling time, min	Amount of MNT, mmol	Yield of MNT, %	p/o ratio
MoO_3	0	1.23 ± 0.23	26.1± 4.83	1.01 ± 0.04
	15	1.61	34.2	0.81
	30	1.95	41.4	0.94
	120	1.31	27.76	0.81
WO_3	0	0.42 ± 0.07	8.83± 1.51	0.67 ± 0.22
	15	0.69	14.74	0.97
	30	0.57	12.06	0.78
V_2O_5	0	0.06	1.21	0
	15	0.47	9.95	0.68
	30	0.71	15.08	0.8
MoO_3+ $NaNO_3$	15	1.17	24.89	0.93
	105	2.4	51.05	1.02
	120	3.11	66.17	1.04
WO_3+$NaNO_3$	120	1.37	29.02	1.24
V_2O_5+$NaNO_3$	120	0.13	2.75	1.25

Table 1.S2 . Nitration of 0.5 ml of toluene with 1.67 g of $NaNO_3$, and 41.63 g catalyst for different catalysts, reaction times, and pre-milling-times

Pre-milled catalyst (and nitrate)	Pre-milling time, min	Reaction time, min	Amount of MNT, mmol	Yield of MNT, %	p/o ratio
MoO_3	30	15	0.39	8.39	1.01 ± 0.04
		30	1.95	41.4	0.81
		45	1.66	35.24	0.94
WO_3	30	15	0.24	5.2	0.67 ± 0.22
		30	0.69	12.06	0.97
		45	0.67	14.28	0.78
MoO_3+ $NaNO_3$	120	0	0.56	11.9	1.3

		5	0.84	17.93	1.27
		10	1.43	30.5	1.34
		15	3.1	65.95	1.35
		30	3.11	66.16	1.04
		45	3.02	64.16	1.42

Table 1.S3. Nitration of toluene with sodium nitrate, 41.63 g of catalyst, reaction time 30 min. Effect of variation of the $NaNO_3$ to toluene mole ratio and pre-milling time.

Pre-milled catalyst (and nitrate)	Pre-milling time, min	Volume of toluene, ml	Mass of sodium nitrate, g	Amount of MNT, mmol	Yield of MNT, %	p/o ratio
MoO_3	30	0.1	1.67	0.35	37.22	1.27
		0.25	1.67	1.04	44.2	1.11
		0.375	1.67	1.11	31.37	1.037
		0.45	1.67	1.38	33.52	1.02
		0.625	1.67	1.27	21.51	0.81
		0.75	1.67	1.41	19.99	0.94
		0.875	1.67	1.15	13.98	0.79
		1	1.67	1.82	19.35	0.93
		1.5	1.67	1.013	7.18	0.88
		2	1.67	0.830	4.402	0.79
		4	1.67	0.82	2.17	0.94
		8	1.67	0.098	0.13	0.66
		1.5	0.305	1.10	7.8	0.9
			1.67	1.013	7.18	0.88
			2.405	1.18	8.36	0.86
			4	1.61	11.43	0.88
			10	1.46	10.34	1.11
MoO_3+ $NaNO_3$	120	0.25	1.67	1.3	55.3	1.64
		0.375	1.67	1.85	52.4	1.44
		0.5	1.67	3.11	66.17	1.038
		0.75	1.67	2.67	37.84	1.27
		1	1.67	2.98	31.69	1.18
		4	1.67	2.12	5.63	0.97
		8	1.67	1.11	1.48	0.99

Chapter 2: Parameters affecting mechanochemical nitration of aromatic precursors

2.1. Abstract

Using MoO_3 as catalyst and $NaNO_3$ as nitronium source, aromatic precursors were nitrated in a planetary ball mill. Reaction times and nitrate/precursor molar ratios varied in the experiments. Nitration was observed with maximum yields approaching 80 %. Product ratios of para to ortho isomers were consistently above 1, indicating reaction on the catalyst surface. Byproducts, including oxidation products and double nitration products, were observed. The product yield approached its theoretical maximum when the aromatic precursor was the limiting reactant; the yields remained well below their expected maxima when the limiting reactant was nitrate. Thus, the catalyst sites necessary to generate nitronium may be blocked by the excess of the aromatic precursor in such cases. Correlation of the reaction rates with characteristics of the precursors suggests the importance of both physical and chemical parameters. Factors affecting the reaction rate include the aromatic activation, basicity, enthalpy of vaporization, reaction enthalpies and viscosity.

2.2. Introduction

Nitroaromatics have wide ranging applications in pharmaceuticals [47], dyes [48], and energetics [49]. The most common method of nitration of aromatics involving mixed acids is associated with a number of drawbacks, namely low selectivity, generation of toxic acid waste and NO_x fumes [50]. The separation and disposal of the produced waste is expensive [51]. With an increased demand for green chemistry methods [52], there has been significant interest in developing solvent-free alternatives. Such solvent-free nitration methods need to produce minimal waste while being compatible with a range of precursors.

Several approaches have been explored recently. Heterogeneous solid catalysts with surface acid sites capable of generating NO_2^+ (nitronium) ions required for nitration have been used with a range of aromatics [51, 53]. Advantages of solid catalysts are the easy separation of the product and reduced quantities of hazardous waste [54]. Solid catalysts also provide para-selective products [53]. For example, for toluene, anisole and chlorobenzene, the para isomers of nitro products are more widely used in applications; hence, an enhanced selectivity is equivalent to an improved productivity. Solid catalysts have been used in both gas-solid and liquid-solid configurations; most commonly results are reported for silica-supported metal oxides, such as MoO_3 [55] and WO_3 [56], and zeolites, including HZSM-5 [57].

Solid catalysts with liquid nitric acid have been used for nitration of chlorobenzene [58], benzene[59], toluene [51, 60], anisole [1] and xylene [61, 62]. Improved para-selectivity has been reported for anisole [1], toluene [60], and chlorobenzene [58] when compared to liquid phase nitration. However, the products contain nitric acid diluted with water, and the contaminated water needs to be separated and disposed of.

Nitration was reported using vaporized nitric acid [63-65] to provide an easier separation of products in gas phase. However, water still is produced making it difficult to design a clean gas-phase separation process.

Solid acid catalysts have also been used with liquid NO_2/N_2O_5 systems for benzene [56, 66, 67], toluene [68] and chlorobenzene [69], eliminating the use of harsh acids. Nitration with high selectivities has been reported. While being solvent-free, related nitration reactions require low temperatures (0^oC) to function effectively.

Combining solid catalysts with solid sources of nitronium ions can remove the need for low temperatures while providing an easy separation of products and eliminating the use of solvents. Only a few studies dealt with purely solid based systems. Initial tests used a clay-supported copper nitrate ("claycop") with montmorillonite clay [70]. Phenol, anisole and cresol were nitrated using ceric ammonium nitrate on pillared clay [71]. While reasonable yields were achieved, use of harmful solvents such as CCl_4 and $CHCl_3$ was necessary making the approach environmentally objectionable.

Recently, mechanochemical reactions has been used to nitrate a broad range of aromatics [72], [73, 74]. Bismuth nitrate and magnesium sulfate were used in Ref. [72] with a diverse group of precursors. Using sodium nitrate serving as a nitronium source and molybdenum oxide catalyst, solvent-free mechanochemical nitration of toluene was reported with high selectivity and yield [73, 74]. More recently, it was found that effective mechanochemical nitration of toluene requires solid catalysts with a high acidity and presence of both Bronsted and Lewis acid sites [75]. Among several tested materials, molybdenum oxide was the preferred catalyst. When the catalyst and sodium nitrate were homogenized by a preliminary milling step, the reaction rate of the nitrate with toluene during subsequent milling increased significantly, approaching the complete conversion of toluene to mononitrotoluene. Effect of nitrate to toluene mole ratio and of the total amount of toluene used in the experiments on the yield, para/ortho isomer (p/o) ratio, and formed byproducts suggested that the reaction primarily involves nitronium ions attached to Bronsted acid sites of the catalyst. It was reported that the amount of toluene in the reactor should be limited to avoid blocking catalyst's acid sites, which are required to generate nitronium and later retain it at the catalyst surface leading to the nitration reaction.

The current work investigates systematic trends in nitration behavior across several aromatic precursors. The goal is to identify characteristics of the precursors affecting their nitration, which will enhance our understanding of the physical and chemical processes leading to mechanochemical nitration of organic compounds [65].

2.3. Experimental

Materials

Sodium nitrate (Alfa Aesar, 99 %) was used as the nitrating source and molybdenum oxide (Alfa Aesar, 99.95%) served as catalyst. The precursors included benzene (Sigma-Aldrich, 99.8%), toluene (Startex, solvent grade), chlorobenzene (Acros organics, 99.8%), ethyl benzene (Acros

organics, 99.8%), p-xylene(Sigma-Aldrich, 99%), 4-nitrotoluene(Sigma-Aldrich, 99%), anisole(Alfa Aesar, 99%) and phenol(ACS reagent, 99 %). Based on the functional group present, the reactivity and selectivity of the ring can change [76]. Some of the functional groups, $-CH_3$ (toluene and xylene), $-CH_2-CH_3$ (ethylbenzene), $-O-CH_3$ (anisole), and -OH (phenol) were expected to activate the aromatic ring, while others, -Cl (chlorobenzene) and $-NO_2$ (mononitrotoluene) were expected to deactivate the ring towards electrophilic nitration [77, 78]. Some of the aromatics, while being activating can also get oxidized easily.

Properties of the precursors that could potentially affect their mechanochemical nitration are included in Table 2.1. Most directly, the rate of nitration is expected to be affected by the relative activation quantified for reaction rates k over the reaction rate for benzene, k_H, using the Hammett equation [78]

$$\rho \cdot \sigma = log_{10}\left(\frac{k}{k_H}\right) \qquad (1)$$

where σ is the substituent constant and ρ is the reaction constant. Values for these parameters were taken from [77, 78]. These changes in k compared to k_H represent the inductive and resonance effects of the functional groups by means of a free energy relationship [79]. The rate of nitration is expected to be further affected by the heats of formation of precursor, $\Delta H_f(P)$, and of the nitroproducts, $\Delta H_f(NP)$.

Independent of chemical properties, mechanochemical nitration may be influenced by physical properties and physical interaction between precursor and catalyst. Specifically, the distribution of the precursor over the catalyst surface is affected by the precursor's density, dynamic and kinematic viscosity, dipole moment, and by how much of the precursor is present as gas vs. condensed phase. The latter is expressed here via the heat of vaporization.

A third group of parameters considered describes chemical interactions of precursors with the catalyst. These parameters include steric factors, proton affinity, gas basicity, and ionization energy. Steric factors may influence the orientation of the precursor molecules at the catalyst surface and affect regioselectivity. Proton affinities and basicity are defined as the enthalpy and free energy of a protonation reaction respectively. These parameters may have affected interactions of the precursors with the weakly bonded hydrogen groups on the surface of the catalyst. Similarly, ionization energy might be affecting how readily the precursor molecules can lose electrons and adhere to catalyst's acid sites.

Table 2.1. Precursors used and their properties [80] that could affect their mechanochemical nitration.

Precursor	Functional group	Relative rate log(k/k_H) [77]	ΔH_f(P) [81-83]	ΔH_f(NP) [84-86]	Kinematic viscosity [87, 88]	Density, ρ[80]	Dynamic viscosity η [87, 88]	ΔH_{vap}(P) [89]	Dipole moment [90]	Steric A-value [91]	Ligand repulsive energies [91]	Proton affinity [92]	Gas basicity [92]	Ionization energy [92]
			kJ/mol	kJ/mol	mm^2/s	g/mL	cP	kJ/mol	Debye	kcal/mol	kcal/mol	kJ/mol	kJ/mol	eV
Nitrotoluene	NO_2	-3.72	-48.2	-66.4	solid	1.1	solid	74.8	1.35	1.10	18	815.2	782.7	9.46
Chlorobenzene	Cl	-0.66	11.5	-48.74	0.92	1.11	1.021	41	1.69	0.53	3.3	753.1	724.6	9.07
Benzene	H	0	49	12.5	0.647	0.876	0.567	33.9	0	0	0	750	725.4	9.24
Ethyl benzene	C_2H_5	0.90	27	-13.22	0.669	0.866	0.579	41	0.59	1.79	34	788	760.3	8.77
Toluene	CH_3	1.02	12	-48.2	0.62	0.867	0.538	37	0.332	1.74	17	784	756.3	8.83
p-Xylene	$(CH_3)_2$	2.04	-24.4	-5.62	0.93	0.86	0.800	42	0	3.48	34	812.1	766.8	8.44
Phenol	OH	2.22	-165	-207	solid	1.07	solid	69.7	1.224	0.60	10	817.3	786.3	8.49
Anisole	OCH_3	4.68	-120	-197	0.99	0.995	0.985	44	1.262	0.75	31	839.6	807.2	8.20

Milling process

A Retsch PM 400MA planetary mill was used for the experiments. The mill was equipped with an air conditioner cooling the compartment containing the milling vials. The rotation direction was changed every 15 minutes and regular, 500-ml hardened steel milling vials were used. Milling parameters were based on previous experiments [74]. Details are summarized in Table 2.2. The MoO_3 catalyst and $NaNO_3$ were milled without any additional process control agent for 120 minutes in order to reduce catalyst particle sizes and distribute the nitrate over the catalyst surface. After this initial step, the vials were cooled for 10 min. The milling vials were then opened briefly, and the precursor was added.

The milling time was systematically varied for all precursors. For these experiments, the volume of the precursor was fixed at 0.5 mL. Additionally, 0.5 mL of the precursor were also added to separate batches of premilled catalyst and nitrate in order to determine how much reaction takes

place without any milling at all. In a separate set of experiments, the amount of the precursor was systematically varied for benzene and chlorobenzene.

Table 2.2. Milling parameters used for testing different precursors

Used in all experiments					Varied in selected experiments, see text	
Milling Media (steel balls) diameter, mm	Ball to powder ratio	Milling speed (rpm)	Mass of MoO_3 (g)	Mass of sodium nitrate (g)	Volume of precursor (ml)	Reaction time (minutes)
6.35	3	350	41.63	1.67	0.25-8	1 - 30

Product extraction

The products were extracted using ethyl acetate (ACS, 99.8%), which readily dissolves the precursors and nitrated products tested. The milling vials were opened in a chemical fume hood. Ethyl acetate (150 ml) was added to each vial. The vials were placed back in the mill and milled for an additional 1 min. Milling balls were separated from the resulting suspension using a sieve with 2.34-mm diameter openings. The suspension was allowed to settle for a day and centrifuged for 5 minutes in a LW Scientific Ultra 8F-centrifuge to remove all solids before analysis.

Product analysis

The yields of nitro products and formed by-products were quantified by gas chromatography–mass spectrometry (GC-MS) using an HP 6890 gas chromatograph. The injection port was held at 200 °C, and the column was heated to 250 °C at 5 °C /min. An HP G2350A mass spectrometer was used to identify the species evolved using the built-in NIST 08 Mass spectral library. In all experiments, xylene (Sunnyside, solvent-grade) was added to the solution as an internal standard with a concentration of 4.06 mmol/L. The standards used to calibrate the measurements of the formed nitro-products are listed in Table 2.3. A calibration curve was obtained comparing peak areas for each nitro-product and xylene using a set of solutions with commercial nitro-product/xylene ratios varied from 0.2 to 2.2.

Table 2.3. Standards used to calibrate measurements of different nitro-products

Precursor	External standard for the nitro-product	Supplier and purity
Chlorobenzene	1-chloro-2-nitrobenzene	Acros organics, 99%
Benzene	Nitrobenzene	ACS, 99%
Ethyl benzene	4-ethylnitrobenzene	TCI America, 99%
Toluene	4-nitrotoluene	Sigma Aldrich, 99%
p-Xylene	3-nitro-o-xylene	Alfa aesar, 99%
Anisole	2-nitroanisole	Sigma Aldrich, 99%
Phenol	4-nitrophenol	Alfa Aesar, 99%

2.4. Results

Effect of milling time on yield of nitro-products

Yields of nitro-product for different precursors as a function of the reaction time are shown in Fig. 2.1. As expected, the yield initially increases with time. Some precursors show a decrease in yield at longer times. The highest initial reaction rate is observed for anisole, which is also the most activated precursor, see Table 2.1. No detectable yield is observed for nitrotoluene, which is the most de-activated precursor used. However, the activation does not directly scale with the observed initial reaction rate for all precursors. Toluene and ethylbenzene, activated more than benzene and chlorobenzene (Table 2.1), show the lowest initial reaction rates based on the 5 min milling runs. The decay in the yield after 6 minutes is observed for anisole and p-xylene. For other precursors, the yield of nitro-products continues to increase with time, although at a consistently lower rate.

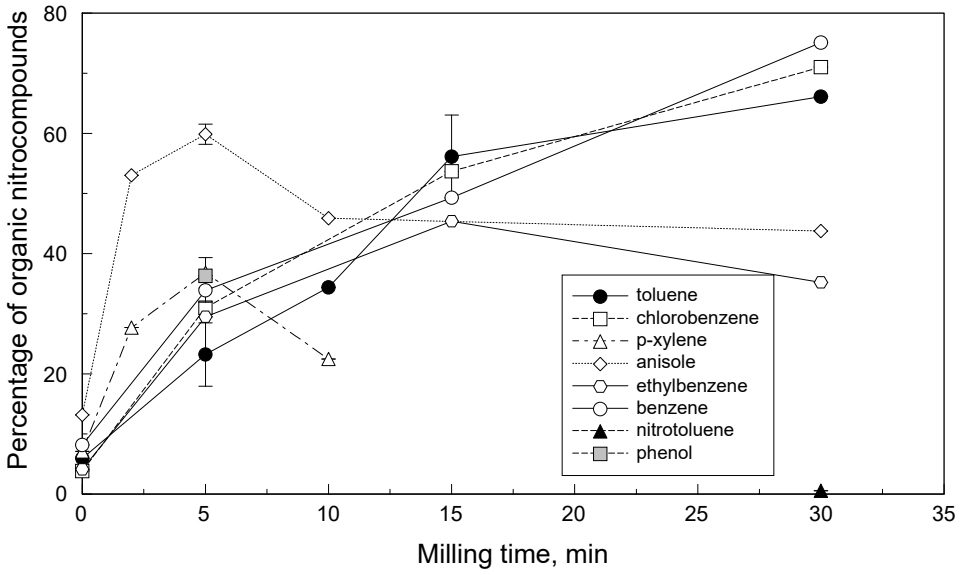

Figure 2.1. Nitration of activated and deactivated aromatic precursors as a function of the reaction milling time.

Regioselectivity

For precursors capable of forming para and ortho isomers of the nitroproduct, the regioselectivity as a function of milling time is shown in Fig. 2.2. Anisole showed an unusually strong increase in selective production of the para isomer of nitroanisole at 30 minutes, when the p/o ratio exceeds 6. For other precursors, the regioselectivity did not change with time appreciably. The effect of the different functional groups on the selectivity suggests that Cl results in a higher para selectivity than CH_3 and C_2H_5. The unusual effect of OCH_3 probably deserves further study.

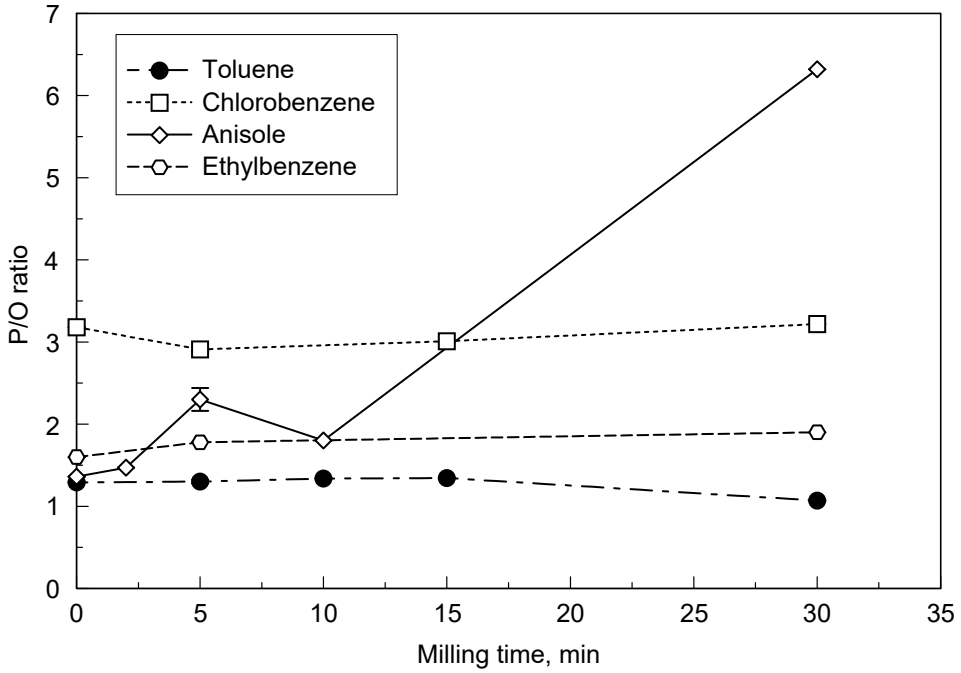

Figure 2.2. Regioselectivity changes as a function of the milling time for nitration of different aromatic precursors.

Effect of the amount of the loaded precursor

In previous work [75] the effect of toluene to nitrate ratio on the yield of mononitrotoluene was characterized. Similar measurements were performed here for benzene and chlorobenzene. In all cases, the reaction milling time was 30 min. The amount of precursor used varied from 0.25 to 8 ml, while the amount of $NaNO_3$ was fixed at 1.67 g. Results are shown in Fig. 2.3, where level of $NaNO_3$ is shown for reference and data for toluene from Ref. [75] are also included for completeness. Additionally, unreacted benzene and chlorobenzene were quantified; these results are also shown in Fig. 2.3. Finally, dinitrated byproducts were quantified for chlorobenzene; these are also shown in Fig. 2.3 and discussed in the next section.

In all cases, the reaction seems to be limited by the amount of precursor available at the high nitrate to precursor ratio. Thus, the yields approach their theoretical maxima. Conversely, for small nitrate to precursor ratios, where the reaction yield might have been limited by the available nitrate, the actual yields are much smaller than their theoretical limits. The peaks observed varied slightly between precursors but fall in the range of reactant ratios of 3-6.

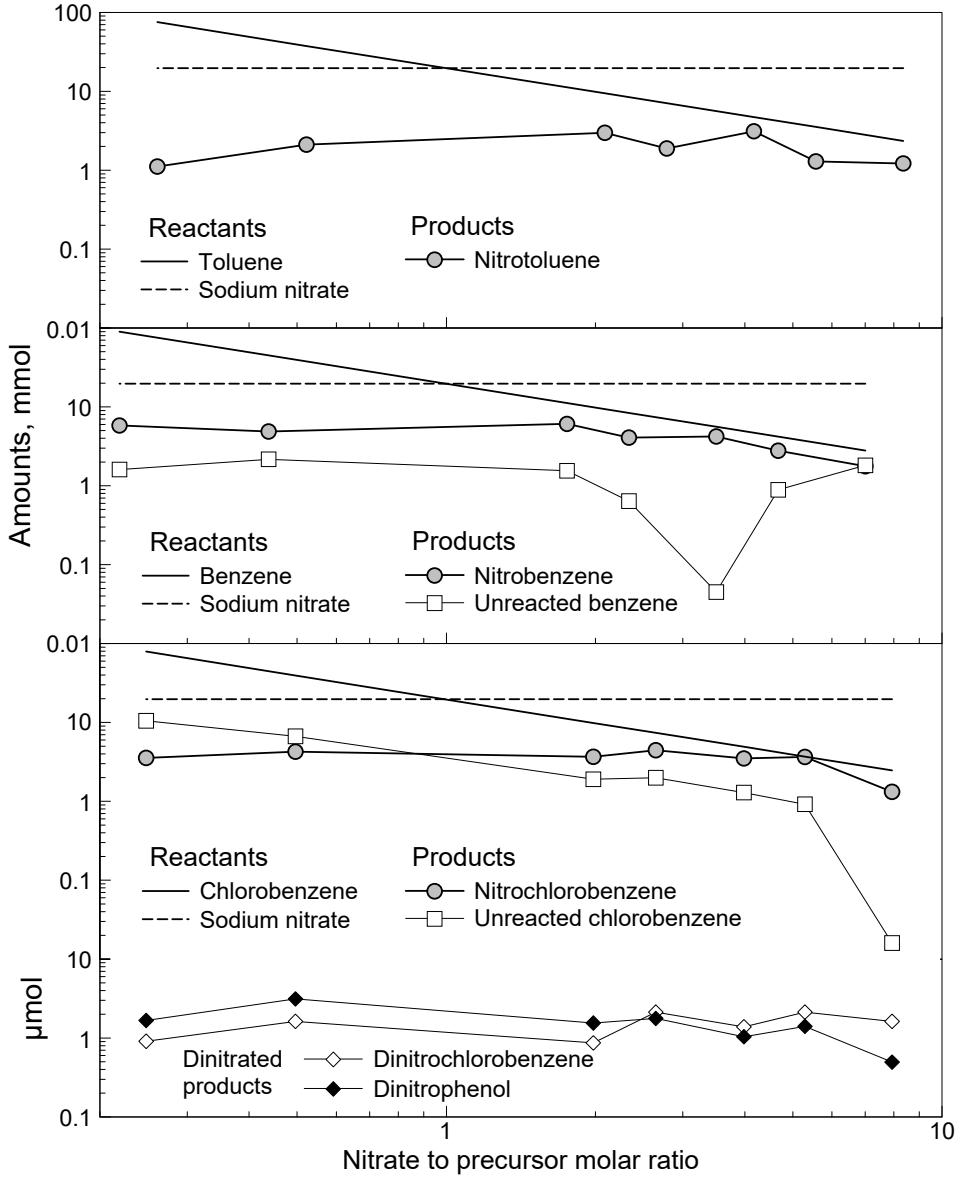

Figure 2.3. Yields of different products as a function of the nitrate to precursor molar ratio for toluene, benzene, and chlorobenzene.

The nitro-products obtained in experiments shown in Fig. 2.3 were examined for regioselectivity for both toluene and chlorobenzene. These results are shown in Fig. 2.4. In both cases, the selectivity increases at higher nitrate to precursor ratio, when relative yields increase also.

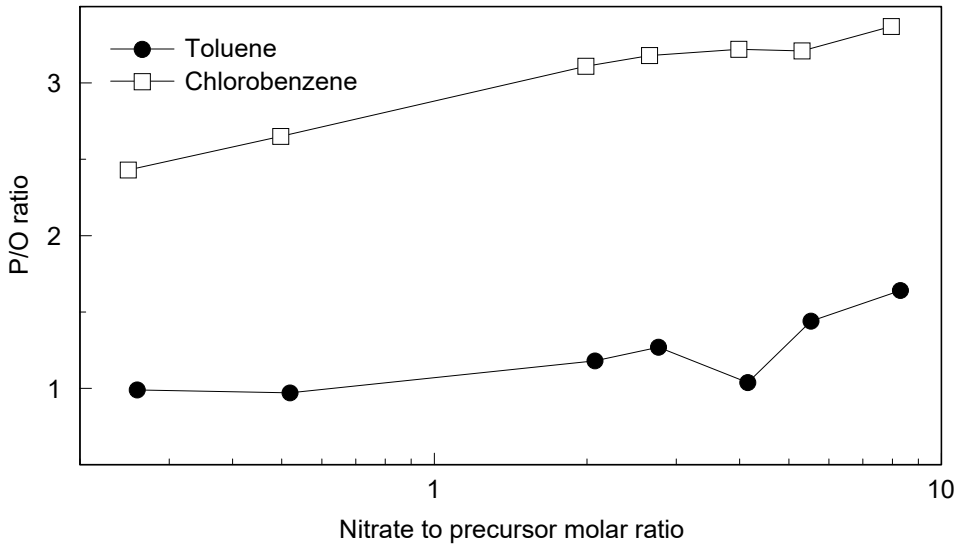

Figure 2.4. Regioselectivity changes for mono nitro toluene and chlorobenzene as a function of nitrate to precursor molar ratio.

Dinitrated and oxidized byproducts

As further illustrated in Fig. 2.3, low concentrations of dinitrated products were observed for chlorobenzene. These included 2,4 dinitrochlorobenzene and 2,6 dinitrochlorobenzene as well 4,6 dinitrophenol along with small traces of 2-chloro 3,5 dinitrophenol. Formation of dinitrophenols suggest that oxidation of dinitroproducts or further nitration and oxidation of nitroproducts has occurred. The oxidation was more significant for the experiments with lower nitrate to precursor ratios. Consistent amounts of 2,4 dinitrochlorobenzene were observed at all molar ratios. The observed dinitroproducts consumed 0.03-0.1 % of the initial chlorobenzene. The changes in the nitroproduct yield with the nitrate to precursor ratios are generally following the changes in the mono-nitrated products.

Although formation of dinitroproducts was not specifically targeted in present experiments,small traces of dinitroproducts were noted to form for all the aromatics tested, as shown in Table 2.4.

Table 2.4. Dinitroproducts observed in experiments

Precursor	Dinitroproduct	Reaction time, min	Total yields, %
Toluene	1-methyl-2,4 dinitrobenzene 1-methyl-4,6 dinitrobenzene 1-methyl-2,6 dinitrobenzene	16	0.03
Benzene	1,3 dinitrobenzene	16	0.029
Ethyl benzene	1-ethyl-2,4 dinitrobenzene	16	0.019
Chlorobenzene	1-chloro 2,4 dinitrobenzene 1-chloro 2,6 dinitrobenzene 1-chloro 2,5 dinitrobenzene	16	0.03
Anisole	1-methoxy 2,4 dinitrobenzene	1	0.025
p-xylene	1,4-dimethyl-2,6 dinitrobenzene	1	0.024

The selective nature of the functional groups (resonance effects) is seen with attachment of the nitro group in either the para or ortho position for all the precursors except benzene. 1,3 dinitrobenzene is formed, which could be attributed to the meta-directing nature of the NO_2 group in nitrobenzene.

Toluene, ethyl benzene and p-xylene, which contain oxidizable functional groups show immediate oxidation of the functional group to benzaldehyde, acetophenone and methyl benzaldehyde respectively as shown in Table 2.5. The mechanism of benzaldehyde formation through interaction of toluene with the metal oxide Lewis sites has been described previously [93]. A similar mechanism is expected to oxidize ethylbenzene [94] and p-xylene. The influence of the oxidation side reaction could explain the drops in nitration rates observed at longer times in Fig. 2.1 for ethyl benzene and p-xylene.

Table 2.5. List of oxidation and nitro by-products

Precursor	Oxidation by-products	Nitro by-products	Dinitro by-products
Toluene	Benzaldehyde	3-nitro benzaldehyde 4-nitro benzaldehyde	2,4 dinitrophenol
Benzene	None	None	2,4 dinitrophenol
Ethyl benzene	Acetophenone Methyl benzaldehyde	4-nitro acetophenone	4,6 dinitrophenol
Chlorobenzene	None	None	4,6 dinitrophenol
Anisole	None	4-nitro phenol	4,6 dinitrophenol
p-xylene	Methyl benzaldehyde Benzaldehyde	3-nitro benzaldehyde	4,6 dinitrophenol

2.5. Correlation of nitration rates with properties of aromatic precursors

To examine the relevance of physical and chemical characteristics of the various precursors shown in Table 2.1 for the formation of nitroproducts, the reaction in the milling vial was described as a first-order process. The simplified nitration reaction is therefore

$$P \longrightarrow NP \tag{2}$$

with a reaction rate r_P that depends only on the reaction rate constant, k, and precursor concentration, C_P:

$$r_P = -k \cdot C_P \,. \tag{3}$$

However, the precursor concentration C_P remaining after extraction could not reliably be determined for all cases. Instead, initial precursor concentration, $C_{P,0}$ was known, so that C_P was estimated based on the concentration of the nitrated product, C_{NP}, and neglecting all byproducts or any other losses:

$$C_P = C_{P,0} - C_{NP} \,. \tag{4}$$

Because of this simplified treatment, only observations with an increase in C_{NP} were useful for the following analysis. Observations with a decrease in C_{NP} (e.g., p-xylene at 10 min, or ethylbenzene at 30 min, see Fig. 2.1) were excluded.

Treating the milling container as batch reactor with constant volume, V, the molar balance becomes:

$$r_P V = dN_P / dt \tag{5}$$

where N_P is the molar amount of nitroproducts, and assuming N= C·V. Substituting Eq. (3) into Eq. (5) yields:

$$-k \cdot C_P = dC_P / dt \tag{6}$$

Introducing the reaction progress X, and approximating it in terms of the nitroproduct concentrations,

$$X = 1 - C_P / C_{P,0} \approx C_{NP} / C_{P,0} \tag{7}$$

Equation (6) is reduced to:

$$k(1 - X) = dX / dt \,, \tag{8}$$

Integrating Eq. (8) produces:

$$kt = -\ln(1 - X) \,. \tag{9}$$

For each precursor, and different milling times, reaction rate constants k were therefore determined as:

$$k = -\ln(1 - X)/t = -\ln(1 - C_{NP} / C_{P,0})/t \tag{10}$$

The reaction rates were then tested for correlation with the parameters ζ_i shown in Table 2.1, using the following relationship:

$$\ln(k) = \ln(k_0) + \sum_i a_i \cdot \zeta_i \qquad (11)$$

The coefficients a_i were determined by multivariate least-squares fitting. Since there are more parameters ζ_i than precursors ($n_P = 6$), a selection must be made as to which parameters ζ_i to consider. On the other hand, there was no a-priori ranking of parameters, and all should be evaluated. To resolve this, all possible combinations of ($n_P - 1 = 5$) or fewer parameters were evaluated. This approach results in a large number of possible parameter combinations, some of which are not physically meaningful. Combinations of closely related parameters were therefore removed from consideration. This includes simultaneous occurrences of gas basicity and proton affinity, kinematic and dynamic viscosity, and the two descriptors of steric effects. With these combinations removed, 1120 possible parameter combinations remain, and were fitted to the data. The results of these model fits were compared against each other using AIC_C, the Akaike information criterion modified for small sample sizes [95]. This parameter calculates the log-likelihood function and applies a penalty based on the number of adjustable parameters used to achieve the fit. The model with the lowest AIC_C value is considered the most prudent, achieving the best fit while using the fewest adjustable parameters. An overview is shown in Fig. 2.5.

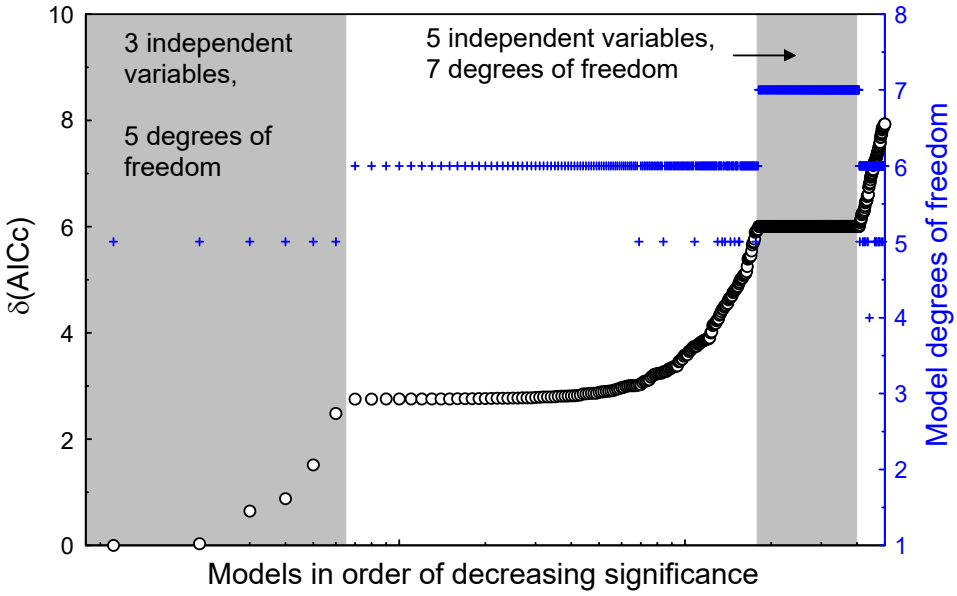

Figure 2.5. Distribution of AICC values of models

Table 2.6 shows the first 12 results of this procedure in order of increasing $\delta_{AIC_C} = AIC_C - \min(AIC_C)$. The first column shows the constant, $\ln(k_0)$, in Eq. (11). Columns 2-14 show the coefficients a_i obtained by the fit corresponding to the parameters ζ_i from Table 2.1. Blank cells indicate that the corresponding parameter was not used in this model. The last two columns show δ-AIC_C and a derived weight associated with each linear model. The

weights, decreasing with increasing δ-AIC_C, were determined from the model likelihood, using the implementation of the R MuMIn library [96]. Differences between the δ-AIC_C values are small, and after the 7th model, δ-AIC_C plateaus. The third column shows weights associated with each model. The weights represent the relative likelihood of the model with a weight of 1.0 being the most likely. These weights decrease as AIC_C increases. Models with greater associated weights are more predictive. The sum of model weights for individual parameters can be taken as an indicator of their relative importance as predictors.

The first two models are statistically nearly equally likely. One describes the observations in terms of the activation parameter ln(k/k_H), the gas basicity and the enthalpy of evaporation of the precursor, while the other uses the enthalpy of formation of the precursor, the enthalpy of formation of the nitrated product and one descriptor of the steric hindrance of the functional group of the precursor. The top two models have no parameter in common, but are both plausible. The relative rate is expected to be important since the values directly correspond to reaction rates observed. Similarly the heat of formation of precursor and product directly corresponds to the energy balance of the reaction.

Table 2.6. The first 12 results of least-squares model fitting against a set of precursor properties, in order of increasing δ-AICC

ln(k_0)	Dipole moment[90]	Dynamic viscosity, η [87, 88]	Ionization energy [92]	Gas basicity [92]	ΔH_{vap}(P) [89]	ΔH_f(P) [81-83]	ΔH_f(NP) [84-86]	Relative rate, log(k/k_H) [77]	Kinematic viscosity, ν [87, 88]	Proton affinity [92]	Density, ρ [80]	Steric A-value [91]	Ligand repulsive energies [91]	δ-AIC_C	model weight, % [96]
	coefficients a_i														
31.8				-0.051	0.074			0.979						0	2.01
-1.79						-0.023	0.012					-0.286		0.030	1.98
-161			8.762						4.233	0.099				0.646	1.45
19.2				-0.031				0.697	1.371					0.880	1.29
20.8		0.921		-0.033				0.754						1.515	0.94
-18.1			1.494					0.446	2.280					2.481	0.58
-1.43						-0.023	0.012				-0.358	-0.304		2.755	0.51
-12.4	-0.498			0.010					3.243			-0.267		2.755	0.51
-12.5	-0.452								2.875	0.011		-0.302		2.755	0.51
-1.60		-0.183				-0.024	0.012					-0.306		2.755	0.51
69.4				-0.099			-0.008	1.279					0.052	2.756	0.51
5.36	-0.494		-1.061						2.667			-0.340		2.756	0.51

The predictions of the top model are compared to the observed data in Fig. 2.6, represented as nitroproduct yield vs. milling time. The experimental data used to obtain the fits are shown; these are the same data as in Fig. 2.1, except for the points showing diminishing yields at longer times. Predictions were calculated from the rate constants k obtained by the model fit, and by solving Eq. (10) for C_{NP}/C_P. The width of the bands in Fig. 2.6 indicates two standard errors of the prediction. The overall trends between the precursors are well reproduced, in particular for short milling times, when the reaction rates are nearly constant. The comparisons for other models with $\delta_{AICc}<2$ show a similar correlation with the experimental data.

Clearly, the models were not designed to predict observed decrease in nitroproduct concentrations, seen at longer times for anisole, p-xylene, and ethylbenzene (see Fig. 2.1). These effects illustrate that the simplified first-order reaction model, and the assumptions of no byproducts and no other losses cannot be used to describe the results observed at different milling times. Nevertheless, since the overall initial trends are reproduced reasonably well, some conclusions can be drawn with respect to the relative importance of precursor properties for nitration by mechanical milling.

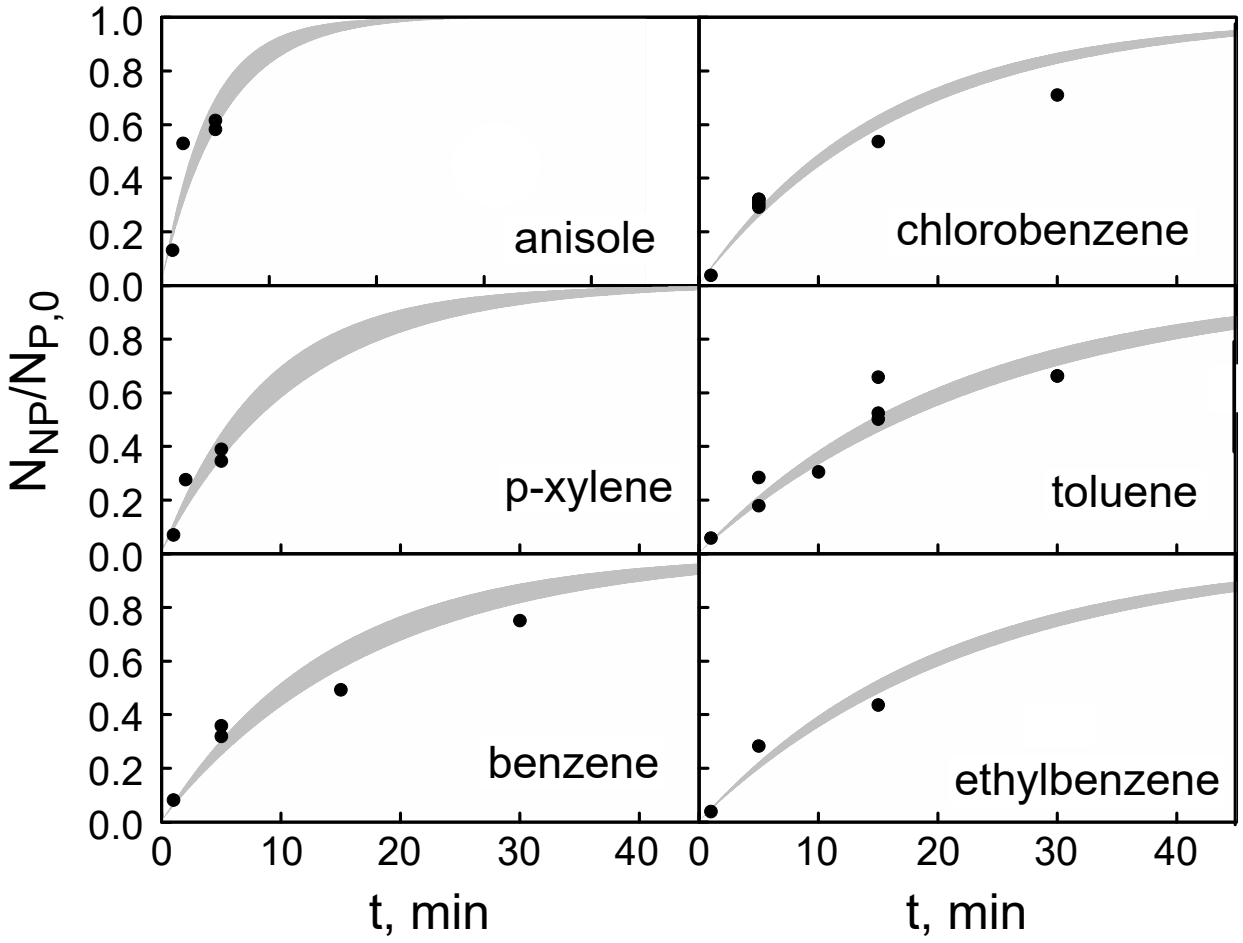

Figure 2.6. Comparison between measurements (filled symbols) and prediction using the model with lowest AICc (gray lines). The two lines show upper and lower prediction limits with a difference of two standard errors.

Figure 2.7 shows the sum of the weights of the models that a given parameter appears in. The top axis (filled bars) show the sum of model weights for all models with $\delta_{AICc}<2$, while the bottom axis (white bars) shows the sum of all model weights up to and including the models with 5 independent parameters (see Fig. 2.5). This suggests that the activation factor and the gas basicity are consistently the most predictive for the nitration rate by mechanical milling. In models where they appear together (e.g., 1st, 4th and 5th models, see Table 2.6), their respective coefficients have opposite signs, suggesting that higher activation promotes nitration, while

stronger gas basicity impedes it. The third most important parameter, kinematic viscosity, is a physical property, and reflects how the precursor behaves mechanically during milling. The generally positive coefficients (Table 2.6) suggest that precursors with higher viscosity form nitrated products more effectively.

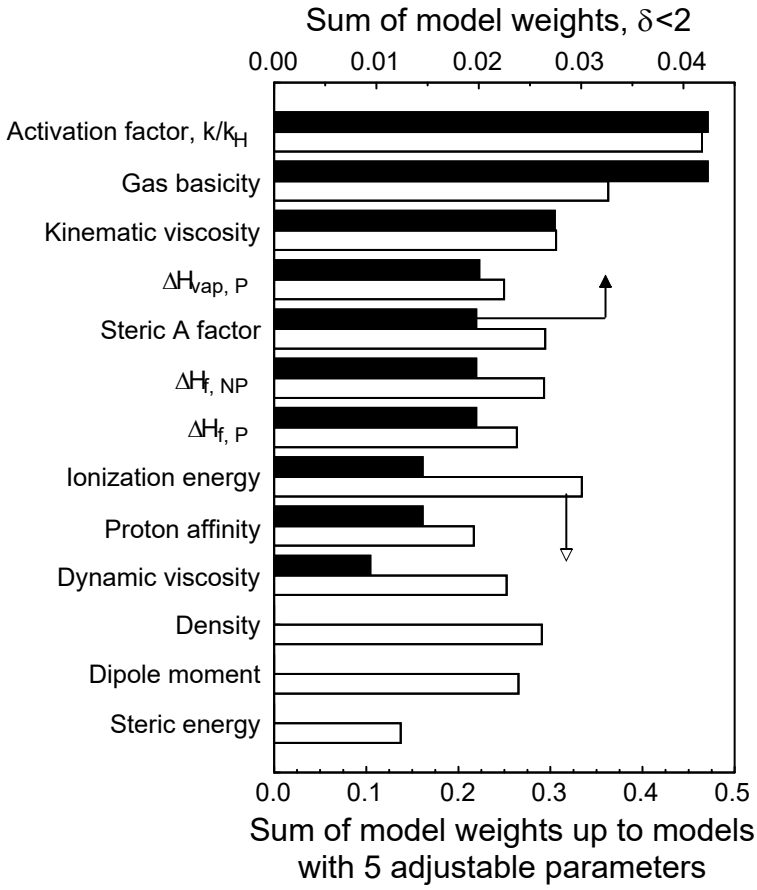

Figure 2.7. Rankings of importance of individual parameters

The top six models with δ_{AICc} values up to 2.48 contain only three parameters. Figure 2.8 shows their respective model weights (top axis, filled bars), and the sum of the model weights of all models containing the respective combinations of parameters (bottom axis, white bars).

The top two models are nearly indistinguishable in terms of their individual model weights. However, the parameter combination of the top model is also more prominent throughout the remaining models, that is, models containing this combination have higher model weights than models containing the parameter combination of the second model. Note that the number of precursors used here limits any model to a maximum of 5 adjustable parameters, therefore no model contains the parameter combinations of both, the first and second top models. The higher sum of associated model weights of the top model gives support for using it for predicting formation of aromatic nitroproducts by mechanical milling.

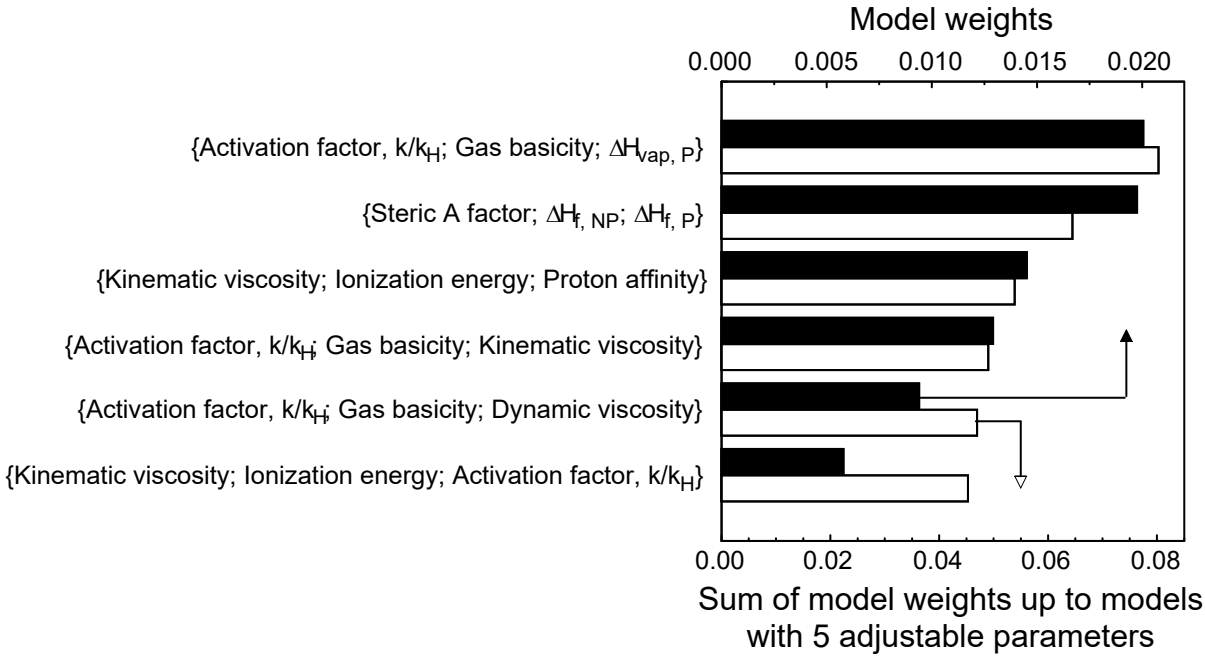

Figure 2.8. Model weights of the top 6 models with the lowest δ-AICc values, and rankings of importance of their respective parameter combinations up to and including models with 5 adjustable parameters.

2.6. Discussion

While the parameter correlation showed which precursor properties generally influence the rate of mechanochemical nitration, there was not sufficient data to account for byproduct formation or physical losses, regioselectivity, or the effect of nitrate to precursor ratio on the yield and selectivity. These results are briefly discussed below.

Several phenomena could limit the amount of nitroproducts observed for different precursors in Fig. 2.1. The most direct factor, limiting yield could be physical losses during handling or extraction. This would apply to all milling times and would not explain the observed decrease of the nitration rate with time or even reduction in the observed yield of nitro products. Data shown in Fig. 2.3 suggest that the yield approaches its theoretical limit when the reaction is limited by the amount of the precursor; however, it is lower than the expected limit, when it could be limited by the available nitrate, i.e., when there is excess of the precursor. To interpret this observation, note that catalyst sites could be blocked by the precursor molecules preventing formation of nitronium ions. Further, at longer milling times, catalyst sites can also be blocked by nitroproducts, inhibiting further nitration. Nitroproducts could either physically block the acid sites if they are not effectively removed from the catalyst surface or otherwise deactivate the sites preventing further reaction. Formation of oxidized byproducts, including oxidation of the already formed products, could be another reason for delaying or even reversing the production of targeted nitroproducts. Finally, secondary nitration was observed to occur for all precursors. While seemingly small quantities of dinitrated products were detected, this offers another avenue leading to decreasing yields of mono-nitrated compounds.

High selectivity or p/o ratio in the mechanochemically produced mono-nitrotoluene was observed previously [75], when sodium nitrate was homogenized with the catalyst using pre-milling. That result was attributed to the mechanism of reaction involving MoO_3 described by [53] and suggesting that toluene is nitrated by nitronium complexes attached to Bronsted acid sites. This reaction preferentially forms the para isomer. Alternatively, nitration slightly favoring the ortho over the para isomer was suggested to proceed through attachment of toluene molecules to Lewis acid sites [97]. The former reaction pathway is thus more likely in present experiments based on the observed p/o ratios. For toluene, the p/o ratios reported in Figs. 2.2 and 4 are similar to those reported elsewhere (1.0-1.3) when MoO_3 served as catalyst for nitration [98] (with nitric acid as a source of nitronium). Similarly, the p/o ratios shown in Figs. 2.2 and 4 for chlorobenzene are close to those reported for its nitration with MoO_3 as catalyst (3.0-3.3) [99](nitric acid added dropwise). For both toluene and chlorobenzene, the p/o ratios remain nearly constant for different milling times, suggesting that the rates of formation and decomposition for both isomers track each other during the milling.

For anisole, at very short milling times (up to 5 min), the p/o ratios observed increase with time (Fig. 2.4) remaining within a range reported earlier (1.3-2) [1]. Further increase in the milling time leads to a significant further increase in the p/o ratio exceeding 6 at 30 min milling time. A possible reasoning for the higher p/o ratios observed for anisole could be a selective breakdown of ortho isomers formed rapidly through the adsorption of precursor to the Lewis sites. It is further interesting that in all cases shown in Fig. 2.3, an increase in yields of mono-nitro products for high nitrate to precursor ratio also leads to a greater para-selectivity (Fig. 2.4). The cases of high nitrate to precursor ratios are particularly suitable for the reactions occurring via nitronium complexes attached to Bronsted acid sites. Because of the low amount of precursor, no sites are blocked by the precursor molecules and attachment of such molecules to Lewis acid sites becomes less likely. Further work is needed to clarify the mechanisms of selective nitration reactions for different precursors.

2.7. Conclusions

Mechanochemical nitration was successfully extended to a series of useful aromatic compounds. The reduced volume of the aromatic used with the fixed mass of metal oxide catalyst was found to enhance the selectivity and increase the yield of the nitroproduct indicating a fast surface reaction with nitronium complexes attached on the catalyst surface. A second nitration of the aromatic ring was observed for all the precursors used. A systematic correlation of physical and chemical properties of the aromatic precursors with their observed nitration rates showed a strong dependence of the formation of the respective nitroproducts on the aromatic activation by the functional group, gas basicity and enthalpy of vaporization of the aromatic precursor, while reaction enthalpies and kinematic viscosity are important secondary parameters. Thus, both chemical and physical properties of aromatic precursors affect the rate of their mechanochemical nitration. The results provide a basis for identifying the reaction mechanism of mechanochemical nitration. They can further be useful to optimize the reaction conditions for the precursors used and determine such conditions for an extended range of aromatics.

Chapter 3: Effect of metal nitrate on mechanochemical nitration of toluene

3.1 Abstract

Mechanochemical nitration of toluene was explored using a planetary mill and MoO_3 as catalyst. Different inorganic nitrate salts were used as the nitronium source. Nitration was carried out by initially milling the nitrate salt and the catalyst, and then adding toluene. The amount of nitrate salt used was systematically varied, while the amounts of both, the catalyst and toluene were held constant. For most nitrates the greatest yield of mononitrotoluene was observed for conditions where the molar reactant ratio of (NO_3^+) to toluene was near 4. Lower yields were observed with either less or more of the nitrate, consistent with limitation by the reactant on one hand, and obscuration of suitable catalytic sites on the other. Observed ratios of para- to ortho-mononitrotoluene were above one, consistently with a mechanism involving nitronium ions positioned at the catalyst surface reacting with toluene directly. Different nitrates resulted in varying mononitrotoluene yields, with copper nitrate showing highest, and potassium nitrate the lowest yields, respectively. The observed yields were found to correlate with the enthalpy of the bulk reaction forming mononitrotoluene and the hydroxide of the cation of the respective nitrate used.

3.2 Introduction

Nitration of aromatic hydrocarbons typically involves use of aggressive acids [100] and both, formation and purification of the nitrated products generate hazardous waste [50]. Recently, it was shown that mechanochemical nitration of toluene and other aromatics is feasible with a metal oxide catalyst and metal nitrate as a source of nitronium ion [73-75, 101]. Nearly complete conversion of organic precursor to nitroproducts was demonstrated; the reaction mechanism was also discussed [75, 101]. Mechanochemical nitration uses readily scalable ball-milling equipment; it involves benign materials and generates no hazardous waste.

Previous efforts determined how the type of organic precursor and the type of catalyst affect mechanochemical nitration [75]. Results suggested that the properties of the aromatic to be nitrated [101], as well as the properties of the catalyst [75] affect the rate of mechanochemical nitration significantly. The effect of the nitrate serving as a nitronium source has not been explored, however. All previous work [73-75, 101] used sodium nitrate as the source of nitronium because of its availability, stability, ease of handling, benign reaction products and low cost. Nevertheless, commercial $NaNO_3$ is manufactured and purified, and may not always be the most economical choice in a potential mechanochemical production of nitrated aromatics. It has also not been clarified whether it leads to the fastest and most complete mechanochemical nitration. Therefore, the current work explores how different metal nitrates affect the mechanochemical nitration of aromatic compounds. To limit the amount of data to be generated and processed, the present experiments addressed only nitration of toluene as representative example. Molybdenum oxide, MoO_3, was used as the most effective catalyst [75]. The current work focuses on the different nitrates as well as the effect of reactant ratios and reaction milling time.

3.3 Experimental

Molybdenum oxide (Alfa Aesar, 99.95%) served as the catalyst to test the nitration of toluene (Startex, solvent grade). The nitrates listed in Table 3.1 were used as sources of nitronium ions. Also shown are mass loadings for different nitrates used in experiments with different reactant ratios. The reactant ratio is defined here as the ratio of number of moles of NO_3^- over the number of moles of toluene, C_7H_8, used in experiments.

Table 3.1. Nitrates used in experiments

Nitrate	Source	Mass in g for reactant ratio, (moles of NO_3^-)/(moles of C_7H_8)			
		2	4	6	8
$NaNO_3$	Alfa Aesar, 99%	0.80	1.60	2.40	3.20
KNO_3	Alfa Aesar, 99%	0.95	1.91	2.86	3.82
$Ca(NO_3)_2 \cdot 4H_2O$	Alfa Aesar, 99%	1.11	2.22	3.33	4.44
$Cu(NO_3)_2 \cdot 2.5H_2O$	Alfa Aesar, 98%	1.30	2.60	3.90	5.20
$Bi(NO_3)_3 \cdot 5H_2O$	Beantown chemicals 98%	1.52	3.04	4.58	6.16
$Mn(NO_3)_2 \cdot 6H_2O$	Alfa Aesar, 98%	1.18	2.36	3.54	4.72

Mechanical milling was carried out using a Retsch PM 400 planetary mill in 500 mL-hardened steel milling vials. The mill was operated at 350 rpm with the rotation direction versed every 15 minutes. The milling compartment was chilled by an added air conditioner. The process included two milling stages: pre-milling of the nitrate and molybdenum oxide and reactive milling with toluene. Previous work [75] showed that the rate of nitration is increased significantly as a result of pre-milling. Therefore, molybdenum oxide and a nitrate powder were first homogenized by milling them without any process control agents for 120 min. The obtained pre-milled powder was used for the second stage reactive milling with toluene. Between the milling stages, the vials were cooled for 10 minutes. Toluene was then introduced by opening the milling vials, adding toluene with a pipette, and resealing the milling vials. The milling parameters used were similar to previous work [75]; details are shown in Table 3.2. The mass of MoO_3 was fixed at 41.63 g, and a constant amount of toluene of 0.5 mL was used. The mass of nitrate was varied as shown in Table 3.1 to obtain different reactant ratios. The time of reactive milling was varied for several nitrates at all reactant ratios. A set of reference experiments were conducted with no reactive milling by adding 0.5 mL of toluene to 43.3 g of premilled catalyst-nitrate composite for 15 min without any agitation.

Surface areas of the pre-milled catalyst-nitrate composites were measured using the Brunauer-Emmett-Teller (BET) method on a Quantachrome Instruments Autosorb IQ ASIQM000000-6. Before recording the adsorption isotherms, the powder was degassed at 300 °C for 8 h.

Table 3.2. Milling parameters common for all experiments.

Milling media (steel balls) diameter, mm	Ball to powder mass ratio	Milling speed (rpm)	Mass of MoO_3 (g)	Volume of toluene (mL)	Mass of nitrate (g)	Time of reactive milling (min)
6.35	3	350	41.63	0.5	0.8-12.16	1 - 30

After reaction milling the products were extracted with ethyl acetate (ACS, 99.8% by VWR International) as an effective solvent for dissolving the nitroproducts and any remaining toluene. The milling vials were opened in a chemical fume hood. Ethyl acetate (150 mL) was added and the mixture was milled for one additional minute. This one minute is added to the time of reactive milling for the following presentation of all results. For example, the experiments performed with no reactive milling are shown as having 1 min of milling time. The milling balls were separated using a 60-mesh brass sieve with 2.5 mm diameter openings. The mixture was allowed to settle for 12 h and then loaded in a LW Scientific Ultra 8f-centrifuge to remove solids. The recovered liquid containing dissolved products was analyzed using gas chromatography-mass spectrometry (GC-MS). The same procedure was applied for samples prepared with all milling times, including those prepared with no reactive milling.

The yields of the nitroproducts along with any dinitrated, oxidized or other by-products were quantified by GC-MS using an HP 6890 gas chromatograph. The inlet port was maintained at 200 °C and the column was heated to 250 °C at 5 °C/min. An HP G2350A mass spectrometer was used to identify the species evolved using the built-in NIST08 mass-spectral library. In all experiments, xylene (Sunnyside, solvent-grade) was added to the solution to serve as the internal standard. A calibration curve was obtained comparing peak areas for each nitro-toluene and xylene.

3.4 Results

Figure 3.1 shows the surface areas obtained after premilling MoO_3 catalyst and corresponding nitrates to form composites. The experiments used varying masses of nitrates (see Table 3.1). For consistent presentation, and to aid comparison, results are plotted in terms of the (NO_3^-)/toluene molar ratio (or reactant ratio) of the subsequent reaction milling. For the nitrates where multiple measurements were performed, $Cu(NO_3)_2$, $Mn(NO_3)_2$, $Bi(NO_3)_3$, and $NaNO_3$, the surface area of the obtained composite powders were not strongly affected by the nitrate amounts used. Among the nitrates, alkali nitrates without any structural water resulted in lower surface areas of the resulting powders compared to nitrates with multivalent cations and structural water.

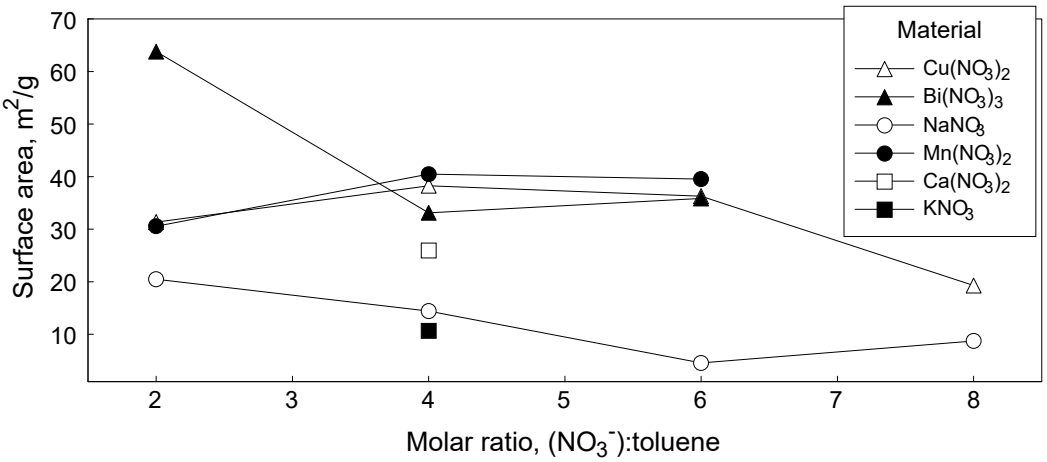

Figure 3.1. Specific surface areas of MoO3 catalyst after premilling with different nitrates for 120 min

The main product of the nitration reaction was mononitrotoluene (MNT). Significant byproducts was benzaldehyde, dinitrophenol, and dinitrotoluene. Comprehensive results are reported in the supplement in Table 3.S1.

Results of the nitration experiments are presented as MNT yields as function of two main experimental variables, reactant ratio and milling time. The time evolutions of the MNT yields for different nitrates grouped by reactant ratio are shown in Fig. 3.2; the respective variations in the MNT yield as a function of the reactant ratio at different times are presented in Fig. 3.3.

The slopes of the curves shown in Fig. 3.2 represent the net reaction rates. Some common features are observed for all metal nitrates. The most consistent trends of MNT yield vs. milling time are noted for reactant ratios of 2 and 4. The reaction rate appears nearly constant initially, and decreases then at longer milling times. This is expected if the reaction rate depends on the concentration of the remaining reactants toluene and metal nitrate. The decrease in reaction rate is accompanied by an increased concentration of benzaldehyde, most clearly observed for milling time of 16 minutes and reactant ratio of 2 (see below).

As the reactant ratio increases from 2 to 4, the observed MNT yields and reaction rates increase. For Cu and Bi nitrates, the MNT yield saturates at 16 min reaction milling time, with a corresponding sharp decrease of the reaction rate. Increasing the reactant ratio to 6 does not increase the reaction rate further. For Bi nitrate, the rate is observed to decrease.

At reactant ratio of 8, inconsistent results are observed. The MNT yield for Cu nitrate decreases after 11 min of milling. Non-monotonic trends are also observed for Mn and Ca nitrates.

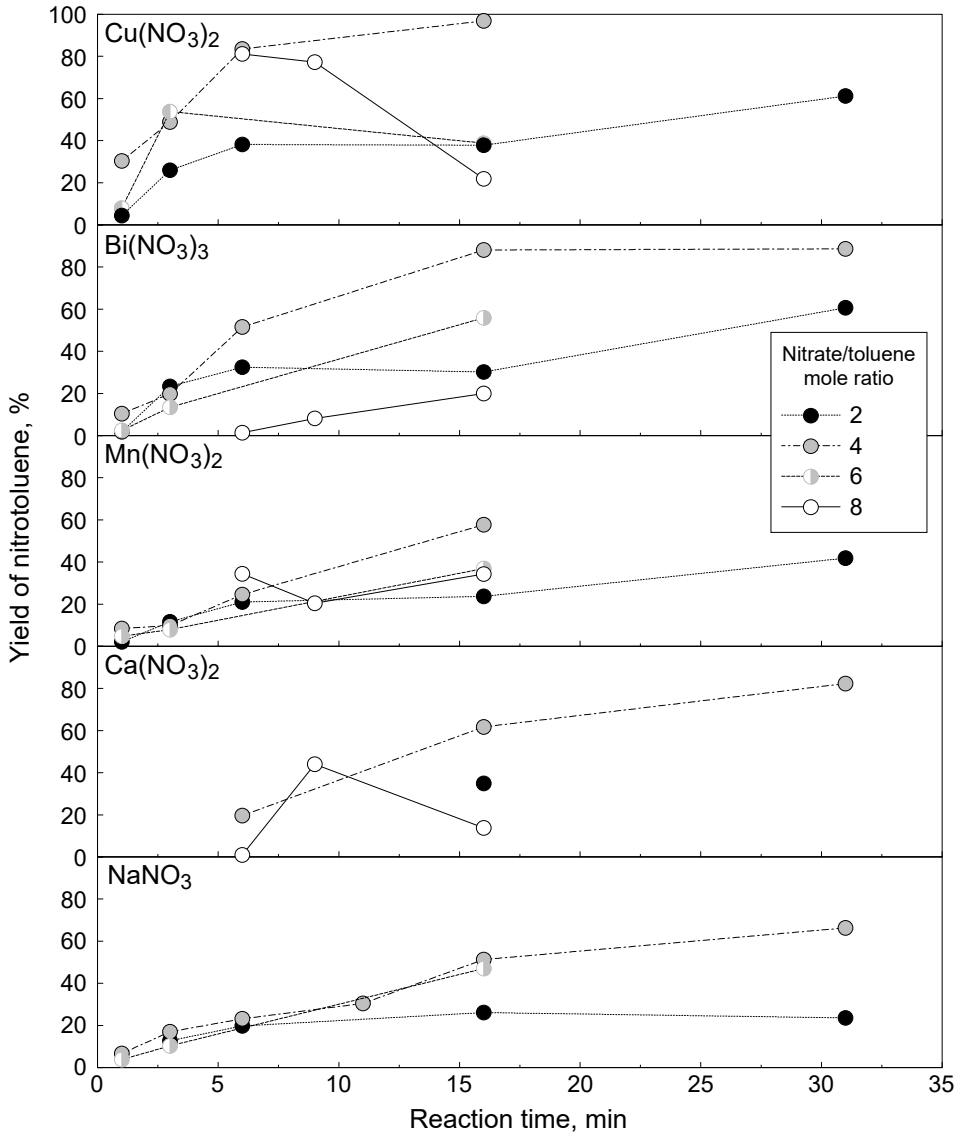

Figure 3.2. Effect of time of reaction milling on yield of MNT with different nitrates serving as sources of nitronium ions. Different symbols and lines represent different reactant ratios of nitrate to toluene

The same results shown in Fig. 3.3.2 are also presented in Fig. 3.3.3, where MNT yield is plotted as a function of the reactant ratio while different trends represent different milling times. This includes measurements for KNO_3 where only one milling time was examined. Only milling times up to 16 min are represented, as only a few experiments were conducted at longer milling times. The common trend is most clearly observed for the milling time of 16 min: for all nitrates, the MNT yield peaks at or near a reactant ratio of 4. The only exception is $NaNO_3$, for which the MNT yield varies little at reactant ratios greater than 4, but does not peak as distinctly as for the other nitrates.

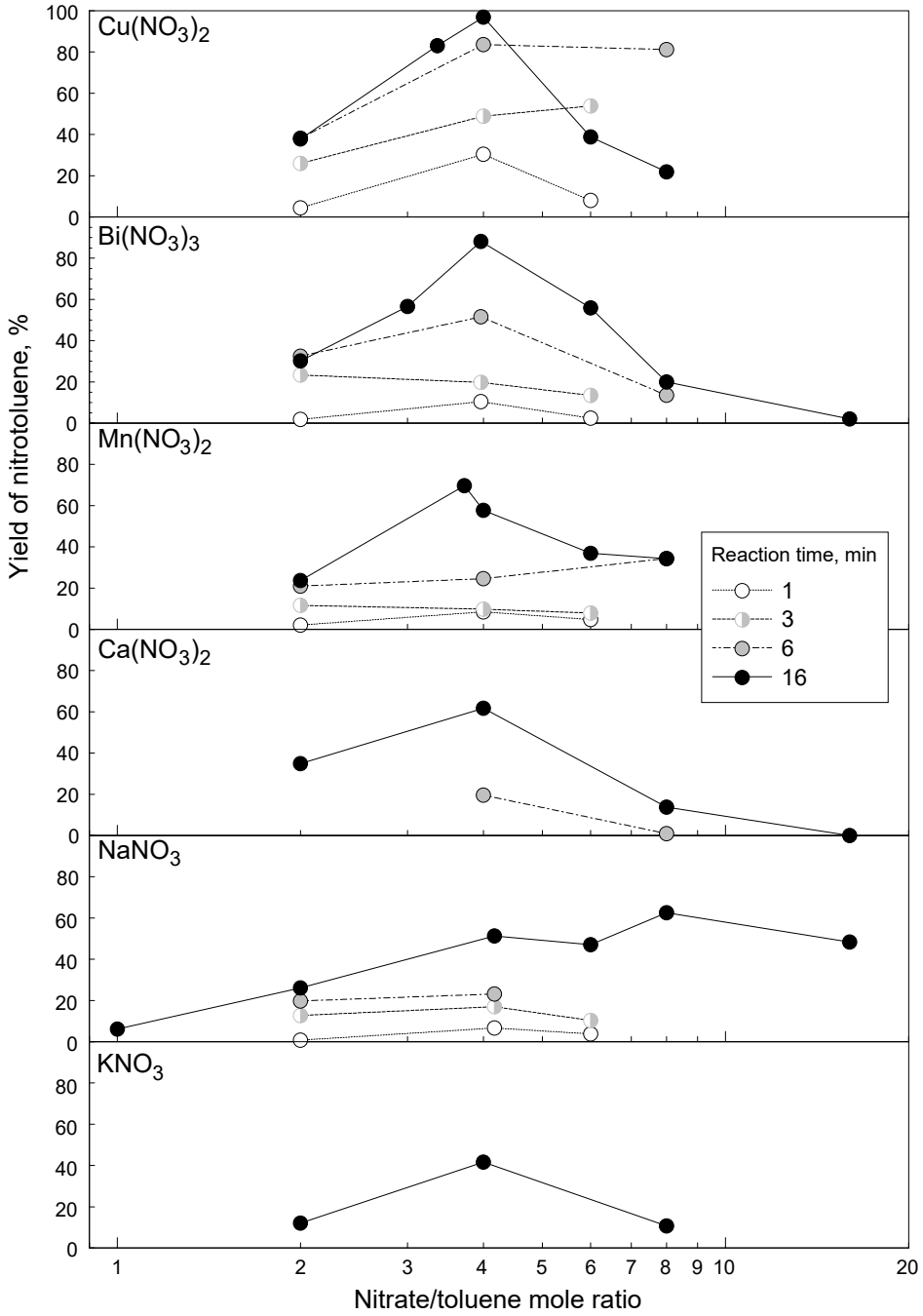

Figure 3.3. Effect of reactant ratio on yield of MNT with different nitrates serving as sources of nitronium ions. Different symbols and lines represent experiments using different reaction milling times.

In addition to the total amount of MNT, the GC-MS measurements allowed to distinguish the different isomers, ortho-, para- and meta-MNT. Of these, only the ortho and para isomers were present in measurable quantities. The ratios of the para and ortho isomers of MNT vs. the reactant ratio for the different nitrates used are shown in Fig. 3.3.4. Despite substantial scatter of

the data, two observations can be made. The para/ortho (p/o) ratio generally exceeds one and is not substantially affected by the milling time. It is decreasing slightly but consistently for most cases with increase amounts of nitrate used. No significant effect of the type of nitrate on the p/o ratio in the MNT product is observed.

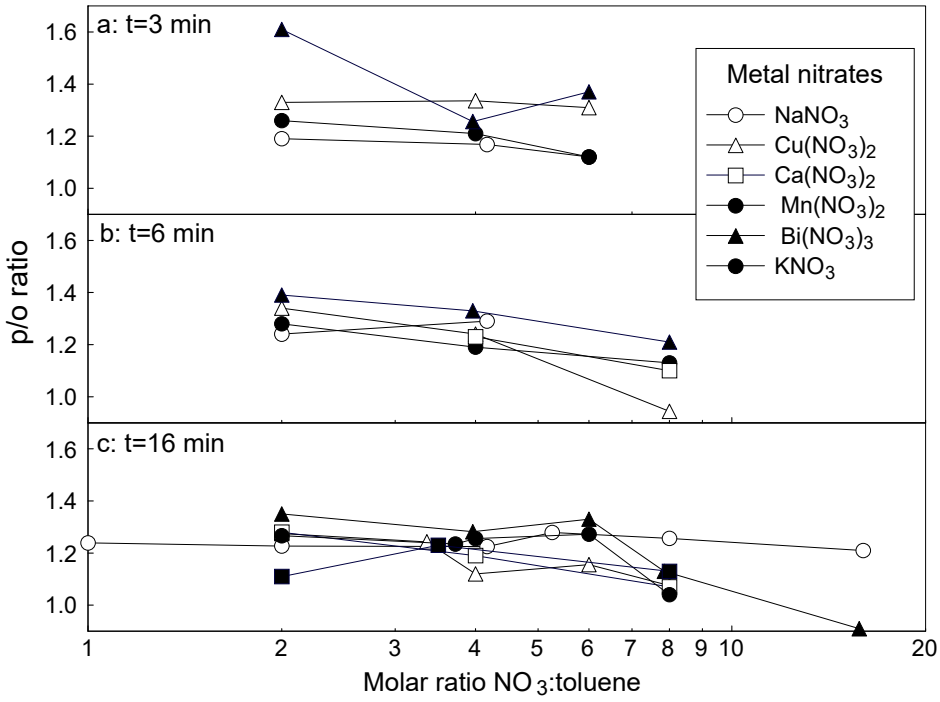

Figure 3.4. Regioselectivity changes at different molar ratios after a) 3 minute reaction milling b) 6 minute reaction milling c) 16 minute reaction milling.

Formation of benzaldehyde, the major oxidized byproduct of toluene nitration observed here, is illustrated in Figs. 3.5 and 6. Benzaldehyde was detected in most cases, however in small amounts. The effect of milling time is illustrated in Fig. 3.3.5. For all nitrates and a reactant ratio of 2, the benzaldehyde formation peaks for a milling time of 16 min. For $Ca(NO_3)_2$ and $NaNO_3$ and a reactant ratio of 4, benzaldehyde formation increased for milling times longer than 16 min, while for $Bi(NO_3)_3$ the amount remained constant at the same milling time. As with the MNT yield, the effect of milling time on benzaldehyde formation is not consistent for larger reactant ratios.

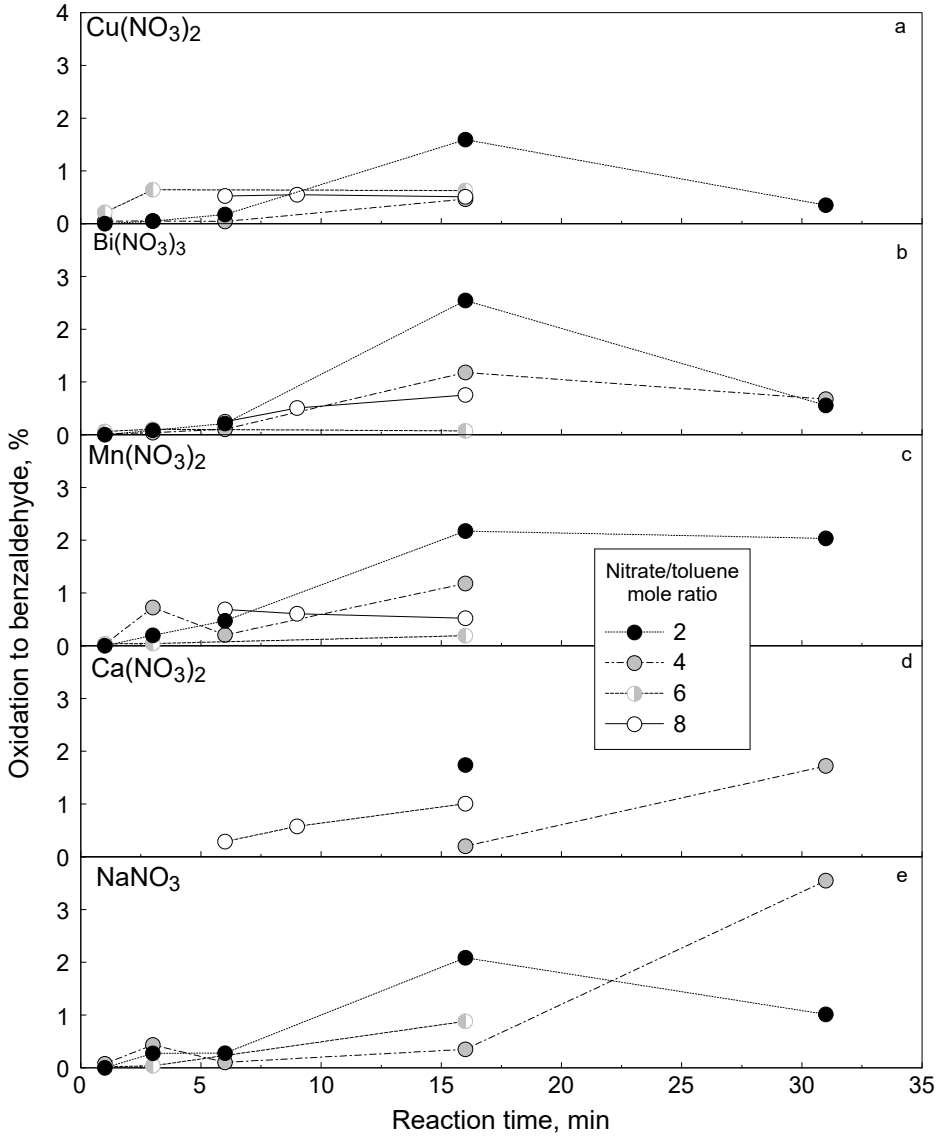

Figure 3.5. Effect of time of reaction milling on benzaldehyde formation. Different symbols and lines represent different reactant ratios of nitrate to toluene.

The same data as in Fig. 3.5 emphasizing correlation between benzaldehyde formation and reactant ratios for different nitrates are shown in Fig. 3.6. It is apparent that for the milling time of 16 min, the greatest amount of benzaldehyde forms for lower reactant ratios, especially for a ratio of 2. For greater reactant ratios, the total amount of benzaldehyde formed is reduced and the effect of milling time is less pronounced.

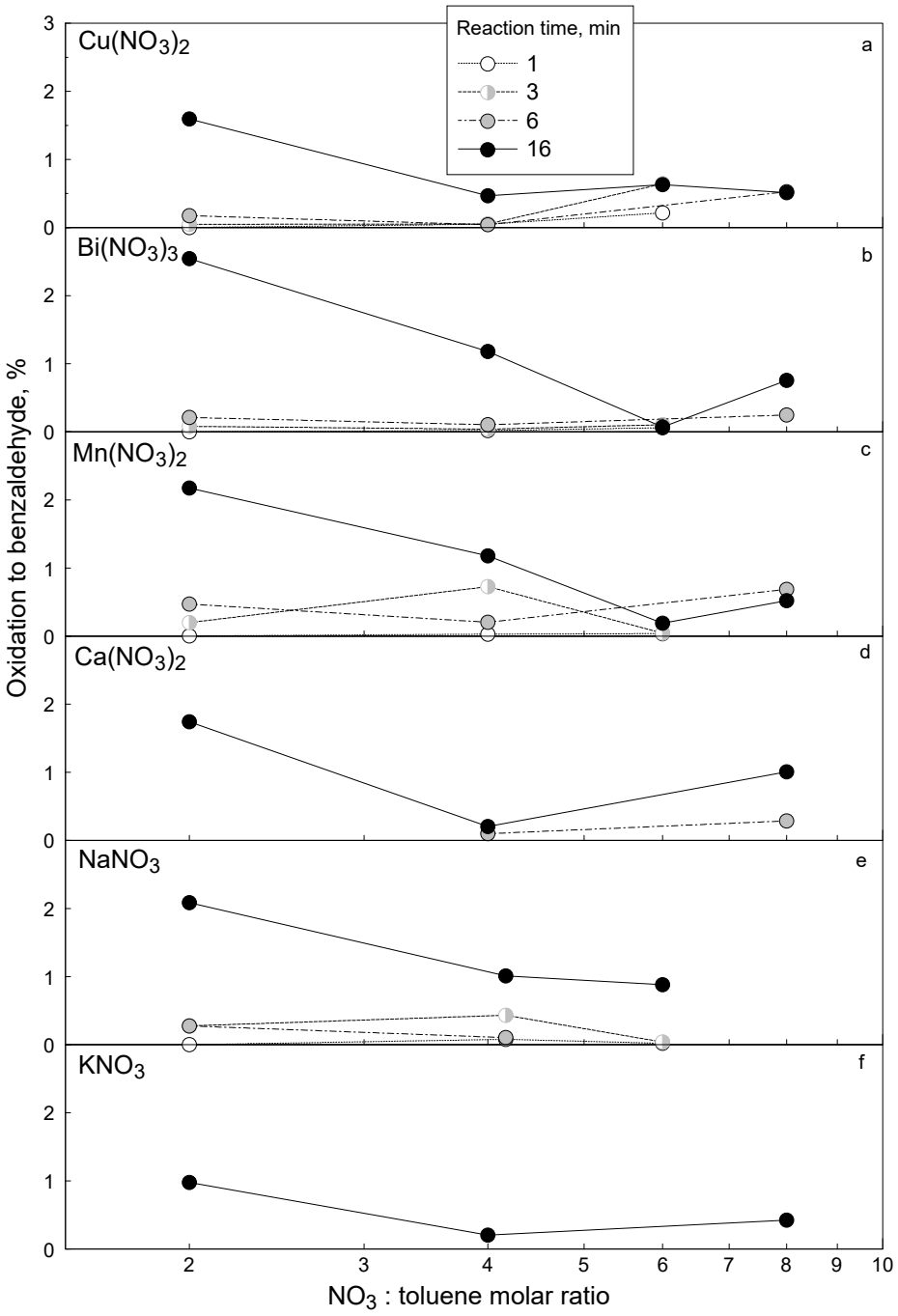

Figure 3.6. Effect of reactant ratio on benzaldehyde formation. Different symbols and lines represent experiments using different reactive milling times.

In all experiments dinitrotoluene (DNT) was detected in the recovered products. Respective yields as a function of the reaction milling time are shown in Fig. 3.7. Comparing these results with the yield of MNT shown in Fig. 3.2 it is observed that a greater MNT yield does not necessarily correlate with a greater yield of DNT. Interestingly, by far the greatest DNT yield

was observed for $Ca(NO_3)_2$, for a reactant ratio of 4 and milling time of 31 min. Note the different vertical scale in Fig. 3.7 for $Ca(NO_3)_2$.

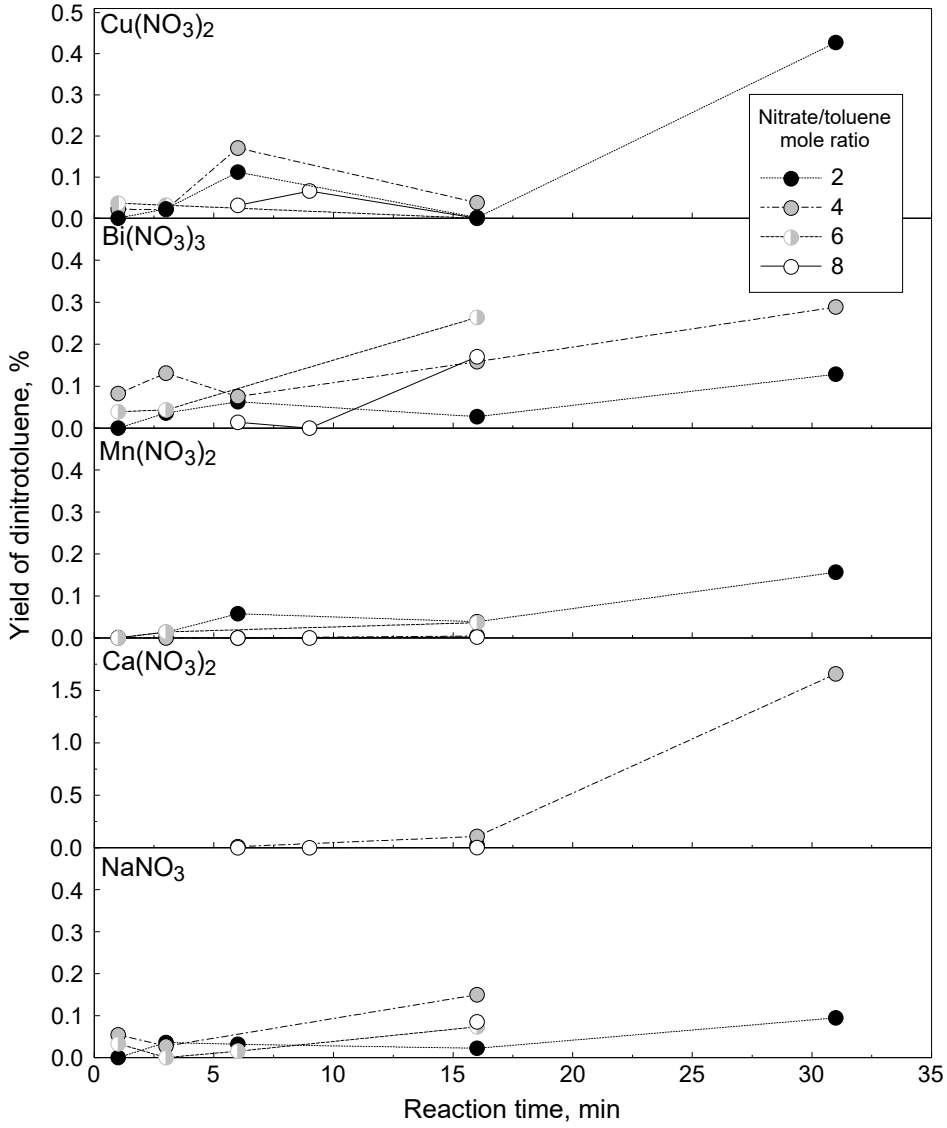

Figure 3.7. Effect of time of reaction milling on yield of DNT. Different symbols and lines represent different reactant ratios.

3.5 Discussion

The surface areas determined here (see Fig. 3.1) as having formed after the premilling step were expected to represent the active surface during reaction milling. This is a relatively crude approximation because during milling, the powder is continuously refined and new surface is generated. It can, nevertheless, be useful for initial estimates because the reaction times were much

shorter than the time of premilling. Results suggested that the premilling MoO_3 catalyst with the different nitrates in the amounts used here did not lead to substantially different active surface areas. Slightly higher specific surface area were observed for nitrates of multivalent cations, which also were also nitrates with structural water. Whether any water released from the nitrates during premilling interacted with the MoO_3 catalyst, or the mechanical properties of the nitrates themselves were systematically different and influenced the refinement of the MoO_3 could not be conclusively determined.

The MNT yield observed in the present experiments (Figs. 3.2, 3.3) was different for different nitrates. To examine effect of the nitrate properties, it was considered whether the yields correlated with electronegativity of the metal and enthalpy of formation of metal nitrate taken per mole of nitrate ion. The electronegativity may reflect the bonding in the nitrate and the ability to produce NO_2^+. However, no clear correlation between yield and electronegativity was observed (results are plotted in supplement, Figs. 3.S1-3.S3). Attempts to consider yield normalized per surface area, using the data shown in Fig. 3.1, did not lead to better correlations with electronegativity, likely due to the only minor variations in the observed specific surface areas.

The enthalpies of formation of the nitrates used, expressed relative to the amount of NO_3^- in the nitrate, likewise, did not show any consistent correlation with the observed MNT yields. However, the yields were observed to correlate with the enthalpies of the global reactions of the nitrate with toluene forming MNT, the hydroxide of the respective cation, and excess water. The individual reactions are shown in Table 3.3. A similar correlation accounting for the anhydrous oxide of the respective metal cation instead of the hydroxide was not successful. The enthalpies of reaction in Table 3.3 were calculated using reference values for enthalpies of formation of the respective metal nitrates, hydroxides, MNT, and water [87, 102, 103]. The enthalpy of formation for copper nitrate hemipentahydrate (as used in experiments) was approximated from the values available for the anhydrous and hexahydrate forms found in [87, 104].

Table 3.3. Global toluene nitration reactions forming hydroxides.

Global reaction	ΔH_r, kJ/mol of NO_3^-
$KNO_3 + C_7H_8 \rightarrow KOH + C_7H_7NO_2$	8.5
$NaNO_3 + C_7H_8 \rightarrow NaOH + C_7H_7NO_2$	-18.23
$Ca(NO_3)_2 \cdot 4H_2O + 2C_7H_8 \rightarrow Ca(OH)_2 + 2C_7H_7NO_2 + 4H_2O$	-58.31
$Bi(NO_3)_3 \cdot 5H_2O + 3C_7H_8 \rightarrow Bi(OH)_3 + 3C_7H_7NO_2 + 5H_2O$	-110.99
$2Cu(NO_3)_2 \cdot 5H_2O + 4C_7H_8 \rightarrow 2Cu(OH)_2 + 4C_7H_7NO_2 + 5H_2O$	-118.06

The MNT yield vs. the enthalpy of the global reactions in Table 3.3 is shown in Fig. 3.8. The subplots show different reactant ratios, and data are grouped by milling time. The trends are clearest for a reactant ratio of 4 and for milling times of 6 and 16 min. Generally, greater yields

are observed if the reaction enthalpy is more exothermic. The sensitivity of the yield to the enthalpy of global reaction increases when that enthalpy becomes smaller than -80 kJ/mol of NO_3^-.

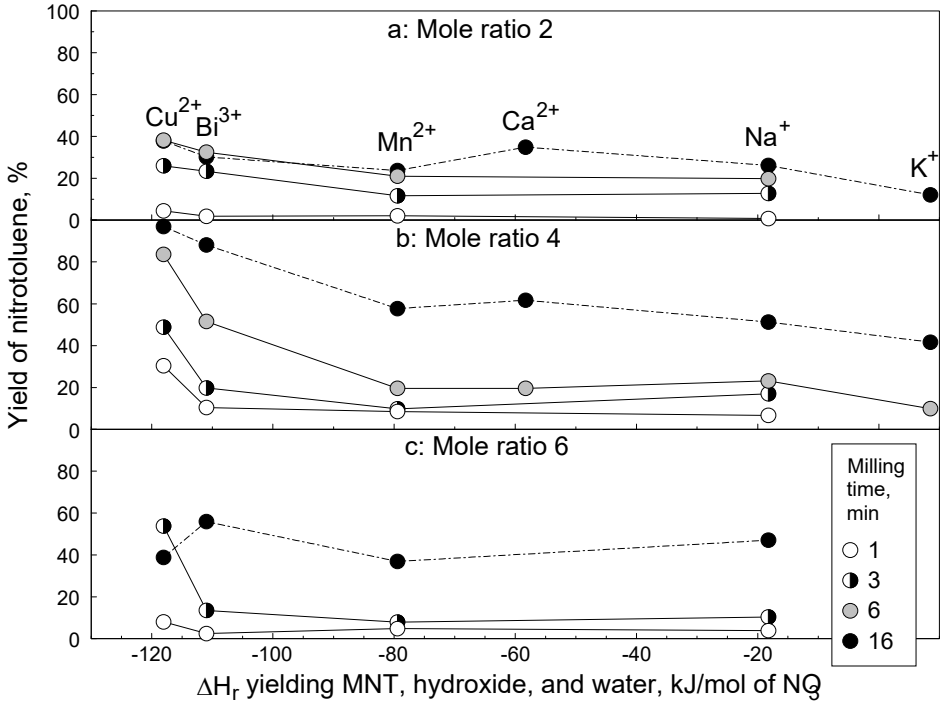

Figure 3.8. MNT yields as function of global reaction enthalpies as defined in Table 3.3.

Rate constants for global MNT formation can be estimated if reaction rate laws are known. Details of the reaction mechanism remain unclear, however. Therefore, consistently with previous research on mechanochemical nitration of different aromatic precursors, first order reactions were considered as the simplest approach to describe correlating decrease in both the reaction rates and the amount of reactant and obtain systematic rate information from the measured yield data. Combining a first order rate law with the batch reactor species balance gives the following equation:

$$X_{Tol} = 1 - exp(-k_1 t) \qquad (1)$$

where X_{Tol} is the conversion of toluene and k_1 is the 1st-order rate constant. The toluene quantification in the reaction products was not as reliable as the quantification of MNT, therefore it was assumed that MNT was the only major product so that conversion of toluene equals to yield of MNT: $X_{Tol} \approx Y_{MNT}$. This is justified in the sense that the amounts of the byproducts benzaldehyde and dinitrated toluene were generally about 2 orders of magnitude smaller than the MNT amounts (see Tables S1-S6). Rate constants were then determined by fitting equation (1) to the observed yield data. Only data up to reaction milling times of 16 minutes (15 min nominal milling time + 1

min milling for extraction) were included, and cases where obvious decrease of MNT yield with time was observed were excluded, such as Cu nitrate at 16 min with reactant ratio of 8. The obtained rate constants as a function of the global reaction enthalpies as defined in Table 3.3 are shown in Fig. 3.9.

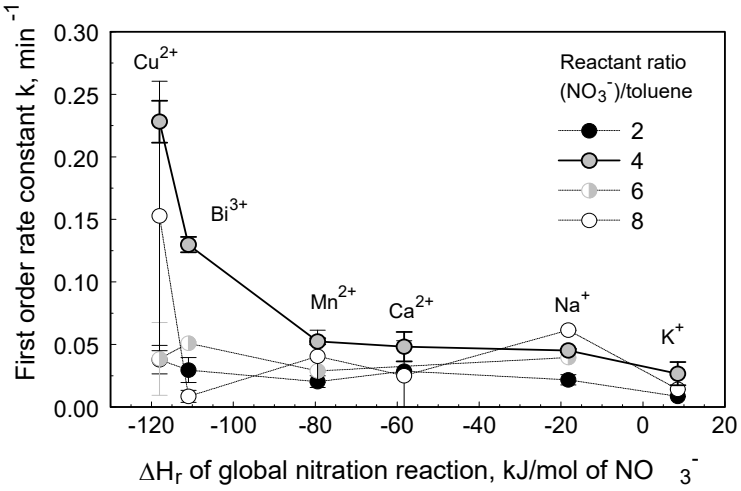

Figure 3.9 Global nitration rate constant for a first order reaction model used to describe the MNT yield for different metal nitrates. The reaction constant is calculated using yields obtained for the reaction times less than 16 min.

Since most of the nitrates showed peak yields at a reactant ratio of 4 (see Fig. 3.3), the results for reactant ratio 4 need to be emphasized in Fig. 3.9. These results show the most consistent trend with the global reaction enthalpies. Results for other reactant ratios, where yields were lower, show considerably more scatter. Figure 3.9 shows that, consistent with higher observed yields of MNT, the reaction rates are higher for Cu and Bi nitrates compared to the other nitrates. The dependence of the reaction rate on the global reaction enthalpies shown in Fig. 3.9 becomes weaker for global reaction enthalpies above -80 kJ/mol of (NO_3^-), consistently with the yield data in Fig. 3.8.

An attempt to include in this analysis the nitrate amount used, by describing the nitration as a second order process did not give consistent results. This can be rationalized from the observation that the yields peak at a certain reactant ratio. The proportionality assumed in a second order rate law would require monotonic behavior of the observed yields with the amounts of nitrate used. The first order reaction model, therefore, remains a more useful approximate description of the data.

It is interesting to compare the results for $NaNO_3$ shown in Fig. 3.3 with similar results reported earlier [75]. Unlike the present work, the amount of sodium nitrate remained fixed whereas the reactant ratio was adjusted by varying the amount of precursor (toluene here) [75]. For varying amounts of toluene, the effect of the reactant ratio on yield of MNT was qualitatively different from that seen in Fig. 3.3. In the present work, increasing the reactant ratio by adding more $NaNO_3$

during the premilling results in a gradual increase of the observed yield, with a weak maximum or plateau above $n(NO_3^-)/n(toluene) = 10$. When the amount of $NaNO_3$ during premilling was constant at 1.67 g [75], close to the amount used to target a reactant ratio of 4 in the current work, and the reactant ratio was varied by introducing varying amounts of toluene in the reaction milling step, the highest yield, and therefore reaction rate were also observed near a reactant ratio of 4 with a pronounced decrease at higher reactant ratios. The decrease in yield at higher (NO_3)/toluene reactant ratios was explained by the decrease in the amount of toluene available for the reaction [75]. In the current work the amount of toluene is constant, and the saturation of the reaction rate for sodium nitrate, or distinct decrease for the other nitrates at higher reactant ratios must be explained by decreasing availability of suitable sites for toluene to react with.

After premilling the nitrate with the MoO_3 catalyst, nitronium groups are distributed over available catalytically active surface sites, specifically Brønsted acid sites [105]. It was proposed that high p/o ratios for MNT are caused through interaction of catalyst-bound nitronium groups with toluene [53]. From our results, drops in p/o ratios are observed with increased reactant ratios for the nitrates tested. From this point, distinct reaction pathways are conceivable:
(a) toluene can react with the nitronium at the Brønsted acid site;
(b) the nitronium may desorb and, within its limited lifetime, react with a toluene molecule removed from the MoO_3 surface; or
(c) toluene can itself form a complex with an existing Lewis acid surface site, which in turn can react with the adsorbed nitronium,

The observed p/o ratios greater than 1 suggest that pathway (a) is dominant. When higher amounts of nitrate are used, there may be lack of available surface for binding nitronium that is required to facilitate all three reaction pathways. Free surface, but also existing nitronium groups at the surface may be obstructed by byproducts of the nitrate salt decomposition, e.g. oxides, hydroxides, water, or even directly by remaining unaltered nitrate. Lack of active sites to bind nitronium impedes all pathways. If pathway (a) leading to the more selective formation of para-MNT is the fastest, impeding it equally along with pathways (b) and (c) will be accompanied with a reduced para-selectivity, consistently with the result shown in Fig. 3.4.

Further, the excess of nitrate may limit interaction of the toluene with the active surface. This specifically impedes pathway (c). The reaction pathway (c) is based on the interaction of toluene and vanadium pentoxide [93], which gives rise to benzaldehyde formation. With low nitrate (and thus nitronium) concentrations, toluene can readily bind to metal defects. Once bound nitronium emerges nearby, e.g., as a result of surface generation continuing (at a relatively low rate) during milling, the reaction pathway (c) is enabled. This process becomes likely at low reactant ratios. Indeed, the relatively high benzaldehyde amounts formed at the lowest molar ratio and longer milling times (Figs. 3.5, 3.6) can be associated with the occurrence of this pathway.

Based on the results, at reactant ratio 4, the reactant to surface balance appears to be optimal with (a) being the preferred reaction pathway. The results further suggest that the negative effect of excess of nitrate limiting availability of the active sites on surface of the catalyst become critical

at the reactant ratios exceeding 6. The present discussion suggests that the specific reactant ratios identified here as leading to optimized reaction rates could be considered as proxies for the nitrate to catalyst ratios. Because both amounts of toluene and MoO_3 catalyst remained fixed, one ratio is directly related to another. The reactant ratio 4 observed to be optimal represents a nitrate to catalyst ratio of approximately 0.065.

3.6 Conclusions

Different nitrates used as sources of nitronium complexes necessary to produce MNT mechanochemically lead to different reaction rates. Among the nitrates tested, the highest nitration rate is observed for $Cu(NO_3)_2$. It is generally observed that the yield of MNT as well as the reaction rate correlate with the enthalpy of the global nitration reaction under the assumoption that the decomposition of the nitrate forms the corresponding metal hydroxide. More MNT forms at greater reaction rates if the global reaction is more exothermic. This effect is strongest for global reaction enthalpies more exothermic than -80 kJ/mol of (NO_3^-) in the nitrate.

In addition to MNT, formation of non-negligible amounts of dinitrotoluene is observed with all nitrates. The DNT yield increases at longer milling times.

The highest yield for the same reactive milling time is observed for an initial molar ratio of (NO_3^-) to toluene close to 4 for all metal nitrates tested. This approximately represent a nitrate to MoO_3 catalyst ratio of 0.065. At higher ratios, the reaction rate may be very high at very short milling times; however, the reaction products appear to decompose rapidly making the nitration difficult to control. At low ratios, the reaction rate is lower; the reaction tends to be more selective in terms of producing para-MNT, but also producing greater amounts of benzaldehyde.

Chapter 3 Supplement

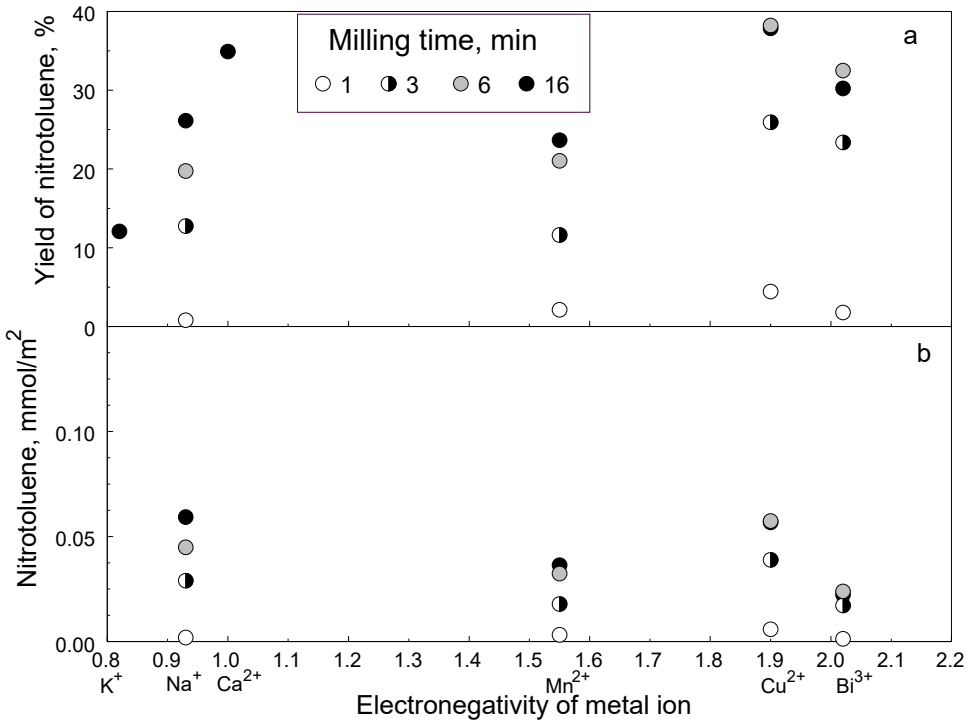

Figure 3.S1. Effect of electronegativity on production of MNT for reactant ratio 2: a) Yield of MNT for various reaction times; b) MNT generated per surface area for various reaction times.

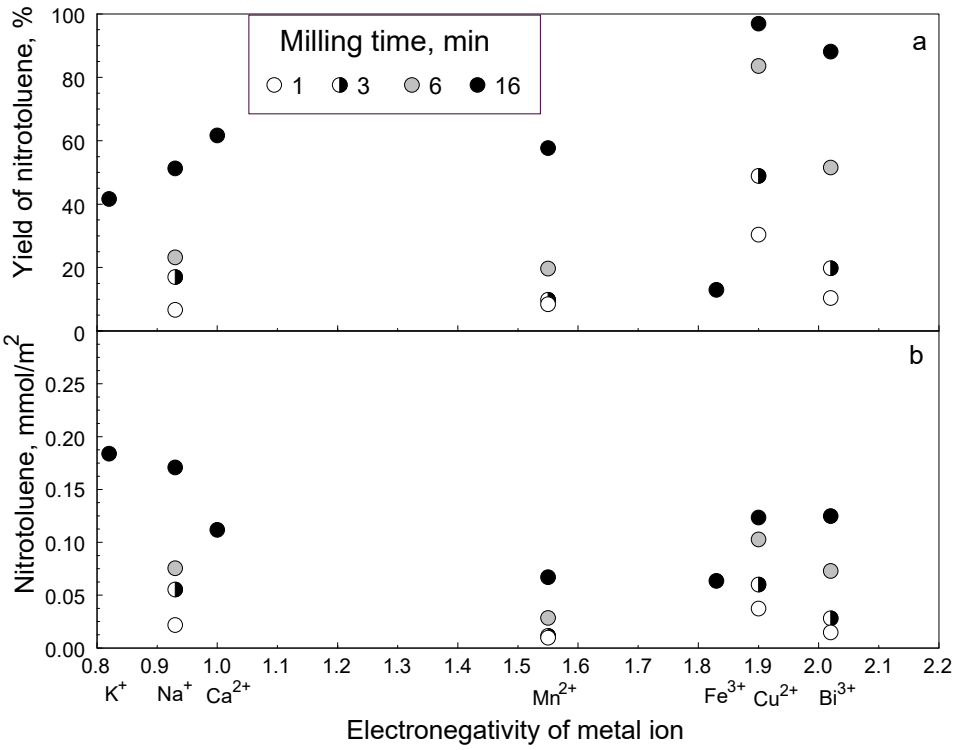

Figure 3.S2. Effect of electronegativity on production of MNT for reactant ratio 4: a) Yield of MNT for various reaction times; b) MNT generated per surface area for various reaction times.

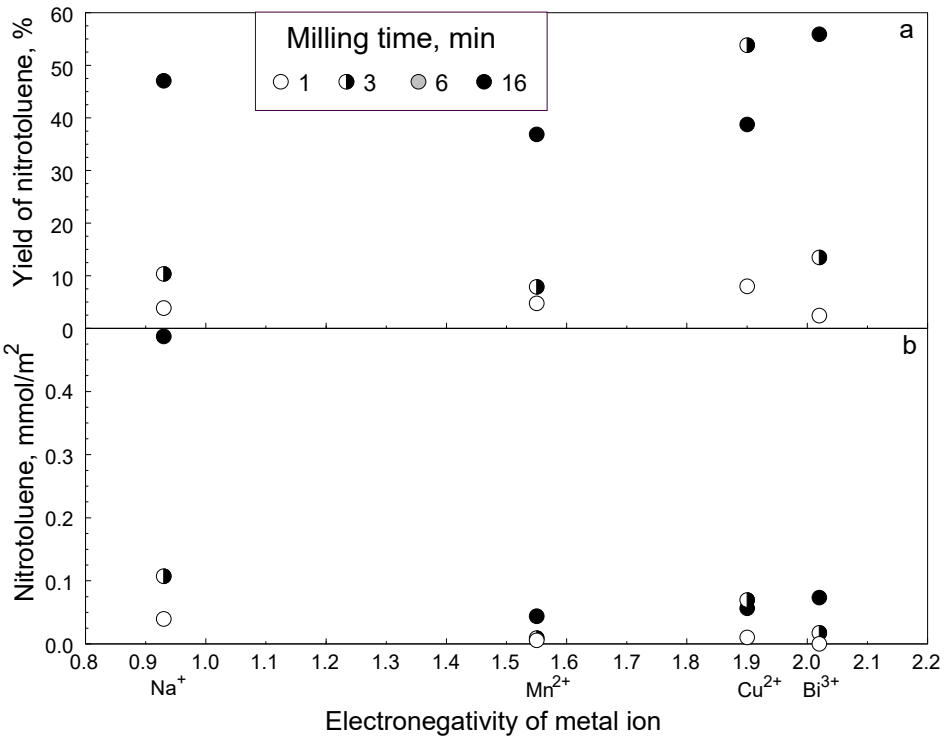

Figure 3.S3. Effect of electronegativity on production of MNT for reactant ratio 6: a) Yield of MNT for various reaction times; b) MNT generated per surface area for various reaction times.

Table 3.S1. Summary of results for mechanochemical nitration of toluene with copper, bismuth, sodium, manganese, calcium and potassium nitrates

Premilled powder: molybdenum oxide (41.63 g) and copper nitrate										
Reaction mixture: molybdenum oxide (41.63 g), copper nitrate and toluene (0.5 ml)										
Nitrate, g	Molar ratio (NO_3: toluene)	Milling time, min		Conversion, in % of toluene						MNT p/o ratio
		Nominal	Effective	MNT	Toluene recovered	Benzal-dehyde	DNT	Di-nitro-phenol	Toluene loss	
1.3	2	0	1	4.45	20.96	0.01	0.0005	0.59	73.99	1.15
1.3	2	2	3	25.92	20.14	0.47	0.02	0.61	52.84	1.33
1.3	2	5	6	38.23	17.33	0.18	0.01	0.53	43.72	1.34
1.3	2	15	16	37.86	17.73	1.59	0.002	0.02	42.79	1.28
1.3	2	30	31	61.27	0.33	0.35	0.04	0.59	37.42	1.33
2.2	3.38	15	16	83.07	1.63	0.08	1.62	0.01	13.6	1.3
2.6	4	0	1	30.36	29.7	0.05	0.02	0	39.87	1.5
2.6	4	2	3	48.9	26.78	0.05	0.02	0	24.25	1.34
2.6	4	5	6	83.55	10.22	0.04	0.17	0.03	5.99	1.24
2.6	4	15	16	93.48	1.34	0.75	0.01	0.04	4.35	1.16
2.6	4	15	16	100.3	0.93	0.67	0.01	0.07	-2.04	1.08
3.9	6	0	1	8.01	32.45	0.07	0.04	0.7	58.73	1.32
3.9	6	2	3	53.82	32.79	0.64	0.03	1.13	11.59	1.31
3.9	6	15	16	38.76	11.12	0.57	0	0	49.55	1.16
5.2	8	5	6	81.2	0.3	0.52	0.03	0.03	17.92	0.94
5.2	8	8	9	77.32	13.93	0.55	0.001	0.07	8.2	0.95
5.2	8	15	16	21.88	49.15	0.5	0	0	28.47	1.08

Premilled powder: molybdenum oxide (41.63 g) and bismuth nitrate										
Reaction mixture: molybdenum oxide (41.63 g), bismuth nitrate and toluene (0.5 ml)										
1.52	2	0	1	17.93	21.63	0.04	0	0.55	59.85	1.12
1.52	2	2	3	23.38	26.37	0.08	0.04	0.63	49.50	1.61
1.52	2	5	6	32.48	23.31	0.2	0.06	0.6	43.35	1.47
1.52	2	15	16	30.23	16.93	2.54	0.03	0.49	49.78	1.35
1.52	2	30	31	60.66	0.65	0.15	0.13	0.49	37.91	1.39
2.3	3	15	16	56.57	12.37	0.58	0.21	0.23	30.04	1.32
3.04	4	0	1	10.42	37.46	0.02	0.08	0	52.02	1.48
3.04	4	2	3	19.8	32.67	0.04	0.13	0	47.36	1.26
3.04	4	5	6	51.53	24.4	0.1	0.10	0.08	23.79	1.32
3.04	4	15	16	88.12	7.41	0	0.16	0.38	3.93	1.28
3.04	4	30	31	88.6	1.34	0.74	0.29	0.06	8.97	1.21
4.58	6	0	1	0.24	27.08	0.06	0.04	0.59	71.99	1.33
4.58	6	2	3	13.46	43.6	0.1	0.04	0.95	41.85	1.37
4.58	6	15	16	31.25	9.62	0.07	0.26	0	58.8	1.33
6.16	8	5	6	1.36	15.89	0.25	0.01	0.08	82.41	1.21
6.16	8	8	9	8.14	11.03	0.51	0	0.05	80.27	1.07
6.16	8	15	16	19.92	29.15	0.87	0.17	1.32	48.57	1.13
6.16	8	15	16	19.62	36.52	0.75	0	0.17	42.94	1.16
12.32	16	15	16	2.06	40.78	0.62	0	0	56.54	0.91
Premilled powder: molybdenum oxide (41.63 g) and sodium nitrate										
Reaction mixture: molybdenum oxide (41.63 g), nitrate and toluene (0.5 ml)										
0.4	1	15	16	6.18	20.26	3.4	0	0	70.16	1.24
0.8	2	0	1	0.82	25.38	0.01	0	0.07	73.72	0.88
0.8	2	2	3	12.76	25.3	0.28	0.04	0.04	61.58	1.19

0.8	2	5	6	19.76	21.1	0.28	0.03	0.05	58.78	1.25
0.8	2	15	16	26.14	24.01	2.09	0.02	0.03	47.71	1.23
0.8	2	30	31	23.66	2.49	1.01	0.1	0.23	72.51	1.24
1.67	4.17	0	1	6.65	29.13	0.08	0.05	0.05	64.04	1.28
1.67	4.17	2	3	16.99	30.7	0.04	0.03	0.03	52.21	1.17
1.67	4.17	5	6	23.2	36.6	0.15	0		40.05	1.31
1.67	4.17	15	16	50.2	10.64	0.55	0.15		38.46	1.24
1.67	4.17	15	16	52.39	12.63	0.16	0.08		34.74	1.22
1.67	4.17	30	31	66.3	14.74	3.55	0		15.41	1.08
2.4	6	0	1	3.86	30.99	0.02	0	0.06	65.07	1.22
2.4	6	2	3	10.36	32.46	0.04	0	0.07	57.07	1.12
2.4	6	15	16	47.03	9.6	0.88	0.07	0.03	42.39	1.26
3.2	8	5	6	15.89	14.01	0.03	0.02	0.01	70.04	1.23
3.2	8	15	16	62.6	14.21	0.75	0.09	0.03	22.32	1.28
6.4	16	15	16	48.38	0.99	0.58	0.02	0.01	50.02	1.21
Premilled powder: molybdenum oxide (41.63 g) and manganese nitrate										
Reaction mixture: molybdenum oxide (41.63 g), manganese nitrate and toluene (0.5 ml)										
1.18	2	0	1	2.12	22.87	0.02	0.001	1.65	73.34	1.08
1.18	2	2	3	11.62	30.04	0.19	0.01	1.66	56.48	1.26
1.18	2	5	6	21.03	23.33	0.47	0.06	1.41	53.7	1.28
1.18	2	15	16	23.67	24.07	2.17	0.04	0.12	49.93	1.27
1.18	2	30	31	41.88	3.8	2.03	0.16	1.15	50.98	1.27
2.2	3.78	15	16	69.68	4.88	1.04	0.19	1.18	23.03	1.25
2.2	3.78	15	16	68.64	7.21	0.55	0.10	1.22	22.28	1.22
2.36	4	0	1	8.46	31.56	0.03	0.11	0.2	59.64	1.36
2.36	4	2	3	9.82	30.43	0.82	0.1	0.17	58.66	1.21

2.36	4	5	6	24.56	26.25	2.03	0	0.6	46.66	1.19
2.36	4	15	16	57.71	16.99	1.18	0.01	0.23	23.88	1.26
3.54	6	0	1	4.77	32.5	0.04	0	1.68	62.01	1.26
3.54	6	2	3	7.87	40.55	0.04	0.01	1.77	50.76	1.25
3.54	6	15	16	36.87	15.23	0.19	0.04	0.23	47.44	1.27
4.72	8	5	6	34.36	25.2	0.68	0	0.47	39.29	1.13
4.72	8	8	9	20.38	30.52	0.6	0	0.19	48.31	1.12
4.72	8	15	16	34.31	33.74	0.68	0.04	0.04	31.19	1.04
Premilled powder: molybdenum oxide (41.63 g) and calcium nitrate										
Reaction mixture: molybdenum oxide (41.63 g), calcium nitrate and toluene (0.5 ml)										
1.11	2	15	16	34.92	15.56	1.74	0.03	0.24	47.51	1.28
2.22	4	5	6	19.66	23.78	0.1	0.01	0.13	56.32	1.35
2.22	4	15	16	61.72	12.01	0.2	0.11	0.37	25.53	1.19
2.22	4	30	31	82.28	12.01	0.2	0.11	3.4	2.0	1.24
4.44	8	5	6	0.98	18.22	0.29	0	0	80.51	1.11
4.44	8	8	9	44.01	10.69	0.63	0.03	0.01	44.63	1.22
4.44	8	15	16	13.85	31.2	1.01	0.09	0.2	53.65	1.07
Premilled powder: molybdenum oxide (41.63 g) and potassium nitrate										
Reaction mixture: molybdenum oxide (41.63 g), potassium nitrate and toluene (0.5 ml)										
0.95	2	15	16	12.09	17.31	0.97	0.36	0.21	69.06	1.11
1.91	4	5	6	9.91	16.65	0.33	0.13	0	72.98	1.22
1.91	4	15	16	41.69	11.66	0.51	0.12	0.14	45.88	1.23
3.92	8	15	16	10.69	21.07	0.42	0.01	0.09	67.73	1.13

Conclusions and Implications for Future Research

This experimental effort systematically addressed the effect of solid catalyst, organic precursor, and nitrate serving as nitronium source on mechanochemical nitration of organic compounds. It was found that effective mechanochemical nitration of organic precursors requires solid catalysts with high acidity and both, Bronsted and Lewis sites. Among the tested materials, MoO_3 was the preferred catalyst. Homogenizing the catalyst with nitrate by a preliminary milling step accelerates ensuing mechanochemical nitration significantly.

Mechanochemical nitration involving MoO_3 catalyst was successful for multiple useful aromatic compounds. The selectivity was enhanced and the yield of the nitroproduct was increased when the volume of the aromatic precursor was reduced while the mass of metal oxide catalyst was fixed. This suggests that the reaction preferably involves nitronium complexes attached on the catalyst surface. A systematic correlation of physical and chemical properties of the aromatic precursors with their observed nitration rates showed the formation of nitroproducts depends on the aromatic activation by the functional group, gas basicity and enthalpy of vaporization of the aromatic precursor. Reaction enthalpies and kinematic viscosity were found to be important as well.

Different nitrates were tested as sources of nitronium complexes for nitration of toluene. All nitrates were preliminarily homogenized with MoO_3 catalyst. Different MNT rate formation were observed for different nitrates with the highest nitration rate observed for $Cu(NO_3)_2$. The yield of MNT as well as the reaction rate correlated with the enthalpy of the global nitration reaction for which the decomposition of the nitrate was assumed to form the corresponding metal hydroxide. More MNT formed at greater reaction rates if the global reaction was more exothermic.

In multiple experiments, a second nitration of the aromatic ring was observed for all the precursors used. Nearly complete mechanochemical nitration could be achieved in many experiments. In this work, achieving the complete nitration was not targeted; instead, conditions, materials, and process parameters affecting the reaction were established.

The present results establish a path to further scale-up and optimization of mechanochemical nitration of organic compounds. The most readily achievable practical goal is to develop a technology for single-nitrated products of aromatic precursors. Such development would benefit from the found relationships between the process parameters, materials, and yield and reaction rate for the nitroproducts. The main challenges would be to determine conditions necessary to transfer the reaction parameters for the attritor mill configuration and to develop methods for in-situ separation of the reaction products from the milling tools and catalyst. Furhter, the efforts aimed at reusing or recycling the catalyst are needed. Although a detailed mechanism of mechanochemical nitration is still missing, the present work offers guidance for future experiments and models aimed to describe such mechanism in detail.

References

1. Adamiak, J., *Controlled nitration of anisole over HNO3/PO4/MoO3/SiO2/solvent systems.* Journal of Molecular Catalysis A: Chemical, 2015. **407**: p. 81-86.
2. Wang, P.C., K. Yao, and M. Lu, *Preparation of heteropoly acid based amphiphilic salts supported by nano oxides and their catalytic performance in the nitration of aromatics.* RSC Advances, 2013. **3**(7): p. 2197-2202.
3. Yang, H., et al., *Regioselective mononitration of aromatic compounds using Keggin heteropolyacid anion based Brønsted acidic ionic salts.* Industrial and Engineering Chemistry Research, 2011. **50**(19): p. 11440-11444.
4. You, K., et al., *H3PW12O40 synergized with MCM-41 for the catalytic nitration of benzene with NO2 to nitrobenzene.* RSC Advances, 2015. **5**(89): p. 73083-73090.
5. Friščić, T., *New opportunities for materials synthesis using mechanochemistry.* Journal of Materials Chemistry, 2010. **20**(36): p. 7599-7605.
6. Wang, G.W., *Mechanochemical organic synthesis.* Chemical Society Reviews, 2013. **42**(18): p. 7668-7700.
7. Lagoviyer, O.S., et al., *Mechanochemical Nitration of Aromatic Compounds.* Journal of Energetic Materials, 2017: p. 1-11.
8. Topchiev, A.V., *Nitration of Hydrocarbons and Other Organic Compounds*. 2013: Elsevier Science.
9. R. W. Millar, a., et al., *New Synthesis Routes for Energetic Materials Using Dinitrogen Pentoxide [and Discussion].* Philosophical Transactions: Physical Sciences and Engineering, 1992(1654): p. 305.
10. Schofield, K., *Aromatic Nitration*. 1980: Cambridge University Press.
11. Agrawal, J.P. and R.D. Hodgson, *Organic Chemistry of Explosives*. Organic Chemistry of Explosives. 2007. 1-384.
12. Ono, N., *The Nitro Group in Organic Synthesis*. 2003, New York: Wiley
13. Jalal Albadi, F.S., Bahareh Ghabezi, Tayebeh Seiadatnasab, *Melamine trisulfonic acid catalyzed regioselective nitration of aromatic compounds with sodium nitrate under solvent-free conditions.* Arabian Journal of Chemistry, 2012. **10**: p. S509-S513.
14. Stamatis, D., et al. *Consolidation of reactive nanocomposite powders*. 2009. Denver, CO.
15. Akhavan, J., *The Chemistry of Explosives*. 2015: Royal Society of Chemistry.
16. Zukas, J.A. and W. Walters, *Explosive Effects and Applications*. 2013: Springer New York.
17. Williams, D.F. and W.H. Schmitt, *Chemistry and Technology of the Cosmetics and Toiletries Industry*. 1996: Springer.
18. *Nitrobenzene and nitrotoluene*, in *Kirk-Othmer encyclopedia of chemical technology*, J.I. Kroschwitz, Editor. 2004, Wiley-Interscience: Hoboken, N.J.
19. A., C.F., *Organic Chemistry*. 2nd ed. 1992: McGraw-Hill, Inc.
20. Vassena D., K.A., Prins R.,, *Potential routes for the nitration of toluene and nitrotoluene with solid acids.* Catalysis Today, 2000. **60**: p. 275-287.
21. Meyers, R.A., in *Encyclopedia of environmental analysis and reme-diation*. 1998, Wiley.
22. Ganjala, V.S.P., et al., *Eco-friendly nitration of benzenes over zeolite-β-SBA-15 composite catalyst.* Catalysis Communications, 2014. **49**: p. 82-86.
23. Peng, X., H. Suzuki, and C. Lu, *Zeolite-assisted nitration of neat toluene and chlorobenzene with a nitrogen dioxide/molecular oxygen system. Remarkable enhancement of para-selectivity.* Tetrahedron Letters, 2001. **42**(26): p. 4357-4359.

24. Adamiak, J.T., W., Skupinski, W., *Interaction of nitromethane with MoO3/SiO2and its influence on toluene nitration.* Catalysis Communications, 2012. **29**: p. 92-95.
25. Gong, S., et al., *Stable and eco-friendly solid acids as alternative to sulfuric acid in the liquid phase nitration of toluene.* Process Safety and Environmental Protection, 2014. **92**(6): p. 577-582.
26. Adamiak, J., et al., *Characterization of a novel solid catalyst, H3PO4/MoO3/SiO2, and its application in toluene nitration.* Journal of Molecular Catalysis A: Chemical, 2011. **351**: p. 62-69.
27. Xinhua Peng, H.S., Chunxu Lu, *Zeolite-assisted nitration of neat toluene and chlorobenzene with a nitrogen dioxide/molecular oxygen system. Remarkable enhancement of para- selectivity.* Tetrahedron Letters, 2001. **42**: p. 4357-4359.
28. Pervez, H., et al., *Selective functionalisatlon. Part 10. The nitration of phenols by pyridine derivatives carrying a transferable nitro group1 1 Part 9. S.O. Onyiriuka and C.J. Suckling, J. Org. Chem., 1986, 51, 1900.* Tetrahedron, 1988. **44**(14): p. 4555-4568.
29. Takacs, L., *The historical development of mechanochemistry.* Chemical Society Reviews, 2013. **42**(18): p. 7649-7659.
30. Boldyrev, V.V. and K. Tkáčová, *Mechanochemistry of solids: Past, present, and prospects.* Journal of Materials Synthesis and Processing, 2000. **8**(3-4): p. 121-132.
31. Friščić, T., *Supramolecular concepts and new techniques in mechanochemistry: Cocrystals, cages, rotaxanes, open metal-organic frameworks.* Chemical Society Reviews, 2012. **41**(9): p. 3493-3510.
32. Kaupp, G., *Mechanochemistry: The varied applications of mechanical bond-breaking.* CrystEngComm, 2009. **11**(3): p. 388-403.
33. Baláž, P., *Mechanochemistry in nanoscience and minerals engineering*. Mechanochemistry in Nanoscience and Minerals Engineering. 2008. 1-413.
34. Baláž, P., et al., *Hallmarks of mechanochemistry: From nanoparticles to technology.* Chemical Society Reviews, 2013. **42**(18): p. 7571-7637.
35. Huot, J., et al., *Mechanochemical synthesis of hydrogen storage materials.* Progress in Materials Science, 2013. **58**(1): p. 30-75.
36. Baláž, P., et al., *Chalcogenide mechanochemistry in materials science: insight into synthesis and applications (a review).* Journal of Materials Science, 2017. **52**(20): p. 11851-11890.
37. Baláž, P., et al., *Mechanochemical Solvent-Free Synthesis of Quaternary Semiconductor Cu-Fe-Sn-S Nanocrystals.* Nanoscale Research Letters, 2017. **12**(1).
38. Côa, F., et al., *Coating carbon nanotubes with humic acid using an eco-friendly mechanochemical method: Application for Cu(II) ions removal from water and aquatic ecotoxicity.* Science of the Total Environment, 2017. **607-608**: p. 1479-1486.
39. Dong, B.X., et al., *Mechanochemical synthesis of COx-free hydrogen and methane fuel mixtures at room temperature from light metal hydrides and carbon dioxide.* Applied Energy, 2017. **204**: p. 741-748.
40. Lomovsky, O.I., I.O. Lomovskiy, and D.V. Orlov, *Mechanochemical solid acid/base reactions for obtaining biologically active preparations and extracting plant materials.* Green Chemistry Letters and Reviews, 2017. **10**(4): p. 171-185.
41. Siddhanti, D.A., et al., *The safer and scalable mechanochemical synthesis of edge-chlorinated and fluorinated few-layer graphenes.* Journal of Materials Science, 2017. **52**(20): p. 11977-11987.
42. S.L. James, C.J.A., C. Bolm, D. Braga, P. Col-lier, T. Friić, F. Grepioni, K.D.M. Harris, G. Hyett, W. Jones, A. Krebs, J. MacK, L. Maini, A.G. Orpen, I.P. Parkin, W.C. Shearouse, J.W. Steed, D.C.

Waddell, *Mechanochemistry: Opportunities for new and cleaner synthesis.* Chemical Society Reviews,, 2012. **41**: p. 413-447.
43. Todres, Z.V., *Organic Mechanochemistry and Its Practical Applications*. Boca Raton, FL: CRC Press Taylor and Frances Group.
44. Balaz, P., *Mechanochemistry in Nanoscience and Minerals Enineering*. 2008, Berlin: Springer-Verlag.
45. Choksi, T. and J. Greeley, *Partial Oxidation of Methanol on MoO3 (010): A DFT and Microkinetic Study.* ACS Catalysis, 2016. **6**(11): p. 7260-7277.
46. Tatibouet, J.M., *A Structure-Sensitive Oxidation Reaction: Methanol on Molybdenum Trioxide Catalysis.* Journal of Catalysis, 1981. **72**(2): p. 375-378.
47. Firth, D., *Nitration reactions in the manufacture of pharmaceutical intermediates.* Innovations in Pharmaceutical technology, 2000. **1**: p. 133-139.
48. Schofield, V.K., *Aromatic nitration*. Angewandte Chemie. Vol. 93. 1980, Cambridge: Cambridge university press.
49. Sickman, D.V., *Chemistry and Technology of Explosives. Volume I.* Journal of the American Chemical Society, 1965. **87**(13): p. 3031-3031.
50. Duehr, J., *Nitration Technology for Aromatics As Described in the Patent Literature*, in *Chemistry, Process Design, and Safety for the Nitration Industry*. 2013, American Chemical Society. p. 71-82.
51. Vassena, D., A. Kogelbauer, and R. Prins, *Potential routes of nitration of toluene and nitrotoluene with solid acids.* Catalysis today, 2000. **60**(3-4): p. 275-287.
52. Anastas, P.T. and J.C. Warner, *Green chemistry : theory and practice*. 2000, New York: Oxford University Press.
53. Adamiak, J., W. Tomaszewski, and W. Skupiński, *Interaction of nitromethane with MoO_3/SiO_2 and its influence on toluene nitration.* Catalysis Communications, 2012. **29**: p. 92-95.
54. Umbarkar, S., et al., *Vapor phase nitration of benzene using mesoporous MoO_3/SiO_2 solid acid catalyst.* Green Chemistry 2006. **8**.
55. Kemdeo, S.M., V.S. Sapkal, and G.N. Chaudhari, *TiO_2–SiO_2 mixed oxide supported MoO_3 catalyst: Physicochemical characterization and activities in nitration of phenol.* Journal of Molecular Catalysis A: Chemical, 2010. **323**(1): p. 70-77.
56. Sato, H. and K. Hirose, *Vapor phase nitration of benzene over solid acid catalysts (1): Nitration with nitrogen dioxide (NO_2).* Research on Chemical Intermediates, 1998. **24**(4): p. 473-480.
57. Smith, K. and G.A. El-Hiti, *Use of zeolites for greener and more para-selective electrophilic aromatic substitution reactions.* Green Chemistry, 2011. **13**(7): p. 1579-1608.
58. Choudary, B.M., M.R. Sarma, and K.V. Kumar, *Fe^{3+}-Montmorillonite catalyst for selective nitration of chlorobenzene.* Journal of Molecular Catalysis, 1994. **87**(1): p. 33-38.
59. Kulal, A.B., M.K. Dongare, and S.B. Umbarkar, *Sol–gel synthesised WO_3 nanoparticles supported on mesoporous silica for liquid phase nitration of aromatics.* Applied Catalysis B: Environmental, 2016. **182**: p. 142-152.
60. Kwok, T.J., et al., *Application of H-ZSM-5 Zeolite for Regioselective Mononitration of Toluene.* The Journal of Organic Chemistry, 1994. **59**(17): p. 4939-4942.
61. Patil, P.T., et al., *Regioselective nitration of o-xylene to 4-nitro-o-xylene using nitric acid over solid acid catalysts.* Catalysis Communications, 2003. **4**(8): p. 429-434.
62. Adamiak, J. and M. Chmielarek, *Efficient and selective nitration of xylenes over MoO_3/SiO_2 supported phosphoric acid.* Journal of Industrial and Engineering Chemistry, 2015. **27**: p. 175-181.

63. Koskin, A.P., I.V. Mishakov, and A.A. Vedyagin, *In search of efficient catalysts and appropriate reaction conditions for gas phase nitration of benzene.* Resource-Efficient Technologies, 2016. **2**(3): p. 118-125.
64. Sato, H., et al., *Vapor phase nitration of benzene over solid acid catalysts IV. Nitration with nitric acid (3); supported sulfuric acid catalyst with co-feeding of a trace amount of sulfuric acid.* Applied Catalysis A: General, 1999. **180**(1): p. 359-366.
65. Umbarkar, S.B., et al., *Vapor phase nitration of benzene using mesoporous MoO_3/SiO_2 solid acid catalyst.* Green Chemistry, 2006. **8**: p. 488-493.
66. You, K., et al., *$H_3PW_{12}O_{40}$ synergized with MCM-41 for the catalytic nitration of benzene with NO_2 to nitrobenzene.* RSC Advances, 2015. **5**(89): p. 73083-73090.
67. Zhou, S., et al., *Metal salts with highly electronegative cations as efficient catalysts for the liquid-phase nitration of benzene by NO₂ to nitrobenzene.* Front. Chem. Sci. Eng., 2017. **11**(2): p. 205-210.
68. Jiao, Y., et al., *Sulfated SO_4^{2-}/WO_3 as an efficient and eco-friendly catalyst for solvent-free liquid phase nitration of toluene with NO_2.* Research on Chemical Intermediates, 2017. **43**(7): p. 3961-3974.
69. Deng, R., et al., *Low-temperature and highly efficient liquid-phase catalytic nitration of chlorobenzene with NO_2: Remarkably improving the para-selectivity in O_2-Ac_2O-Hβ composite system.* Applied Catalysis A: General, 2020. **594**: p. 117468.
70. Gigante, B., et al., *Mild and Selective Nitration by Claycop.* The Journal of Organic Chemistry, 1995. **60**(11): p. 3445-3447.
71. Pérez, C., et al., *Nitration of phenol, cresol, and anisole using ceric ammonium nitrate supported on a clay and on a pillared clay.* Organic Preparations and Procedures International, 2005. **37**(4): p. 387-396.
72. Guo, F., M. Ji, and P. Zhang, *Facile nitration of aromatic compounds using $Bi(NO_3)_3{\cdot}5H_2O/MgSO_4$ under mechanochemical conditions.* Green Processing and Synthesis, 2017. **7**(5): p. 453-459.
73. Lagoviyer, O.S., et al., *Mechanochemical Nitration of Aromatic Compounds.* Journal of Energetic Materials, 2017. **36**(2): p. 191-201.
74. Lagoviyer, O.S., M. Schoenitz, and E.L. Dreizin, *Effect of process parameters on mechanochemical nitration of toluene.* Journal of Materials Science, 2018. **53**(19): p. 13690-13700.
75. Vasudevan, A.K., M. Schoenitz, and E.L. Dreizin, *Mechanochemical nitration of toluene with metal oxide catalysts.* Applied Catalysis A: General, 2020. **601**: p. 117604.
76. Stock, L.M. and H.C. Brown, *A Quantitative Treatment of Directive Effects in Aromatic Substitution*, in *Advances in Physical Organic Chemistry*, V. Gold, Editor. 1963, Academic Press. p. 35-154.
77. Hansch, C., A. Leo, and R.W. Taft, *A survey of Hammett substituent constants and resonance and field parameters.* Chemical Reviews, 1991. **91**(2): p. 165-195.
78. Jaffé, H.H., *A Reëxamination of the Hammett Equation.* Chemical Reviews, 1953. **53**(2): p. 191-261.
79. Wold, S. and M. Sjöström, *Erratum to: Multiparameter Extensions of the Hammett Equation*, in *Correlation Analysis in Chemistry: Recent Advances*, N.B. Chapman and J. Shorter, Editors. 1978, Springer US: Boston, MA. p. 547-547.
80. Lide, D.R., *CRC Handbook of Chemistry and Physics: A Ready-Reference of Chemical and Physical Data, 85th ed Edited by David R. Lide (National Institute of Standards and Technology). CRC Press LLC: Boca Raton, FL. 2004. 2712 pp.* 85 ed. CRC Handbook of Chemistry and Physics: A Ready-Reference of Chemical and Physical Data. 2004: CRC Press LLC: Boca Raton,.

81. Roux, M.V., et al., *Critically Evaluated Thermochemical Properties of Polycyclic Aromatic Hydrocarbons.* Journal of Physical and Chemical Reference Data, 2008. **37**(4): p. 1855-1996.
82. Geiseler, G., *J. D. Cox und G. Pilcher: Thermochemistry of Organic and Organometallic Compounds. Academic Press, London and New York 1970. 643 Seiten. Preis: 170s.* Berichte der Bunsengesellschaft für physikalische Chemie, 1970. **74**(7): p. 727-727.
83. Cox, J.D., *The heats of combustion of phenol and the three cresols.* Pure and Applied Chemistry, 1961. **2**(1-2): p. 125.
84. Lenchitz, C., et al., *Thermodynamic properties of several nitrotoluenes.* The Journal of Chemical Thermodynamics, 1971. **3**(5): p. 689-692.
85. Lebedeva, N.D., Y.A. Katin, and Y.G. Akhmedova, *Standard Enthalpy of Formation of Nitrobenzene.* Journal of physical chemistry, 1971. **45**: p. 1192-1193.
86. Sabbah, R. and M. Gouali, *Energetics of Intra- and Inter-molecular Bonds in the Three Nitrophenols.* Australian Journal of Chemistry, 1994. **47**(9): p. 1651-1660.
87. Kroenlein, K., et al., *NIST Standard Reference 202: TRC Web Thermo Tables (WTT) Version 2-2012-1* 2012, National Institute of Standards and Technology.
88. Van Velzen, D., R. Lopes Cardozo, and H. Langenkamp, *Liquid Viscosity and Chemical Constitution of Organic Compounds: A New Correlation and a Compilation of Literature Data. EUR 4735*, in *EUR series on nuclear research*. 1972, European Atomic Energy Commission.
89. Acree, W.J. and J.S. Chickos, *Phase Transition Enthalpy Measurements of Organic and Organometallic Compounds. Sublimation, Vaporization and Fusion Enthalpies From 1880 to 2010.* Journal of Physical and Chemical Reference Data, 2010. **39**(4): p. 043101.
90. Nelson, R.D.J., D.R. Lide, and A.A. Maryott, *Selected values of electric dipole moments for molecules in the gas phase*. NSRDS-NBS10. Vol. 10. 1967: National Bureau of standards.
91. White, D.P., J.C. Anthony, and A.O. Oyefeso, *Computational Measurement of Steric Effects: the Size of Organic Substituents Computed by Ligand Repulsive Energies.* The Journal of Organic Chemistry, 1999. **64**(21): p. 7707-7716.
92. Hunter, E.P.L. and S.G. Lias, *Evaluated Gas Phase Basicities and Proton Affinities of Molecules: An Update.* Journal of Physical and Chemical Reference Data, 1998. **27**(3): p. 413-656.
93. Brückner, A., et al., *Selective oxidation of toluene to benzaldehyde: Investigation of structure-reactivity relationships by in situ-methods*, in *Studies in Surface Science and Catalysis*, A. Corma, et al., Editors. 2000, Elsevier. p. 359-364.
94. Rahman, M.M., et al., *Recent Development of Catalytic Materials for Ethylbenzene Oxidation.* Journal of Nanomaterials, 2020. **2020**: p. 7532767.
95. Hurvich, C.M. and C.L. Tsai, *Regression and time series model selection in small samples.* Biometrika, 1989. **76**(2): p. 297-307.
96. Bartoń, K., *MuMIn: multi-model inference. R package version 1.43.17.* 2020.
97. Brückner, A., *Looking on Heterogeneous Catalytic Systems from Different Perspectives: Multitechnique Approaches as a New Challenge for In Situ Studies.* Catalysis Reviews, 2003. **45**(1): p. 97-150.
98. Adamiak, J., et al., *Characterization of a novel solid catalyst, $H_3PO_4/MoO_3/SiO_2$, and its application in toluene nitration.* Molecular Catalysis, 2011. **351**: p. 62-69.
99. Cheng, G., X.Q. Qi, and C. Lu, *Selective Nitration of Chlorobenzene on super-acidic metal oxides.* Central European Journal of Energetic Materials, 2007. **4**(4): p. 59-65.
100. Albright, L.F., R.V.C. Carr, and R.J. Schmitt, *Nitration: An Overview of Recent Developments and Processes*, in *Nitration*. 1996, American Chemical Society. p. 1-9.
101. Vasudevan, A.K., M. Schoenitz, and E.L. Dreizin, *Parameters affecting mechanochemical nitration of aromatic precursors.* Chemical Engineering Science, 2021. **in press**.

102. Donald D. Wagman, W.H.E., Vivian B. Parker, Richard H. Schumm, Iva Halow, Sylvia M. Bailey, Kenneth L. Churney, and Ralph L. Nuttall *Erratum: The NBS tables of chemical thermodynamic properties. Selected values for inorganic and C1 and C2 organic substances in SI units.* Journal of Physical and Chemical Reference Data, 1989. **18**: p. 1807-1812.
103. Kodama, H., *Synthesis of a New Compound, Bi5O7NO3, by Thermal Decomposition.* Journal of Solid State Chemistry, 1994. **112**(1): p. 27-30.
104. Varma, A., et al., *Solution Combustion Synthesis of Nanoscale Materials.* Chemical reviews, 2016. **116**.
105. Malysheva, L., V. , E. Paukshtis, A. , and K. Ione, G. , *Nitration of Aromatics by Nitrogen Oxides on Zeolite Catalysts: Comparison of Reaction in the Gas Phase and Solutions.* Catalysis Reviews, 1995. **37**(2): p. 179-226.

Final Report for ARL Contribution to SEMS Project WP19-1383

Mechanochemical Nitration of Organic Compounds

Army Research Laboratory
Aberdeen Proving Ground, MD 21005

ARL Contributors:

Leah Wingard, Ph.D. (WMRD, ARL)
Melissa Garner (ARL Summer Student)

Contents:

DEPARTMENT OF THE ARMY

U.S. ARMY RESEARCH LABORATORY

Aberdeen Proving Ground, MD 21005-5066

STANDING OPERATING PROCEDURE 1 July 2019

SAFETY

Mechanochemical Nitration

1. PURPOSE: To establish safe operating procedures and assign responsibilities for mechanochemical nitration procedures. This SOP applies to operations utilizing the SPEX Certiprep 8000D Mixer Mill.

2. SCOPE: This Standing Operating Procedure (SOP) applies to operations. Operations not adequately covered by this SOP will be addressed in a separate SOP or a supplement to this SOP, and will include a documented risk analysis approved at the appropriate level of risk acceptance.

3. APPLICABILITY: This SOP applies to all elements of the Army Research Laboratory and other personnel assigned to support these operations.

4. RESPONSIBILITY:

   a. The Branch Chief (BC), is responsible for the overall enforcement of this SOP. The Branch Chief is further responsible to ensure that only properly trained personnel are assigned to these operations and that all personnel are informed of all hazards associated with this test procedure.

   b. The Branch Chief, will ensure that personnel have been properly trained in their duties and that they have been thoroughly briefed as to the nature of the hazards involved prior to starting work. The Branch Chief will ensure that personnel are not unnecessarily exposed to any hazard and take any special precautions that may be required. The Branch Chief is further responsible for ensuring compliance of operating personnel with the provisions of this procedure.

   c. The Experimenter/Researcher (P-IX) or Explosive Processor (P-IV) is responsible for application and enforcement of this SOP and overall on-site supervision of the tests, to include taking the necessary actions to protect all personnel, equipment, and facilities from any blast, fragments, or fire resulting from a test under his or her control. The Experimenter/Researcher (P-IX) or Explosive Processor (P-IV) also maintains responsibility for providing a daily safety briefing to mixing operation personnel.

   d. Each individual assigned to this operation is responsible for their personal compliance with the applicable provisions of this SOP.

5. PERSONNEL LIMITS:

   a. Personnel will be limited to the minimum required for safe and efficient operations.

   b. A minimum of two qualified persons must be present for any hazardous operation.

   c. Observer personnel will be limited to those having an official interest in the operation or test.

6. HAZARDOUS MATERIAL LIMITS:

   a. The quantity of energetic materials to be used in any one operation will be limited to 1 grams of energetic material with Classification 1.1 or Classification 1.3. Amounts over 1 gram are not appropriate for the equipment and require approval from the Explosives Safety Office. Hazardous material at the test site shall be limited to the amount necessary for safe and efficient operations.

b. Storage of explosives and propellants before and after experiments will be in approved facilities.

c. Chemical compatibility of materials to be used in a mechanochemical nitration operation must be determined prior to mixing and storage.

7. GENERAL SAFETY REQUIREMENTS (Additional safety requirements specific to mixing energetic containing materials are listed in Section 8):

a. An operational safety shower shall be available at all times.

b. Only non-sparking tools shall be used on explosives or propellants.

c. Good housekeeping is essential and the area will be kept in a clean and orderly condition. Personnel shall remove PPE and wash their hands immediately after completing a task requiring handling of hazardous materials.

d. Non-energetic materials produced in the mixing operation should be handled and stored as described in Lethality's Chemical Synthesis SOP. All energetic materials (products or waste) shall be placed in an electrostatic discharge approved container and stored or disposed of in accordance with existing regulations.

e. There is an ABS Fire extinguisher located just outside the door. There are 2 fire extinguishers (1 ABC, 1 for metal powders) located in the front lobby of the building.

f. All opening and closing of vials, and loading and unloading of material into the milling vials will be done in the chemical fume hood with the sash as low as possible to provide additional protection.

8. PERSONAL PROTECTIVE EQUIPMENT REQUIREMENTS:

a. 100% Cotton lab coats or other ARL safety approved apparel and suitable protective gloves shall be worn when handling and processing hazardous material.

b. Safety glasses shall be worn when in the lab. Face shield and protective respirators shall be worn when handling hazardous materials as needed.

c. Blast shields will be placed around the mixer mill while the mill is in operation.

d. Researcher should remain in the opposite corner of the lab, with ready access to remote shut-off while the milling operation is underway.

9. SEQUENCE OF OPERATIONS: Only a certified Experimenter/Researcher(PI-X) or Explosive Processor (P-IV) will perform mechanochemical nitration operations.

a. OPERATING PROCEDURE FOR MECHANOCHEMICAL NITRATION

i. Clean and air-dry the milling vials as per the mill manufacturer's instructions. Make sure the threads are cleaned on both vial and lid prior to use.

ii. Gather all materials and supplies needed for the loading: reactants, milling balls, weighing dishes, syringe, spatula, and balance.

iii. Weigh out desired amounts of reactants (MoO_3 and $NaNO_3$), and the desired amount of new milling balls (usually 25g).

iv. Move the vials to the fume hood, open, and load reactants into the milling vials, followed by the milling balls. The vials need to be equal weight to balance the mill. Then weigh out the organic substrate to be nitrated into the milling vials and quickly cover the vials with lids if the substrate is volatile. Substrates should be non-energetic only. Screw on the vial cover rings and hand tighten.

v. Place the vials into the vial holders inside the mill, tighten both the vial holders and lock nuts by hand.

vi. Close and lock the mill cover.

vii. Place blast shields around mill.

viii. While unplugged, turn on the power switch on the back of the mill. Then plug the mill into an inactive powerstrip. Turning the powerstrip on and off will turn on and off the mill.

ix. Start a timer (maximum 30 minutes) and turn on the mill. New reactions should begin with a maximum milling time of 10 minutes to ensure that overheating of the sample is not occurring. Gradually increasing milling time in increments until 30 minutes is achieved to allow for monitoring of the reaction temperature.

Temperature will be monitored using an infrared temperature sensor to check the temperature of the outside of the vial.

x. Once the desired milling time is complete, turn off the mill and allow the vials to cool for a minimum of 5 minutes before removing them from the mill. If the vials are still warm to the touch, allow them to cool until they reach room temperature.

xi. Move the vials to the fume hood. Open each vial and add 15 mL of extraction solvent in the fume hood. Replace the covers and place both vials back in the mill. Tighten the lock nuts, close and lock the mill cover, and turn on mill for 30 seconds.

xii. Remove the vials and open in the fume hood. Remove the liquid via pipette or filtration.

xiii. Save the solid fraction for future analysis, or discard in the appropriate waste container.

xiv. Clean the milling vials following the manufacturer's instructions. Make sure the threads are cleaned on both vial and lid. Milling balls are to be discarded after single use.

xv. Store energetic materials IAW SOP Sup 1 (Storage of Small Scale Energetic Material in Laboratories).

10. TRANSPORTATION

a. Explosives and propellants shall be transported between laboratories and storage facilities in an appropriate container within approved ARL explosives transport boxes.

11. EMERGENCY PROCEDURES: In case of accidental ignition, the Experimenter/Researcher (P-IX) or Processor (P-IV) should stop the mill and dial 911. Do not continue milling procedures.

a. In case of a vial coming loose inside the milling equipment, turn off power via powerstrip near door. This allows remote shut-off without approaching the mill.
b. In case of any detonation or thermal runaway, use remote shut-off if safe to do so and call 911. Contact safety office as well at 306-4750 or 306-0210. Contact Explosives Safety Office at 278-9065.
c. In case of electrical storm, stop milling procedure and follow the procedure for post milling process. Caution: Forecast must be known prior to process starting.

12. POSTING REQUIREMENTS: A copy of this SOP, and any related SOPs, will be prominently displayed at the site of this operation.

2. Experimental Design

ARL's contribution focused on the evaluation of the mechanochemical nitration technique developed by NJIT as viable nitration technique for a range of substrates of interest. Following approval of the SOP, the procedure outlined in section 9a (OPERATING PROCEDURE FOR MECHANOCHEMICAL NITRATION) was applied to both commercially available substrates and non-energetic precursors designed and synthesized at ARL. Following milling, products were extracted with ethyl acetate. Analysis by NMR and IR was conducted on crude collected products. Further purification of the products via silica column chromatography was performed on some product mixtures.

3. Results

Replication of NJIT's mechanochemical nitration procedure was successful at ARL (Figure 3.1), producing nitrotoulenes in ratios similar to those described by NJIT. 1-Nitronapthalene was produced through milling naphthalene as a substrate (Figure 3.2).

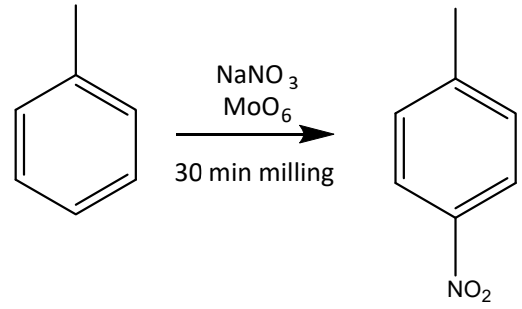

Reagents/Products	Health	Fire	Reactivity
Toluene (0.5 mL)	2	3	0
Sodium Nitrate (1.67 g)	2	1	3
Molybdenum (VI) Oxide (41.63 g)	0	0	0
Nitrotoluene (0.5 mL)	2	1	0
Ethyl Acetate (15 mL)	1	3	0

Figure 3.1 Reaction using toluene as a substrate.

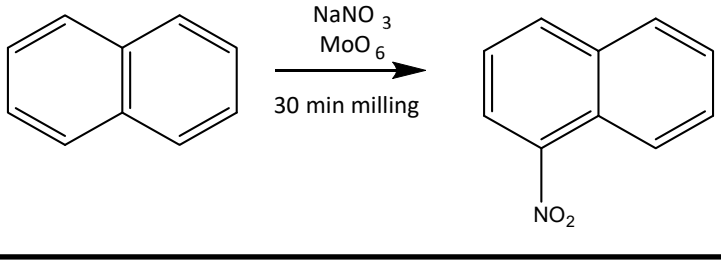

Reagents/Products	Health	Fire	Reactivity
Napthalene (0.5 g)	2	2	0
Sodium Nitrate (1.67 g)	2	1	3
Molybdenum (VI) Oxide (41.63 g)	0	0	0
1-Nitronapthalene (0.5 mL)	2	1	0
Ethyl Acetate (15 mL)	1	3	0

Figure 3.2 Reaction using naphthalene as a substrate.

Milling was also tested with the following list of commercially available substrates:

Isoxazole (Figure 3.3)
1,2-Benzisoxazole
Maleimide
Pyrazole
Pyrrole

Reaction mixtures all showed some production of nitrated products via IR. NMR analysis revealed low yields (<20%) of nitrated products along with unreacted substrate and decomposition products. In the case of the pyrazole substrate, a highly hygroscopic product was formed, and decomposed too rapidly for accurate analysis.

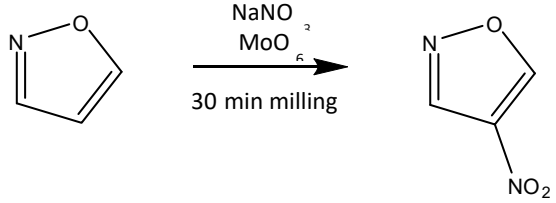

Reagents/Products	Health	Fire	Reactivity
Isoxazole (0.5 g)	0	3	0
Sodium Nitrate (1.67 g)	2	1	3
Molybdenum (VI) Oxide (41.63 g)	0	0	0
Product	?	?	?
Ethyl Acetate (15 mL)	1	3	0

Figure 3.3 Reaction using isoxazole as a substrate.

Finally, mechanochemical nitration was tested on 2 ARL designed precursors, 5,5'-Dihydroxymethyl-3,3'-bis-isoxazole[1] and 2,2'-([3,3'-biisoxazole]-5,5'-diyl)bis(Ethan-1-ol)[2]. These readily form their respective nitrate ester energetic compounds in high yields (>90%) through traditional wet nitration chemistry. While the nitrated compounds are relatively insensitive to impact and friction, concern with milling nitrate esters prompted using very small amounts of precursor (100 mg or less) in the milling process. Analysis showed some degree of nitration, but reactions were clearly much lower yielding than traditional nitration reactions.

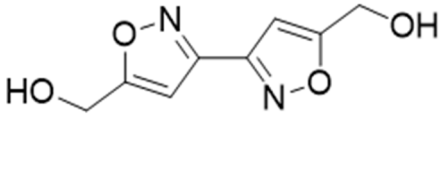

5,5'-Dihydroxymethyl-3,3'bis-isoxazole

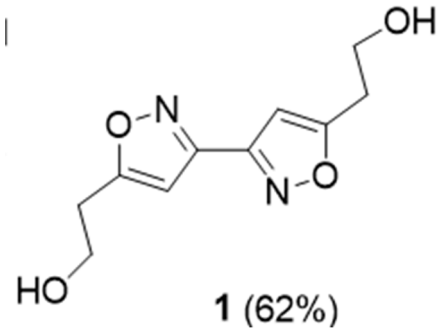

2,2'-([3,3'-biisoxazole]-5,5'diyl)bis(Ethan-1-ol)

Figure 3.4 ARL substrates

4. References

1. L. A. Wingard, P. E. Guzmán, E. C. Johnson, J. J. Sabatini*, G. W. Drake, E. F. C. Byrd

"Synthesis of bis-isoxazole-bis-Methylene Dinitrate: A Potential Nitrate Plasticizer and Melt-Castable Energetic Material" *ChemPlusChem*, **2017**, *82(2)*, 195.

2. L. A. Wingard, R. C. Sausa, P. E. Guzmán, R. A. Pesce-Rodriguez, J. J. Sabatini, G. W. Drake "Synthesis of bis-Isoxazole-bis-ethylene Dintrate and bis-Isoxazole-tetra-ethylene Tetranitrate: Potential Energetic Plasticizers" *Propellants, Explosives, Pyrotechnics*, **2019**, DOI: 10.1002/prep.201800315.